8-18-2016

Micro-grid Reliability Modeling and Analysis Approaches

Xiaofang Shi
xiaofang.shi@uconn.edu

Micro-grid Reliability Modeling and Analysis Approaches

Xiaofang Shi

B.E., Tianjin Polytechnic University, 2013

A Thesis

Submitted in Partial Fulfillment of the

Requirements for the Degree of

Master of Science

At the

University of Connecticut

2015

APPROVAL PAGE

Masters of Science Thesis

Micro-grid Reliability Modeling and Analysis Approaches

Presented by

Xiaofang Shi, B.E.

Major Advisor_____
Dr. Ali M. Bazzi

Associate Advisor_____
Dr. Yang Cao

Associate Advisor_____
Dr. Shalabh Gupta

University of Connecticut

2015

ACKNOWLEDGEMENTS

First, I would like to express my sincerest gratitude to my advisor, Professor Ali M. Bazzi, who assisted me throughout the whole M.S. degree studying especially during the thesis preparation. His guidance, mentoring and constant encouragement and education are the most important power to help me overcome all hardness. I would also like to thank my associated advisors, Professor Yang Cao and Professor Shalabh Gupta for all supports for my thesis writing.

In my daily work and study, I received assistance from my colleagues in the Advanced Power Electronics and Electric Drives Lab (APEDL), Weiqiang Chen, Yiqi Liu, Michael Stettenbenz, Artur Ulatowski, and Christian Ratliff. I would like to express my thankfulness to all of them, since I was not able to so smoothly finish my M.S. study without their help. Some of my thesis work was partially supported by Pareto Energy, so I would like to thank colleagues from Pareto Energy for their comments. Also I thank James Hare for his help on our cooperative paper.

What's more, I would like to bring my deepest gratitude to my parents, Enwei Shi and Guimei Li, who not only financially support me to have the chance studying at University of Connecticut, but also take good care of me thought all my life. Finally I would like to extend my gratitude to my boyfriend, Hongchun Zhang for his support and understanding.

In all, my degree would not have been possible without the encouragement and assistance of all the aforementioned. Thank you all!

CONTENTS

LIST OF FIGURES

LIST OF TABLES

I. INTRODUCTION

1.1 Motivation

In August 2003, Northeastern US and Ontario, Canada, experienced a cascading failure leading to large power blackout affecting about 50 million people with an estimated economic loss of around $4-$10 billion [1]. The blackout affected the power generation, water supply, transportation, communication, and industry operation. In September 2003, a black which lasted for more than two days affected more than 56 million people in Italy and Switzerland. The mobile communication failed, the power sources ran out of battery power, people were trapped on trains and flights were cancelled. An incident on European electricity network in November 2006 has led to blackouts all over the grid. It affected 10 million people in Germany, France, Belgium, Spain and Austria. The main reason of this event was a fault in the transmission system [2]. Since power system blackouts have become a phenomenon which comes to be more important and causes a large series of consequences, people are seeking to improve the grid resilience and also well-designed backup power systems which have the capability to satisfy the demand of the customers.

Micro-grids are becoming of more interest worldwide to achieve reliable electrical energy infrastructure during natural hazards and catastrophic situations due to their ability to operate in both grid-connected and islanded modes. They typically include distributed generation resources that could provide heat and electricity and are expected to have significant clean energy penetration.

1.2 Challenges

A typical micro-grid system contains generators, transformers, transmission lines breakers, converters, and loads, and each of these can have different types of failures.

Faults and failures can occur in the micro-grid without early warnings due to a wide range of possible events such as equipment failures, animal/tree contacts, falling trees, lightning strikes, malicious attacks, etc.. When a fault occurs in a certain region or part of the micro-grid system, other regions of the micro-grid may become overloaded or isolated through tripped switchgear due to load redistribution. This continuous load redistribution often leads to a cascading phenomenon that is propagated throughout the micro-grid system and in turn can lead to a catastrophic failure causing power disruptions even within the micro-grid itself and negative impacts on society especially that micro-grids are expected to be resilient. Examples of a failed solar photovoltaic and a failed transformer are shown in Fig.1.

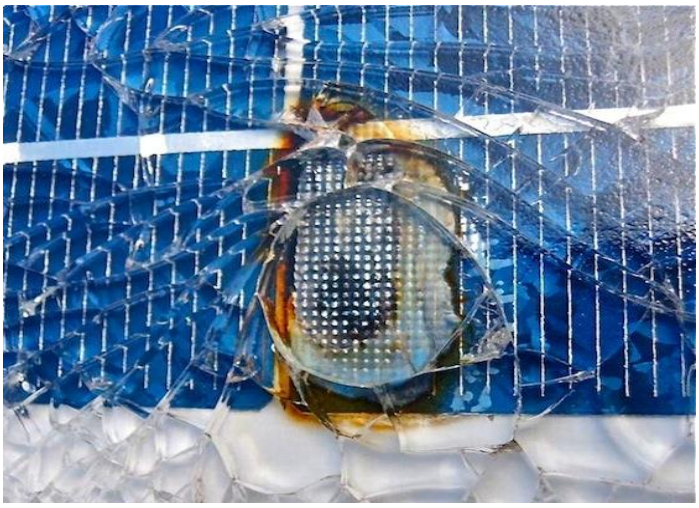

Fig.1 (a). Example of a failed solar photovoltaic panel due to degradation of the antireflection coating [3]

Fig.1 (b). Example of a failed transformer due to current arcing [4]

"Reliability is the ability of an item to perform a required function, under given environment and operational conditions and for a stated period of time" (ISO8402) [5]. Micro-grid system reliability is critical for system design and maintenance since it is commonly used as a backup power system especially during the main grid blackouts or failures. The study of micro-grid reliability can give system designers, operators, and customers potential failure modes of its subsystems and components and can provide lifetime estimation by estimating the time before the first physical failure of the micro-grid. Therefore, reliability analysis of micro-grids is significant at both design and operation stages.

1.3 Contribution

Reliability theory has been widely used in system reliability analysis [6-10], but using reliability modeling and analysis methods to evaluate micro-grid reliability at a lower level than standard power systems has not been common in the literature. This thesis thus focuses on the intersection of system theory, reliability theory, and micro-grid concepts as illustrated in the shaded area in Fig.2, and on comparing various reliability modeling and analysis methods as applied to micro-grids. The main focus is on failure of physical components in a micro-grid

which is treated as a "system" and the effects of such failures on the micro-grid's performance to meet a desired reliability objective, e.g. supporting a critical load. This approach is not common in the micro-grids literature and therefore several reliability modeling and analysis methods are applied to different micro-grids to illustrate their application methodology. The reliability modeling methods shown in this thesis can be applied for lifetime estimation and can therefore be used to enhance the micro-grid system's reliability at the design stage. Since different methods have their own characteristics, they can complement each other when analyzing micro-grid reliability to fill gaps between each method's capabilities and the other. It is important to note that failure rate numbers used later in the thesis are from literature references shown in the references section. However, the main objective of this thesis is to illustrate how micro-grids can be treated as systems for reliability purposes to open up a system-theoretic and reliability-theoretic door for micro-grid reliability modeling and analysis rather than provide numerical answers to micro-grid reliability evaluation or prediction. It is also important to note that stochastic loads and resources (e.g. wind, solar irradiance) are not considered in this thesis but are essential for future work.

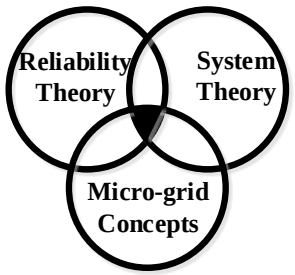

Fig.2. Highlighted focus area where system and reliability theories are applied to micro-grid concepts

Reliability metrics such as mean time to failure (MTTF), reliability function $R(t)$, the failure rate (λ), mean residual life (MRL), component importance (I), and component's success probability can be used to iteratively "design for reliability" and system hardening for operational and economic benefits. An example introducing an approach to design for reliability is also presented to illustrate how one of the reliability methods introduced can be applied to choose a design power electronic converter for micro-grids.

The thesis proceeds as follows. Chapter II reviews major faults in micro-grid components and introduces RBD, FTA and MRM methods as applied to a simple three-component system. Chapter III describes micro-grids used as case studies. Three methods applied for reliability modeling and analysis of the University of Connecticut micro-grid are described, and the results are shown in Chapter IV. Chapter V shows King's Plaza and New York University micro-grids reliability analysis results. An example introducing a design-for-reliability approach is in Chapter VI. In Chapter VII, discussions of the results are presented along with brief comparison of the three methods, and Chapter VIII is the conclusion.

II. LITERATURE REVIEW

2.1 Review of the Major Faults in the Micro-grid System

An example of a micro-grid is shown in Fig. 3 and includes the integration of sensing, communication and control technologies with distributed power generation systems. This forms an efficient and reliable micro power system that is capable of delivering power even in the event of failures on the main utility grid. Micro-grids are configured as DC or AC grids connected to low or medium voltage distribution networks [11]. Clean energy generation systems commonly include wind turbines, photovoltaic (PV) panels, and fuel cells. Conventional generation systems, e.g. diesel or natural gas generators, are used when clean energy systems cannot provide sufficient power or are highly intermittent. Most distributed generation systems require power electronic converters to connect to building loads or the utility grid and are mainly interconnected through cables and possibly distribution-level transmission lines forming a unified power system for local load support. Before providing a review of the reliability analysis methods, it is useful to have a detailed understanding of the fault universe of the micro-grid's electrical energy infrastructure. Table 1 summarizes the components reviewed in this thesis, their failure modes, and their effects. This literature review has already been published in [12].

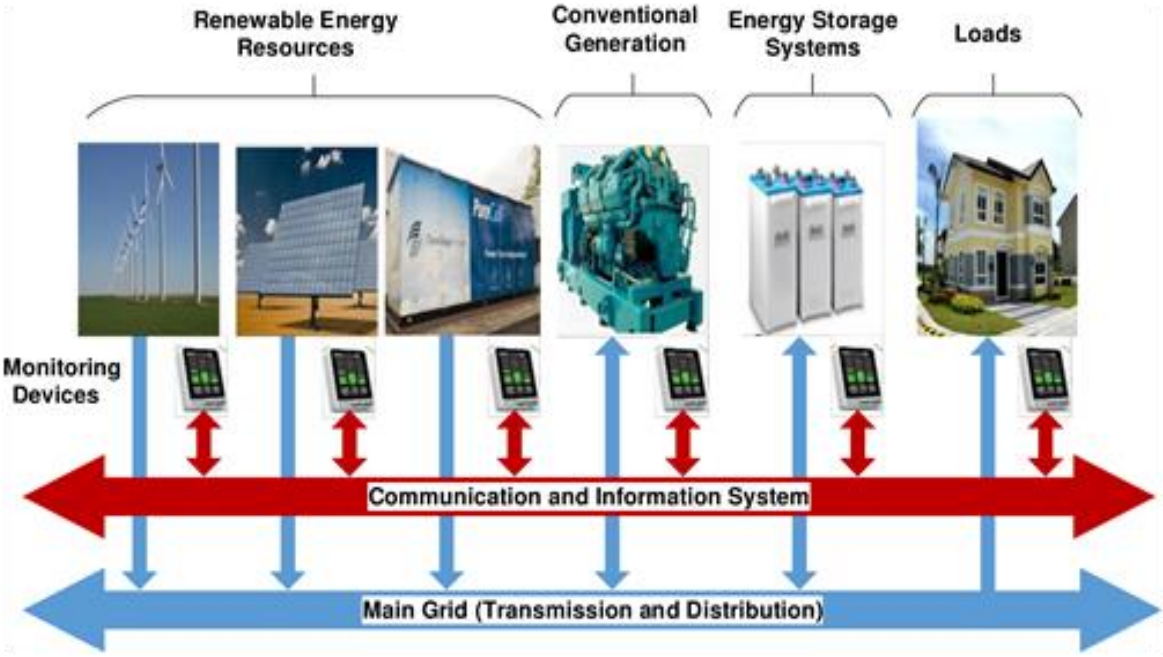

Fig.3. Micro-grid infrastructure [12]

A. Photovoltaic (PV) Panels:

Solar cells generate renewable energy from solar radiation and they consist of glass, metals, polymers and a semiconductor. Faults associated with PV panels include module and cell faults. PV panel failures mainly causes gradual reduction in output power over time or an overall reduction in power due to failure of an individual solar cell in the module.

Module faults [13] include open circuits, short circuits, fractured glass and delamination. Open circuit typically occur in bus wiring and between junction boxes that tie PV panels. Often, manufacturing, transportation and installation defects, and insulation degradation with weather, result in open or short circuits, delamination, cracking or electrochemical corrosion. Short circuits also can occur when panels face severe weather, such as wind, hail, snow, sand, salt, dust and humidity. The top of PV panels is glass, thus exposing it to the outside may shatter it due to

vandalism, thermal stress, handling, wind or hail. Delamination results from the loss of adhesion between the encapsulant and other front surface material of the modules.

Cell failures consist of solar cell degradation, short and open circuited cells, interconnect open circuits and hot spot failure. Solar cell degradation is the most significant one. Degradation of PV cells, modules and panels can be caused by [14]:

1. Front surface soiling: dirty shading the surface of the cells; Impurities on the surface will lead to partial shading of the cell;
2. Optical degradation of the encapsulation material: When exposed to UV-light, temperature changes, or humidity, the encapsulating material of the cell can discolorate;
3. Increase in the cells' series resistance: cells are exposed to the outside environment with variation in temperature and irradiation over time, which lead to an increase of the series resistance. Although series resistance is low by design, it can originate from resistances in the solder bonds, emitter and base regions, cell metallization, and others;
4. Decrease in the cell shunt resistance: crystal damage and impurities in and near the inter junction may cause this decrease. While exposing to light for a longer time, the total number of shunts can increase. With a large number of shunts, the shunt current increases and resistance decreases;
5. Degradation of the cells' anti-reflection coating: This occurs when the PV cells are used for a long time and reduces the efficiency of the cells since less photons are absorbed for power generation;

6. Mismatch of cells: This often occurs when cells are connected in series. If a cell is partially shaded, it can be forced by the other cells to operate in the negative voltage region where it dissipates power instead of producing it. Cell mismatch in general leads to heating of the cells, which in turn can accelerate degradation of this and other cells;
7. Temperature and light induced degradation: With high temperature, the bandgap of the cells will decrease, which will allow the cells to absorb more photons but decrease the open circuit voltage (V_{oc}).

Short circuited cells occur across the cell's inner connections, which is a common failure mode since top and rear contacts are much closer together with each other and more chance of being shorted together by impurities. Open circuited cells mainly occur due to corrosion and result in an increased resistance of the cell. Cell cracking can be caused by thermal stress and hail. Cyclic thermal stress and wind loading lead to interconnect open circuit failures. Hot-spot failures happen when the operating current of the cell is too large. By-pass diode failure operation is mainly due to overheating.

In the grid connected mode, the reliability of PV inverters is important. Failure of a PV inverter may affect the PV array, the power conversion efficiency, and the amount of power going into the micro-grid. Two main fault types are open-circuit and short-circuit faults in inverter components. They can occur in the switch, MOSTETs, IGBTs and other components. Degradation faults in DC link capacitors are also common in central micro-inverters [15].

B. Diesel and Gas Generators:

Diesel and gas generators can be used as alternative power sources on a micro-grid in the event of a power grid failure. They use a diesel or gas engine which spins the shaft of the electric generator. Very little research has been reported on the types of failures for the whole diesel or gas generator as a system, however the diesel engine and electric generator failures have been widely considered.

Diesel and gas engines are subject to fuel leakage, bearing failures, and cracked crankshaft failures. A cracked crankshaft is caused by corrosion or poor assembly and can lead to an inability to generate rotational energy [16]. Fuel leakage causes a decrease in fuel pressure leading to a reduction in the combustion efficiency [17]. Bearing faults are caused by fatigue and metal-to-metal contact and occur in a similar fashion to that of the wind turbine generator bearing faults.

Electric generator failures consist of rotor and stator failures. Stator may fail due to single or multiple phase short circuit, inter-turn short circuit [18], saturation, stator winding ground, and air gap eccentricity [19]. The open or short circuits lead to internal asymmetry which causes extremely high currents in windings thus leading to the degradation of other parts in stator. Inter-turn short circuits are caused by the combination of thermal, electrical, mechanical and environmental stresses. The main effects of stator faults are unbalanced air gap voltage and line currents, disturbances in the current voltage and flux waveforms, increased losses and reduction in efficiency and excessive heating. Rotor failures consist of inter-turn and inter-slot short and open circuit, rotor ground, air gap eccentricity, rotor windings and bending failure. Rotor ground

faults can have several reasons: weakness in the original design, a problem in phases, or the ageing problem. These cause unbalanced air-gap fluxes and line currents, excessive heating, disturbances in the current, voltage and flux waveforms at last reductions of efficiency. Air eccentricity is caused by the formation of different air gap thicknesses between the stator and rotor. In general, two types of air-gap eccentricity faults exist: static and dynamic air-gap eccentricity. Static eccentricity can be caused by stator or rotor positioning incorrectly and oval stator cores. A cause of dynamic eccentricity can be a bent shaft, bearing wear and movement, misalignment of bearings, or mechanical resonances at critical speeds.

C. Fuel Cells:

Proton Exchange Membrane (PEM) fuel cells are the most common type of fuel cells, that generate clean electric power from the chemical energy emitted from the reaction of hydrogen and oxygen. They consist of the membrane, electro-catalyst, catalyst, and gas diffusion layers which are subject to degradation faults [20]. These layers fail due to mechanical, thermal and chemical degradations. Mechanical degradations cause perforations due to improper membrane electrode assembly and humidity cycling. Thermal degradations are caused by a change in hydrations, flooding, and dehydration [21], due to operating at temperatures beyond the rated operating range. Chemical degradations are formed by the presence of foreign cationic ions due to combustion between hydrogen and oxygen. Other failure modes include degradations in the bipolar plate and sealing gasket. Bipolar plate degradation is caused by corrosion and generally leads to a drop in the output voltage. Sealing gasket degradation is caused by force retention

compression loss leading to plate electrical shorting. Fuel cells require compressors to supply air throughout the cell. Compressors also tend to degrade and lock up resulting in a reduced or loss of air flow through the cell [22]. These typically occur due to increased friction in the compressor motor and overheating. In general, fuel cell faults lead to a reduction in generation efficiency, and reduction or loss of output power.

D. Wind turbines:

Wind turbines are subject to failures in the following systems: 1) Gearbox and bearing, 2) Generator, 3) Power electronics and controls, and 4) Rotors, blades and hydraulic controls [23].

Gearbox and bearing faults are the leading causes of wind turbine failures due to mechanical stresses and environmental conditions [24]. Repairing or replacing a damaged gearbox is a difficult and time consuming process which causes significant downtime. Gearbox failures are mainly caused by lack of lubrication, wear of materials, and failures of bearings. Bearing faults typically consist of inner/outer race and ball faults and occur due to abrasive wear, corrosion, lack of lubrication, and accumulation of debris contaminates [25].

Generator failures are caused by bearing, stator, rotor and air gap faults and lead to unbalanced harmonics, reduction in efficiency, decreased average torque, and excessive heating of the windings. Most wind turbines use the induction generators. Faults in the induction generator may produce unbalanced stator voltages and currents, decreased average torque, excessive heating, and low efficiency [26-27].

Power electronics and electric control failures occur due to semiconductor device faults

which include short and open circuits, gate drive circuit faults, and wiring damages. Rotors and blades fail due to corrosion, mechanical damages, and manufacturing defects. Corrosion leads to cracked rotors while mechanical damages caused by ice, lighting, insects, etc. can lead to roughness on the blades' surface causing a loss in efficiency and change in stiffness. Hydraulic control failures cause a reduction of fluid due to air contamination resulting in a leak causing failures in the rotor blades and bearings [28-29].

E. Cables and Transmission Lines

Power cables are essential interconnections between distributed generation and loads in a micro-grid, but distribution-level transmission lines may also be used. Power cables are typically installed underground while transmission lines are installed overhead. Underground cables are subjected to mechanical faults and usual wear and tear, while overhead lines are exposed to natural events that can cause faults such as due to lighting strikes, icing, short circuits, overloading, equipment failures, aging, animal/tree contact, human actions, lack of maintenance, etc. [30]. Three most common types of faults include: i) single line-to-ground, ii) three-phase–to -ground, and iii) line-to-line. The first two occur due to one or three phase(s) short circuiting to ground by physical contact. Line-to-line faults occur due to a short circuit between two phases and are commonly caused by broken insulation or loose connection

F. Transformers

Transformers are electrical components that can be used for energy transfer by electromagnetic induction between two circuits. The faults in transformers can be very dangerous.

The common causes of transformer failures are lighting surges, line surges or external short circuit, poor workmanship-manufacturer, deterioration of insulation, overloading, moisture, inadequate maintenance, sabotage, malicious mischief, and loose connection.

A transformer mainly has the following subcomponents: core, winding, tank, bushing, tap changer, and cooling system. DC magnetization or displacement of the core steel during the construction can cause the core failure. It will reduce the transformer's efficiency. A fault in the winding can occur due to material faults in the cellulose isolation, construction fault, transient overvoltage, and movement of transformer. Careless handing/move, high pressure due to gas generation, and corrosion may cause the tank failure. The main failure mode of the bushing is short circuit. Old capacitors in the motor cause the tap changer fail to control its movement direction. The motor in the tap changer can breakdown because of over voltage. Cooling system will reduce the heat produced in transformers due to copper and iron losses. The failures in the cooling system may increase the heat in the transformer which can affect different parts of the transformer [31-32].

G. Switchgears

Switchgears are electrical devices that include electrical switches, fuses or circuit breakers. They are used to control, protect, and isolate electrical equipment. Failures of switchgear can cause serious injury and damage.

Loose connection is one of the switchgear failures causes, loose and faulty connections can cause an increase of resistance at that localized point. The increased resistance causes increased

heat and will escalate until complete thermal failure of the connection occurs. Insulation breakdowns are likely to occur in jumper cables, bus, and cable terminations. Water immersion due to natural disasters or accidents can lead to instant short circuits, long term insulation damage, and long term metallic component corrosion [33]. The breaker racking may also cause serious injury or damage. A defective ground fault protective device will not offer protection from the ground fault and will cause failures of the switchgear.

H. Inverters and Converters

The reliability of power electronic inverters and converters is a major concern in power system because of their high failure rates. Faults are likely to occur in each of the subcomponents in a converter or inverter during operation, such as MOSFET, rectifier diode, inverter diode, reactor, and capacitor or inductor. Each component can develop two main types of faults: open circuit and short circuit.

Three main causes of the failures are capacitor wear, overuse and over/under voltage. Inverter and converter rely on capacitor to provide smooth output power at different levels of current. The failure in capacitor itself can be a cause of inverter /converter failure. Over using the inverter/converter beyond their operation limit can contribute to their failures. If the current or voltage increases to a higher level than the rated inverter/converter threshold value, it can also cause damage to the components.

Thermal stresses, overload transients, extreme ambient temperature, moisture, and mechanical vibration are the other causes of the converter and inverter failures. The failures in

the converter and inverter can produce a very high transient, an over voltage stress or a rapid voltage decreasing [34].

Table I summarizes major failure modes, causes, and effects of major micro-grid components.

TABLE 1. FAILURE MODES AND EFFECTS OF THE ELECTRICAL ENERGY INFRASTRUCTURE OF MAJOR COMPONENTS IN MICRO-GRIDS

Component	Sub-component	Failure Mode	Cause	Effect
PV Panel	Cell	• Degradation • Short/Open circuit cell • Interconnect open circuit cell • Hot spots	• Over exposer • Decrease in cell shunt resistance • Debris accumulation on the surface • Mismatched cells • Overheating	• Loss/reduction of output power • Decrease in voltage and current waveforms
	Module	• Open/Short circuits • Glass fracture • Delamination	• Manufacturing defects, mechanical loads, corrosion • Natural occurrences • Degradation of cells anti-reflection coating • Overheating	
	By-Pass Diode	• Open/Short circuit	• Overheating	

Component	Sub-component	Failure Mode	Cause	Effect
Diesel and Gas Generators	Stator and Rotor	• Single/Multi-phase • Short circuit • Inter-turn short circuit • Air-gaps • Grounding • Bending/broken rotor • Demagnetization	• Insulation damage leading to winding interconnections • Reduction of lubrication • Manufacturing defects • Overheating	• Phase shift • Unbalanced voltage and current waveforms • Reduction in efficiency • Decreased gas pressure and combustion efficiency • Increased vibration • Decreased efficiency
	Fuel line	Leaking	• Holes/air contamination	
	Bearings	• Inner race • Outer race • Ball	• Vibration, High speeds • Wear, mechanical loads &contamination • Electric arcing • Lack of lubrication • Misalignment	
	Crankshaft	• Cracked crankshaft	• Fatigue • Corrosion • Manufacture defects	

Component	Sub-component	Failure Mode	Cause	Effect
Fuel cell	Membrane, Electrocatalyst, and gas diffusion layers	• Mechanical degradation • Thermal degradation • Chemical degradation	• Perforation, cracks, tears, or pinholes • Humidity cycling • Flooding/drying	• Reduction in efficiency • Loss of output power • Decrease in voltage and current waveforms
	Bipolar Plate	• Loss of conductivity	• Corrosion	
	Sealing Gasket	• Mechanical failure		
	Compressor	• Degradation	• Increased friction	
	Motor	• Locked	• Overheating	

Component	Sub-component	Failure Mode	Cause	Effect
Wind Turbine	Gearbox	• Bearing-inner/outer race and ball faults	Corrosion and contamination	• Unbalanced voltage and current waveforms • Reduction in efficiency • Decreased torque • Phase shift • Increased vibration
	Generator	• Bearing • Stator inter turn short circuit • Cracked rotor • Air gaps • Demagnetization	• Corrosion, contamination, manufacturing defects • Overheating • Reduction of fluid • Insulation damage	
	Power electronics and electric control	• Semiconductor short/open circuit	• Over voltage of components • Manufacturing defects	
	Blades	• Degradation	• Corrosion • Change in stiffness	
	Hydraulic control	• Fuel leak	• Air contamination and mechanical defects	
Cable and Transmission Lines		• Single line to ground • Double line to ground • Line to line	• Physical contact between one/two phases with ground/animal/tree • Broken insulators • Natural events • Overloading	• Introduces fault currents leading to tripped breaker, shutting off power flow
Transformer	Winding	• Wind failure • Dielectric faults	• Copper line resistance thermal losses • DC magnetization • Loosening of conductors • Sealing breaking	• Reduce the transformer's efficiency • Loss of output power • Black out of power
	Core	• Mechanical failure		
	Tank	• Shaft connection		
	Bushing	• Loosen of conductors • Sealing breaking		

Component	Sub-component	Failure Mode	Cause	Effect
Switchgear		• Thermal failure • Overstressed • Short circuit	• Loose connection • Water intrusion or immersion • Jumper cables and cable terminations insulation breakdown • Partial discharge activity	• Burning oil and gas clouds • Explosion
Inverter and converter	MOSFET	• Open circuit • Short circuit	• Electro-mechanical wear on capacitors • Overuse • Over and under voltage • Ultrasonic vibrations	• Reduce the efficiency • Loss of output power
	Rectifier diode			
	Inverter diode			
	Reactor			
	Capacitor/ inductor			

2.2 Review of Major Reliability Modeling and Analysis Methods for Micro-grid Systems

"Reliability is the ability of an item to perform a required function, under given environment and operational conditions and for a stated period of time" (ISO8402). Power system reliability is critical for system design and maintenance and can give system designers, operators, and customers potential failure modes of the subsystems and components.

Main reliability modeling methods include Failure Modes, Effect and Criticality Analysis (FMECA or FMEA), Cause and Effect Diagrams (CEDs), Bayesian Belief Networks (BBNs), Event Tree Analysis (ETA), Probabilistic Risk Assessment (PRA), Stochastic Petri Nets (SPNs), Fault Tree Analysis (FTA), Markov Reliability Modeling (MRM) and Reliability Block Diagrams (RBD). FMECA is an inductive bottom-up method to identify potential failure modes and study effects of failures by focusing on components in a system and examining how fault

modes of each component [35]. CED is used as a quality analysis method to find potential causes for system failures where causes are arranged based on their importance [36]. BBN uses probability distribution allocated to the causal factors to evaluate a network's performance quantitatively [37]. ETA is an inductive technique that examines an initiating event and its possible deviation then explores how this deviation may develop [38]. FTA is a top-down deductive failure analysis approach commonly used to determine root causes of failures where failures and their modes are connected with logic gates and binary numbers [39]. ETA and FTA focus on opposite sides of an undesired event where ETA focuses on the consequences after the event while FTA focuses on causes leading to that event. PRA is based on three basic questions: what parts can fail, what are the detriments, and what are the possibilities that these undesirable events happen [10]? SPN is a dynamic reliability analysis tool used to describe the relations between events and conditions [41]. RBD is another method for studying reliability and can be implemented in parallel with any physical block diagram [42]. MRM is focused on probabilistic transitions between healthy, intermediate, and failed states of a system. Approaches discussed in this thesis are RBD, FTA, and MRM due to their common application and easy implementation in electrical energy systems. Details of these three methods will be introduced in 2.2.2-2.2.4

2.2.1 Quantitative Measures for Reliability [5]

A. Time to Failure

We assume that the time to failure T is continuously distributed with probability density function $f(t)$. Distribution function $F(t)$ denotes the probability that the item fails within the time interval (0, t].

$$F(t) = \Pr(\ T \le t) = \int_0^t \ f(u)du \tag{2.1}$$

B. Reliability Function

Reliability is the probability that the system survives at a time *T*>t. The reliability function of an item is defined by

$$R(\ t) = \ 1 - \ F\ (t\ ) \tag{2.2}$$

R(t) is the probability that the item does not fail in the time interval (0, t].

C. Failure Rate Function

The probability that an item will fail in the time interval (*t, t + Δt*] when we know that the item is functioning at time *t* is

$$\Pr(\ t < T \le t + \Delta t) = \ \frac{\Pr(\ t < T \le t + \Delta t)}{\Pr(\ T > t)} = \ \frac{F(\ t + \Delta t) - F(\ t)}{R(\ t)} \tag{2.3}$$

D. Mean Time to Failure

The time elapsing from when the item is put into operation until it fails for the first time is called the time to failure. The mean time to failure of an item is defined by

$$MTTF = \int_0^\infty R(t)dt \tag{2.4}$$

E. The Exponential Distribution

If an item that is put into operation at time *t* = 0, the time to failure *T* of the item has a probability density function

$$f(t) = \begin{cases} \lambda e^{-\lambda t} & for\ t > 0\ ,\lambda > \ 0 \\ 0 & otherwise \end{cases} \tag{2.5}$$

This distribution is called the exponential distribution with parameter λ and the reliability

function of the item and MTTF are

$$R(t) = \Pr(T > t) = \int_t^{\infty} f(u)\,\mathrm{d}u = e^{-\lambda t} \tag{2.6}$$

$$MTTF = \int_0^{\infty} R(t)dt = \int_0^{\infty} e^{-\lambda t}dt = \frac{1}{\lambda} \tag{2.7}$$

Note that, in the thesis, all the failure distributions are assumed to have exponential distributions.

2.2.2 Reliability Block Diagram (RBD) Method

RBD is a system-level reliability analysis method and can be implemented in parallel with an electrical or other physical layouts or block diagrams by considering the function of each component or subsystem. RBD simplifies the reliability modeling process since the order of fault occurrence does not affect the model and thus eliminates exponential growth in system states which could occur when considering fault occurrence sequences. RBDs are suitable for systems of non-repairable components and where the order of the failures does not matter. Engineers can easily construct, modify, and verify the RBD based on the construction of the system. There are series structures, parallel structures and *k*-out-of-*n* structures in RBDs. A series connection is joined by one path from the "in" node to the "out" node, a parallel connection is joined by multiple paths, and *k*-out –of –*n* is functioning if at least *k* of *n* components are functioning or healthy. Fig. 4 shows a simple RBD of a system of three components (A, B, and C), and multiple paths from the "In" point to the "Out" point.

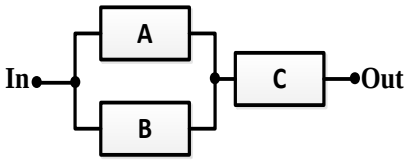

Fig.4. A simple RBD example

Consider a non-repairable system with n series independent components with failure rates λ_i, for i=1, . . . , n , then equations (2.8) and (2.9) show the $R(t)$ and MTTF expressions, while for parallel components, (2.10) and (2.11) are shown. Therefore for Fig. 4, if λ_1 is the failure rate of "a", λ_2 is the failure rate of "b", and λ_3 is the failure rate of "c", $R(t)$ and MTTF of the diagram in Fig. 4 become (2.12) and (2.13).

$$R(t) = e^{-\sum_{i=1}^{n}\lambda_i t} \tag{2.8}$$

$$MTTF = \frac{1}{\sum_{i=1}^{n}\lambda_i} \tag{2.9}$$

$$R(t) = 1 - \prod_{i=1}^{n}(1 - e^{-\lambda_i t}) \tag{2.10}$$

$$MTTF = \frac{1}{\lambda}\sum_{x=1}^{n}\binom{n}{x}\frac{(-1)^{x+1}}{x} \tag{2.11}$$

$$R(t) = e^{-(\lambda_1+\lambda_3)t} + e^{-(\lambda_2+\lambda_3)t} - e^{-(\lambda_1+\lambda_2+\lambda_3)t} \tag{2.12}$$

$$MTTF = \frac{1}{\lambda_1+\lambda_3} + \frac{1}{\lambda_2+\lambda_3} - \frac{1}{\lambda_1+\lambda_2+\lambda_3} \tag{2.13}$$

2.2.3 Fault Tree Analysis (FTA) Method

FTA explicitly shows all different failure modes that are necessary to result in the top event and constructing the fault tree gives a thorough understanding of the logic and basic causes leading to the top event. FTA can give a qualitative and quantitative evaluation of system. Fig.5

shows the fault tree with “AND” gates, “OR” gates, and events of the diagram in Fig.4. An advantage of FTA is that when accurate failure rates are difficult to acquire for a quantitative analysis, qualitative analysis can be achieved using the structure importance coefficient of components or subsystems. The structure importance coefficient is $I_{\Phi(i)}$ calculated as

$$I_{\Phi(i)} = 1 - \prod_{X_i \in K_j} \left(1 - \frac{1}{2^{N_j - 1}}\right) \tag{2.14}$$

where K_j is the cut-set, $N_j\,(j \in K_j)$ is the number of basic events in the cut-set which includes the basic event i; and $X_i \in K_j$ is the basic event i which belongs to the cut set. One important concept used in FTA is the cut-set: It is a list of basic events such that if they occur then the top event occurs. Two other common methods used in FTA are Fuzzy Fault Tree Analysis (FFTA) and Monte Carlo Simulation (MCS).

In order to overcome the limitation of the failure probability or relationship between events, fuzzy numbers are used to describe the probability of an event to occur. FTA-MCS can combine the practical experience from engineering and technical personnel of the practical experience to construct fuzzy membership functions. The common used fuzzy numbers are the triangular fuzzy number, the trapezoidal fuzzy number, the cusp fuzzy number and the normal fuzzy number.

However, in complex power systems, the use of FTA increases in complexity with a large number of basic components and logic gates. MCS is thus a powerful tool to evaluate the reliability of a system by generating random values of uncertain variables and scanning the fault tree thousands of times to get more accurate results. While MCS is computationally intensive, it can accurately predict fault propagation in a fault tree and thus evaluate a system’s reliability. To

apply the MCS to a fault tree, Monte Carlo random sampling is applied, typically in software such as MATLAB, through a random number between 0 and 1 to obtain the failure time of each basic component.

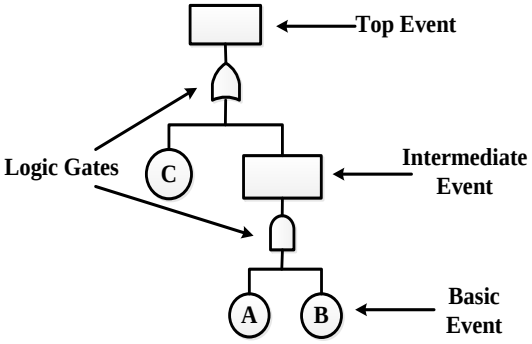

Fig.5. A simple fault tree diagram example

2.2.4 Markov Reliability Modeling (MRM) Method

MRM uses a stochastic process to model the system with several states and transitions between states. A Markov reliability model contains a series of the possible states in the system and uses possible failure rates and repair rates between those states. If $X(t)$ is denoted as a random variable in Markov process, then P_{ij} of transitioning probability from state "i" at t=0 to state "j" at t is P_{ij}=P[X(t)=j |X(0)=i]. The probability of transitioning from state "i" to state "j" does not depend on the global time and only depends on the transition time interval. A simple Markov process for Fig.4 is shown in Fig. 6. The states in Fig. 6 (a) show transition from state 0 which is the healthy state to state 1 when component A fails but the system survives, state 2 when component B fails but the system survives, and state 3 when component C fails and the system fails since component C ties the rest of the system to the output. Staying at a state means that no new fault even happened. State 3 is an absorbing state of system failure since every

physical system is expected to fail at some point in time. Fig. 6 (b) shows failure rates λ and recovery rates μ. Equations (2.15) and (2.16) show the probability of transitioning between different states and the state transition matrix, respectively.

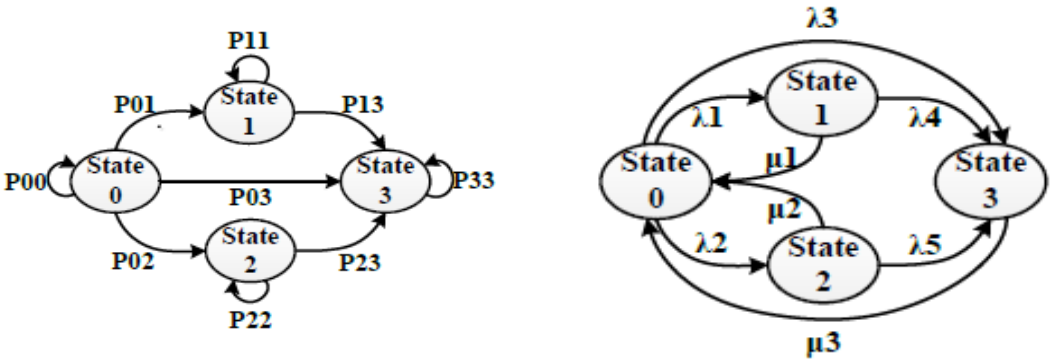

(a) (b)

Fig.6. Markov-based state diagram using MRA for the system in Fig. 4

$$P = \begin{bmatrix} p_{00} & p_{01} & p_{02} & p_{03} \\ 0 & p_{11} & 0 & p_{13} \\ 0 & 0 & p_{22} & p_{23} \\ 0 & 0 & 0 & p_{33} \end{bmatrix} \tag{2.15}$$

$$A = \begin{bmatrix} -\lambda_1 - \lambda_2 - \lambda_3 & \lambda_1 & \lambda_2 & \lambda_3 \\ \mu_1 & -\mu_1 - \lambda_4 & 0 & \lambda_4 \\ \mu_2 & 0 & -\mu_2 - \lambda_5 & \lambda_5 \\ \mu_3 & 0 & 0 & -\mu_3 \end{bmatrix} \tag{2.16}$$

MRM can be simulated based on the failure rates of components and the system state transition matrix. But this method is suitable for small size systems since it is hard to get higher dimension matrices and the corresponding derivation for all the possible states. Take the three component system as an example; to implement this method, all the possible states of the three components in Fig.4 and Fig.5 need to be known, as shown in Table 2. Details of this method can be found in Section 4.3.

TABLE 2 SYSTEM STATES AND RELIABILITY

	A $R(1)$	B $R(2)$	C $R(3)$	System State	Probability of the state at time t
0	Success	Success	Success	Success	$P_{00}(t) = R_1(t) \times R_2(t) \times R_3(t)$
1	Success	Success	Failure	Failure	$P_{01}(t) = R_1(t) \times R_2(t) \times (1 - R_3(t))$
2	Success	Failure	Success	Success	$P_{02}(t) = R_1(t) \times (1 - R_2(t)) \times R_3(t)$
3	Failure	Success	Success	Success	$P_{03}(t) = (1 - R_1(t)) \times R_2(t) \times R_3(t)$
4	Success	Failure	Failure	Failure	$P_{04}(t) = R_1(t) \times (1 - R_2(t)) \times (1 - R_3(t))$
5	Failure	Success	Failure	Failure	$P_{05}(t) = (1 - R_1(t)) \times R_2(t) \times (1 - R_3(t))$
6	Failure	Failure	Success	Failure	$P_{06}(t) = (1 - R_1(t)) \times (1 - R_2(t)) \times R_3(t)$
7	Failure	Failure	Failure	Failure	$P_{07}(t) = (1 - R_1(t)) \times (1 - R_2(t) \times (1 - R_3(t))$

III. MICRO-GRID CASE STUDIES

Micro-grids are becoming of more interest worldwide to achieve reliable electrical energy infrastructure during natural hazards and catastrophic situations due to their ability to operate in either grid-connected or islanded modes. They typically include distributed generation resources that could provide heat and electricity. Three case studies are considered to illustrate the proposed reliability modeling and analysis methods. The first case study is a micro-grid system at University of Connecticut which has a synchronous interconnection and significant clean energy penetration. The second and the third micro-grids are at King's Plaza Mall (KP) and New York University (NYU). The King's Plaza micro-grid utilizes a non-synchronous interconnection strategy using the GridLink technology [43], while the NYU micro-grid has a synchronous interconnection, but with no clean energy penetration and is at a large scale.

3.1 Case Study #1: Micro-grid with significant clean energy penetration at University of Connecticut (UConn)

The micro-grid system under study consists of two photovoltaic (PV) arrays each rated at 3.3 kW, one fuel cell (FC) rated up to 400 kW, two diesel generators (DG) each rated at 150 kW, three buildings with variable loads, interconnecting power electronic converters and transformers, and a point of common coupling (PCC) between the micro-grid and utility as shown in Fig.7. The critical loads can get supply from either micro-grid or utility. An important note is that in this thesis, all the devices are assumed to be of equal operational value to the overall system.

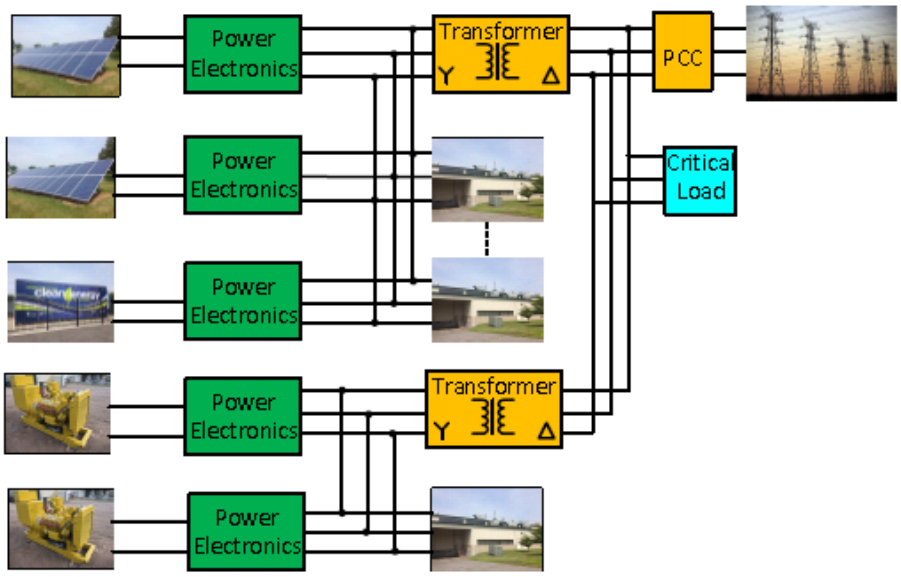

Fig. 7. One line diagram of micro-grid being analyzed for reliability

Three different reliability objectives with different models are using in the first case. RBD, FTA, and MRM were applied to analyze the reliability of the micro-grids shown in Fig. 8. The failure rates shown in Table 3 are estimated from the literature [44-52] and are used here for illustrative purposes. In the calculations and simulations below, the failure rate of the critical load is assumed to be 2.2831×10^{-6} failures/hour or once in 50 years. Since it is difficult to get exact failure rates of all the components in a real system, warranty information is also used to estimate some failure rates. It is important to note that failure rate values can be updated or adjusted but the methodology remains the same.

A. The first objective:

The first objective of the micro-grid is to support a 3.3kW critical load in Fig.8 (a). The critical load is assumed to be at medium voltage in between the utility grid and micro-grid. In the micro-grid system, there always exits a critical load that is expected to receive power at all times.

If the critical load does not receive electrical power, the overall system is assumed to be in a failed state.

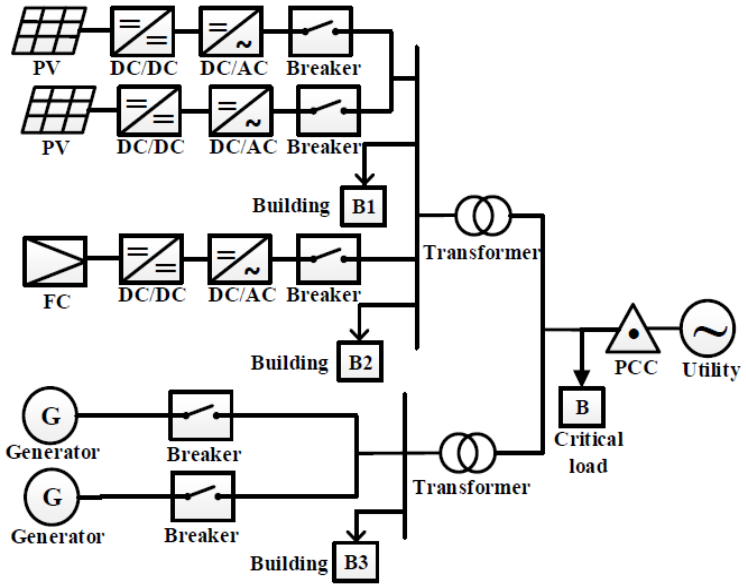

Fig.8 (a). Micro-grid diagram for the first objective: supporting a 3.3kW critical load

B. The second objective:

The second objective of this case is to support a 150kW critical load in Fig.8 (b). Under this situation, PV systems will not affect the overall system reliability due to their low output power. Thus, PV panels and their interconnecting devices and converters are not considered in this case.

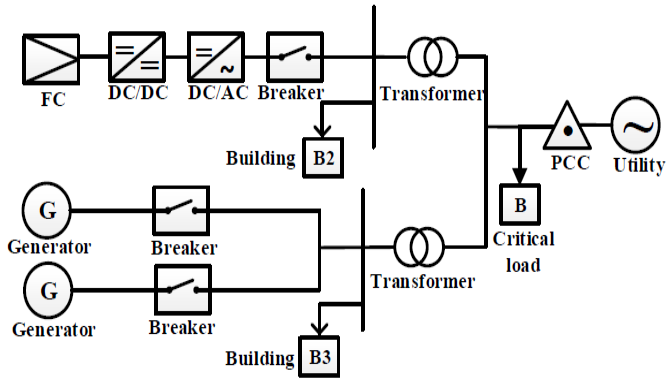

Fig.8 (b). Micro-grid diagram for the second objective: supporting a 150kW critical load

C. The third objective:

The third objective is to support a 400kW critical load in Fig. 8 (c). Here PV and DG are not considered since their low output power compared to the critical load.

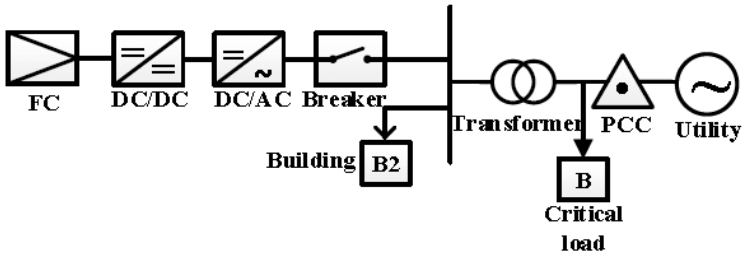

Fig.8 (c). Micro-grid diagram for the third objective: supporting a 400kW critical load

TABLE 3. FAILURE RATES USED TO ESTIMATE THE MICRO-GRID MTTF [44-52]

Component	Failure rate (failures/hour)	Component	Failure rate (failures/hour)
PV Panel	4.5662×10^{-6}	Diesel Generator	11.4155×10^{-6}
DC/DC	14.2694×10^{-6}	Start Generator	11.4155×10^{-6}
DC/AC	14.2694×10^{-6}	Transmission system	2.2831×10^{-6}
Breaker	2.2831×10^{-6}	PCC	2.2831×10^{-6}
Fuel cell	14.2694×10^{-6}	Loads	2.2831×10^{-6}

3.2 Case Study #2: Non-synchronous Micro-grid at King's Plaza (KP)

The one-line diagram of the KP non-synchronous micro-grid is shown in Fig. 9, there are two parallel feeders, each having two transmission parts and one Gridlink (back to back) inverter/rectifier. Four gas engines and two spare diesel generators (not existing in real system) which are distributed generators are in the "Generators" block. Under healthy operating conditions, two feeders support the King's Plaza Mall (load) together while Con-Edison (the utility grid) is available, but when Con-Edison fails, the generators will support the King's Plaza Mall (load) instead. The reliability analysis objective in this study is to support the King's Plaza Mall in Fig. 9.

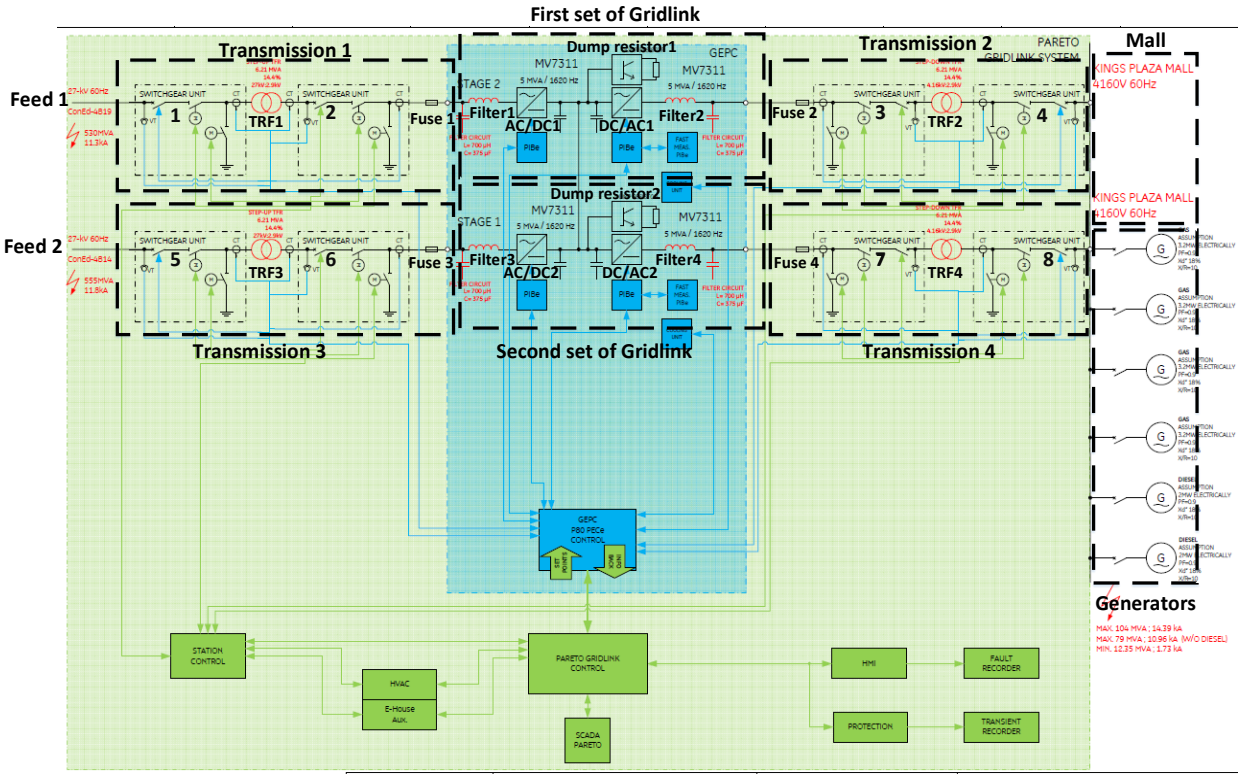

Fig.9. King's Plaza one line diagram

3.3 Case Study #3: Large Synchronous Micro-grid at New York University (NYU)

The NYU micro-grid system is shown in Fig. 10, Central Heating Plant, Silver Tower Garage and Broadway Block Substation NO.3 are assumed to be three critical loads for the sake of illustration and since heating and parking are expected to receive power at all times. If one of the critical loads does not receive electrical power, the overall system is assumed to be in a failed state. Other non-critical loads can be separated by their support buses which are shown in the dotted blocks. Note that Fig. 10 is redrawn from an original one-line diagram to aggregate various other loads based on their critical or non-critical characteristics, or the busses they feed from. The reliability analysis objective in this study is to support the critical loads in Fig. 10.

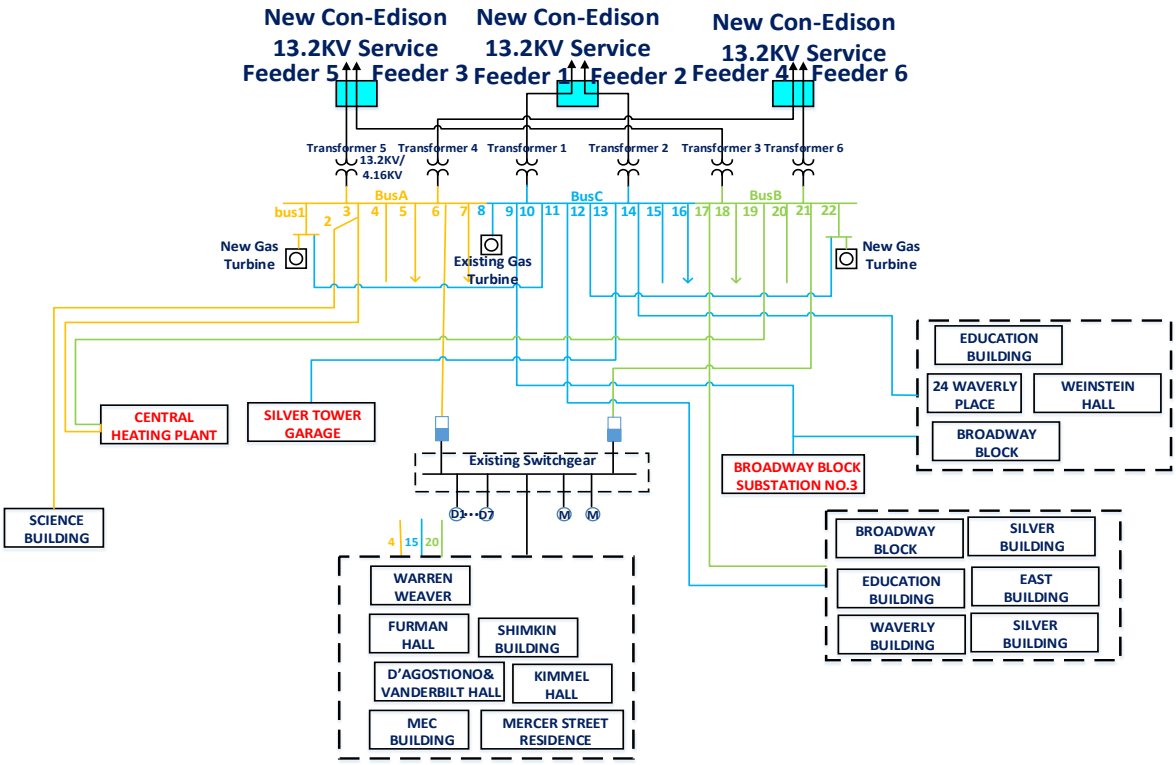

Fig. 10. NYU system one line diagram

IV. RELIABILITY ANALYSIS METHODS APPLIED TO THE FIRST CASE: UCONN MICRO-GRID

4.1 RBD Method for Case #1 UConn Micro-grid System Reliability

The RBDs of the micro-grid shown in Fig. 8 are shown in Fig.11. In Fig.11, λ_{c1}, λ_{c2}, λ_{c3}, are the lumped failure rates of power electronic converters and breakers for two PV arrays, FC and DG branches, λ_{tr} is the failure rate of the transformer and cable. The others are the corresponding failure rates of the components in Figs.8 (a)-(c). The MTTFs of the subsystems in the three dashed rectangles in Fig.11 (a) are calculated in (4.1)-(4.3), where $MTTF_1$ is the MTTF of the two PV array subsystems with PV, DC/DC, DC/AC, and breaker, $MTTF_2$ is the MTTF of the one FC subsystem with FC, DC/DC, DC/AC, and breaker, and $MTTF_3$ is the MTTF of the two DG subsystems with DG and breaker. Since the structure of the FC and DG subsystems are the same with Fig.11 (a), the MTTF in the dashed rectangles in Fig.11s (b) and (c) are not changed. The overall system MTTF of Fig. 11 (a) is calculated in (4.4). Equations (4.5) and (4.6) are the overall micro-grid system MTTF of Fig.11s (b) and (c). MTTFs in (4.4)-(4.6) are similar since the transmission system, the critical load and the PCC have small failure rates compared with the distribute generators. But changing the failure rate of these components gives a different result, especially the failure rate of the critical load.

$$MTTF_1 = 2/\left(\lambda_{c1}+\lambda_{pv}\right) - 1/2\left(\lambda_{c1}+\lambda_{pv}\right) = 4.8387 \ \ years \tag{4.1}$$

$$MTTF_2 = 1/\left(\lambda_{c2}+\lambda_{fc}\right) = 2.020 \ \ years \tag{4.2}$$

$$MTTF_3 = 2/\left(\lambda_{c3}+\lambda_{dg}\right) - 1/2\left(\lambda_{c3}+\lambda_{dg}\right) = 12.50 \ \ years \tag{4.3}$$

$$
\begin{aligned}
MTTF_{all1} &= 1/\left(\lambda_1+\lambda_{load}+\lambda_{tr}\right)+1/\left(\lambda_2+\lambda_{load}+\lambda_{tr}\right)+1/\left(\lambda_3+\lambda_{load}+\lambda_{tr}\right)\\
&+1/\left(\lambda_1+\lambda_2+\lambda_3+\lambda_{load}+2\lambda_{tr}\right)+1/\left(\lambda_1+\lambda_3+\lambda_{load}+\lambda_{pcc}+2\lambda_{tr}\right)\\
&+1/\left(\lambda_2+\lambda_3+\lambda_{load}+\lambda_{pcc}+2\lambda_{tr}\right)-1/\left(\lambda_1+\lambda_2+\lambda_{load}+\lambda_{tr}\right)\\
&-1/\left(\lambda_1+\lambda_{load}+\lambda_{pcc}+\lambda_{tr}\right)-1/\left(\lambda_2+\lambda_{load}+\lambda_{pcc}+\lambda_{tr}\right)-1/\left(\lambda_3+\lambda_{load}+\lambda_{pcc}+\lambda_{tr}\right)\\
&+1/\left(\lambda_{load}+\lambda_{pcc}\right)-1/\left(\lambda_1+\lambda_2+\lambda_3+\lambda_{load}+2\lambda_{tr}+\lambda_{pcc}\right)-1/\left(\lambda_1+\lambda_3+\lambda_{load}+2\lambda_{tr}\right)\\
&-1/\left(\lambda_2+\lambda_3+\lambda_{load}+2\lambda_{tr}\right)+1/\left(\lambda_1+\lambda_2+\lambda_{load}+\lambda_{tr}+\lambda_{pcc}\right)=25.466\ \textit{years}
\end{aligned}
\tag{4.4}
$$

$$
\begin{aligned}
MTTF_{all2} &= 1/\left(\lambda_2+\lambda_{load}+\lambda_{tr}\right)-1/\left(\lambda_2+\lambda_{load}+\lambda_{pcc}+\lambda_{tr}\right)\\
&+1/\left(\lambda_3+\lambda_{load}+\lambda_{tr}\right)+1/\left(\lambda_2+\lambda_3+\lambda_{load}+\lambda_{pcc}+2\lambda_{tr}\right)\\
&-1/\left(\lambda_3+\lambda_{load}+\lambda_{pcc}+\lambda_{tr}\right)+1/\left(\lambda_2+\lambda_3+\lambda_{load}+2\lambda_{tr}\right)=25.213\ \textit{years}
\end{aligned}
\tag{4.5}
$$

$$
MTTF_{all3} = 1/\left(\lambda_2+\lambda_{load}+\lambda_{tr}\right)-1/\left(\lambda_2+\lambda_{load}+\lambda_{pcc}+\lambda_{tr}\right)+1/\left(\lambda_{load}+\lambda_{pcc}\right)=25.0673\ \textit{years} \tag{4.6}
$$

The MTTF of the one PV subsystem (PV-DC/DC-DC/AC-Breaker series connection) is calculated to be 3.2258 years according to Table 3 due to the low assumed reliability of the converter and inverter. So it is important to increase their reliability by implementing more reliable components or refining converter and inverter configurations based on the RBD reliability analysis which is introduced below. The MTTF of the FC subsystem is calculated to be 2.4393 years and the MTTF of one DG subsystem is 8.3334 years.

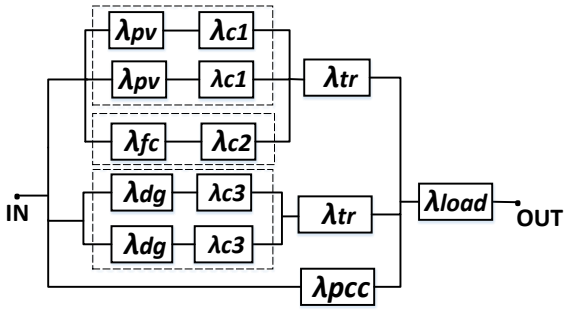

Fig.11 (a). RBD of the micro-grid in Fig.8 (a) where the objective is to support a 3.3kW critical load

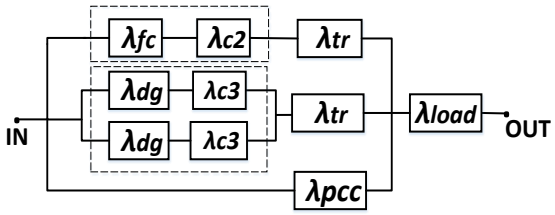

Fig.11 (b). RBD of the micro-grid in Fig.8 (b) where the objective is to support a 150kW critical load

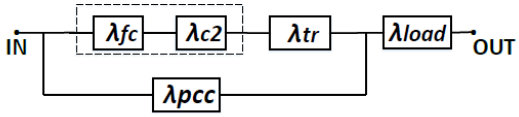

Fig.11 (c). RBD of the micro-grid in Fig.8 (c) where the objective is to support a 400kW critical load

4.2 FTA Method for Case #1 UConn Micro-grid System Reliability

Before building the fault tree, it is necessary to define the FTA reliability objective. In the following case study in this section, the first objective is to support the 3.3 kW critical load, so the fault tree of the micro-grid in Fig.8 (a) is shown in Fig.12 (a), with basic events m_1 to m_{21} defined in Table 4, intermediate events G_1-G_{11}, top event T_{top}, in addition to "AND" and "OR" logic gates. For the PV system, the power electronics block contains a DC/DC converter, a DC/AC inverter, and breaker which are in series with the PV array. Thus, the intermediate event for PV system failure G_1 has an "OR" gate combining m_1, m_2, m_3, and m_4. PV system failure G_1 and G_2 events are in parallel with the FC system failure G_3. We assume that the failure of both PV arrays and the FC is necessary to achieve a failed subsystem G_6. This assumption is to lump clean energy generation on one side of the fault tree while diesel generators are used as a back-up. But other objectives can be used and may result in other different fault trees which are shown in Fig. 12 (b) with the objective of supporting the 150 kW critical load, and in Fig.12 (c) with the objective of supporting

the 400kW critical load.

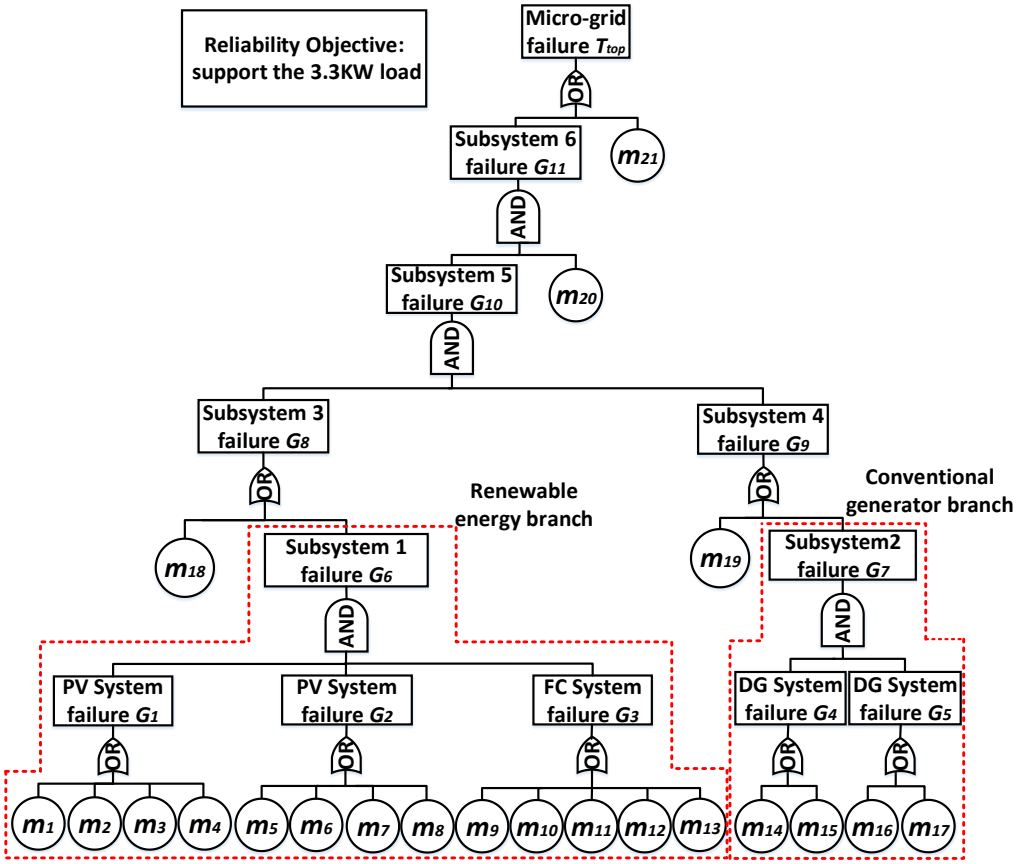

Fig.12 (a). Micro-grid fault tree of the first objective of supporting a 3.3kW critical load

TABLE 4. BASIC EVENTS IN THE MICRO-GRID IN FIG. 12 (A)

Number	Failure	Number	Failure
m_1	PV panel	m_{12}	Start Generator
m_2	DC/DC	m_{13}	Breaker
m_3	DC/AC	m_{14}	Generator
m_4	Breaker	m_{15}	Breaker
m_5	PV panel	m_{16}	Generator
m_6	DC/DC	m_{17}	Breaker
m_7	DC/AC	m_{18}	Transmission
m_8	Breaker	m_{19}	Transmission
m_9	Fuel cell	m_{20}	PCC
m_{10}	DC/DC	m_{21}	Load
m_{11}	DC/AC		

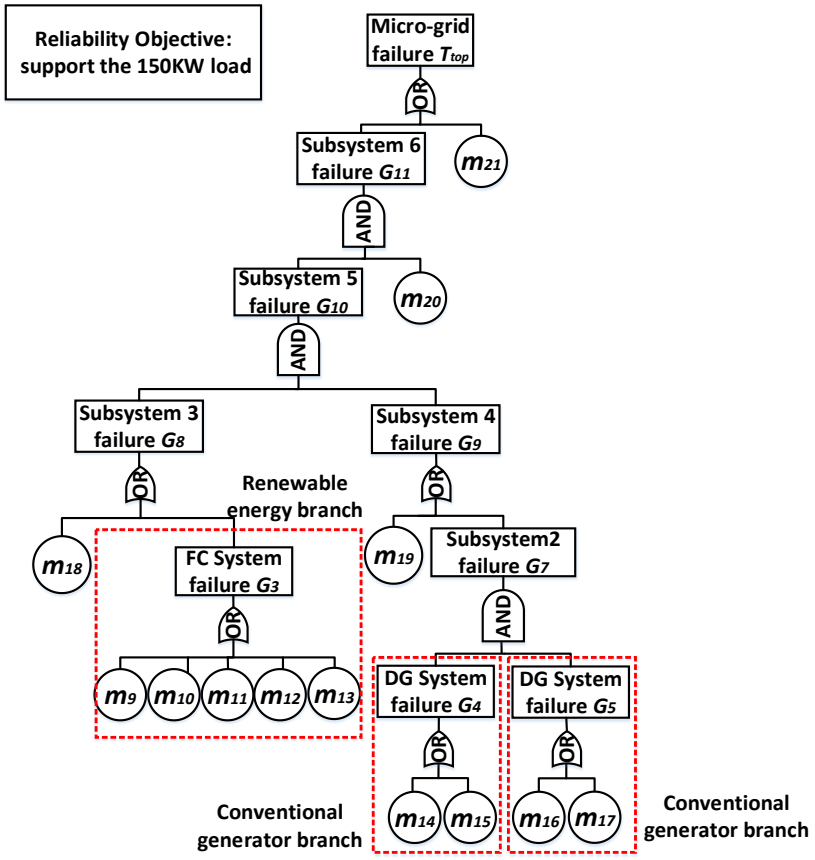

Fig. 12 (b). Micro-grid fault tree of the second objective of supporting a 150kW critical load

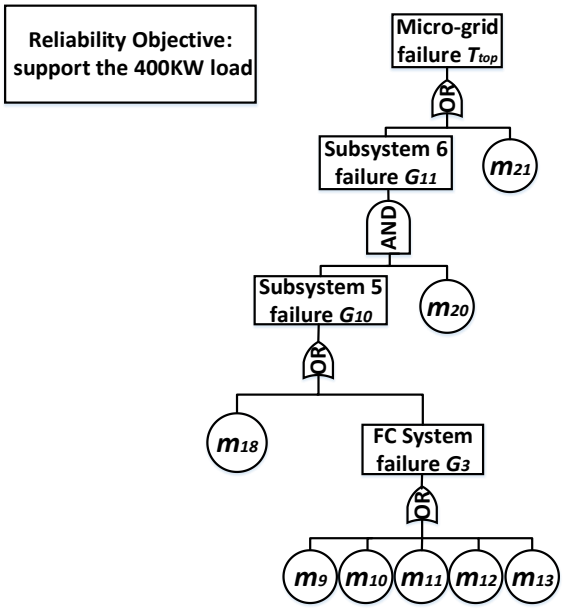

Fig. 12 (c). Micro-grid fault tree of the third objective of supporting a 400kW critical load

4.2.1 Component Importance Coefficient Method

Without component failure rates, based on equation (2.14), the structure importance values of Fig. 12 (a) are calculated as $I(1),\ldots, I(23)$ below. It can be seen that PCC and the critical load are the most critical components in the system with the highest importance value. Therefore, the best way to improve the system is by improving their dependability. The PCC can also be disconnected due to grid-side faults and ensuring that the main grid has less faults that may trip the PCC enhances the micro-grid's reliability to support the critical load. While evaluating the components' importance values can be found and can be a guide to improve the micro-grid's reliability, the lifetime of individual components is not considered in this analysis.

$$I(1)=I(2)=I(3)=I(4)=I(5)=I(6)=I(7)=I(8)=1-(1-\frac{1}{2^{5-1}})^{20}(1-\frac{1}{2^{6-1}})^{80}=0.9783$$

$$I(9)=I(10)=I(11)=I(12)=I(13)=1-(1-\frac{1}{2^{5-1}})^{16}(1-\frac{1}{2^{6-1}})^{64}=0.9533$$

$$I(14)=I(15)=I(16)=I(17)=1-(1-\frac{1}{2^{4-1}})^{2}(1-\frac{1}{2^{6-1}})^{160}=0.9952$$

$$I(18)=1-(1-\frac{1}{2^{3-1}})(1-\frac{1}{2^{4-1}})^{4}=0.5604$$

$$I(19)=1-(1-\frac{1}{2^{3-1}})(1-\frac{1}{2^{5-1}})^{80}=0.9957$$

$$I(20)=1-(1-\frac{1}{2^{3-1}})(1-\frac{1}{2^{4-1}})^{4}(1-\frac{1}{2^{5-1}})^{80}(1-\frac{1}{2^{6-1}})^{320}=0.9999$$

$$I(21)=1-(1-\frac{1}{2^{1-1}})=1$$

The structure importance values of Fig. 12 (b) are calculated as $I(9),\ldots, I(23)$ below.

$$I(9)=I(10)=I(11)=I(12)=I(13)=1-(1-\frac{1}{2^{3-1}})(1-\frac{1}{2^{4-1}})^{4}=0.5604$$

$$I(14)=I(15)=I(16)=I(17)=1-(1-\frac{1}{2^{4-1}})^{12}=0.7986$$

$$I(18)=1-(1-\frac{1}{2^{3-1}})(1-\frac{1}{2^{4-1}})^{4}=0.5604$$

$$I(19)=1-(1-\frac{1}{2^{3-1}})^{6}=0.8220$$

$$I(20)=1-(1-\frac{1}{2^{3-1}})^{6}(1-\frac{1}{2^{4-1}})^{24}=0.9928$$

$$I(21)=1-(1-\frac{1}{2^{1-1}})=1$$

The structure importance values of Fig.12 (c) are calculated below.

$$I(9)=I(10)=I(11)=I(12)=I(13)=I(18)=1-(1-\frac{1}{2^{2-1}})=0.5$$

$$I(20)=1-(1-\frac{1}{2^{2-1}})^{6}=0.9844$$

$$I(21)=1-(1-\frac{1}{2^{1-1}})=1$$

It is clear from importance value result that large critical loads maintain higher dependence on the utility grid where smaller generation becomes less important.

4.2.2 Monte Carlo Simulation Based Fault Tree (FT-MCS) Method

In a complex system, applying the traditional FTA becomes more challenging with a large number of basic components and logic gates. The MCS method is thus a powerful simulation tool to evaluate the reliability of a system by generating random values of uncertain variables and scanning the fault tree thousands of times to get a statistic result. While MCS is computationally intensive, it can accurately predict fault propagation in a fault tree and thus evaluate a system's reliability.

MCS uses statistics to mathematically model a system process in real life and estimate its reliability. To apply MCS to FTA, the Monte Carlo random sampling is applied in MATLAB through a random number η_{ij} between 0 and 1 to obtain the failure time of each basic component. Assuming F is the failure distribution function of the components, during the j^{th} cycle, the occurrence time of event i is $t_{ij}=F^{-1}(\eta_{ij})$. The type of failure distribution function used in the simulation is exponential and the failure rates shown in Table 3 are estimated from datasheets of actual components and the literature.

In the j^{th} cycle, the sampling times for all n components (t_{1j},t_{2j}… t_{nj}) are sorted from the

smallest to the largest (t_{f1},t_{f2}…t_{fn}) and the corresponding basic event order is Z_1,Z_2…Z_n. First, only Z_1 is set to fail then the top event is tested. If it survives, the simulation should continue testing the next basic component Z_2 until the top event fails at t_{fk}. This t_{fk} is the time to failure of the j^{th} cycle. Another important step is recording the failure times of each component by using the time interval method. T_{max} is the maximum simulation time, it is divided into intervals and the number of times during which the system failed due to each component are recorded during each interval. This step can give an importance degree of each component based on the number of times it failed. Detailed simulation steps are shown in the FT-MCS algorithm shown below.

In a fault tree, the "AND" gate structure function should be $\varphi(t) = \prod_{i=a}^{b} x_i$, since the top event after an AND gate is 1 (i.e. $\varphi(t) = 1$) only if all bottom events have occurred (x_i=1). The "OR" gate structure function should be $\varphi(t) = \sum_{i=c}^{d} x_i$, since when only one bottom event occurs, the top event occurs. Below is the FT-MCS algorithm as applied in MATLAB.

FT-MCS Algorithm

(1) Initialize the maximum simulation time T_{max} of the system, simulation interval Δt, failure distribution of each component $F_1(t)$, $F_2(t)$,…, $F_n(t)$, state function (0 or 1) of each component $x_1(t)$, $x_2(t)$,…, $x_n(t)$, simulation cycles W, j=1, top event function $\varphi(t) = \phi(x_1(t), x_2(t), ..., x_n(t))$;

(2) While($j \le W$);

(3) Using Monte-Carlo method to obtain the occurrence time samples of each basic component t_{1j}, t_{2j},…,t_{nj}, $t_{ij}=F^{-1}(\eta_{ij})$ here t_{ij} is the failure occurrence time of the i^{th} basic component. η_{ij} is the random number acquired during the j^{th} sample of event i;

(4) Sort the failure times in increasing values $t_{f1}<t_{f2}<\ldots<t_{fk}<\ldots t_{fn}$;

(5) For k=1 to n;

(6) If $t_{fk}<T_{max}$;

(7) $x_1(t_{fk})=x_2(t_{fk})=\ldots=x_k(t_{fk})=1$, $x_{k+1}(t_{fk})=x_{k+2}(t_{fk})=\ldots=x_n(t_{fk})=0$, calculate the top event $\varphi_k(t_{fk}) = \phi(x_1(t_{fk}), x_2(t_{fk}), ..., x_n(t_{fk}))$;

(8) If $\varphi_k(t_{fk}) = 1$;

(9) Record the failure time t_{fk}, the components which lead to system failure, and the system failure probability distribution;

(10) Else $k=k+1$;

(11) End if;

(12) Else $t_{fk}=T_{max}$, record the failure time t_{fk}, the components which lead to system failure and system failure probability distribution;

(13) End for;

(14) Calculate MTTF, system reliability function, and importance of the basic components;

(15) End while;

Using the MCS method, the PV, FC, and DG subsystems are found to have the reliability

distributions shown in Fig. 13. The curves in Fig. 13 clearly show how the system reliability changes with time and this eliminates the drawbacks of the traditional fault tree method which is static. In Fig. 13 (a), we can see that the reliability of the PV subsystem decreases to being 20% reliable after around 5 year operation. Because of the difference of the components' lifetime, different T_{max} values in simulations are assumed and are shown as the maximum values on the time axes which can be found in Fig. 13. Fig. 14 (a), (b), and (c) show the components' importance degree in each subsystem. From these results we can determine which components are the most critical in the subsystems and the overall system. To improve a subsystem's or system's reliability, the direct way is to improve the reliability of critical components of high importance. Fig. 15 gives the overall micro-grid system reliability function and importance degree of all the components for the first objective to support a 3.3kW critical load. In simulations, the number of iterations W equals to 5000 and based on the components' failure rates used, the system MTTF is found to be 25.683 years. Note that this excludes grid-side faults which can be translated into a significantly higher failure rate of the PCC. Fig .16 and Fig.17 are the results of the second and third objectives with the MTTFs equal to 25.415 and 25.083 years, respectively. Fig.18 shows the comparison of three objectives.

Using the MCS method, MTTF or failure rate values of an overall micro-grid can be approximated as a micro-grid is being designing, and this approximation is based on the micro-grid's component hierarchy. The micro-grid's subsystems, failure rates, and reliability objectives may lead to different final results, but the FTA and FT-MCS can be used for sensitivity

analysis and rough reliability models.

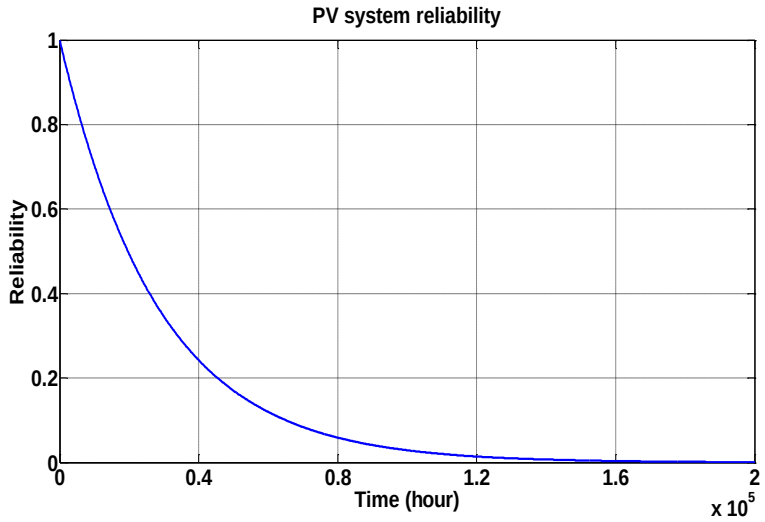

Fig.13 (a). PV subsystem reliability function using a combined PV failure rate of λ_{pv}=35.388x10^{-6} failures/hour

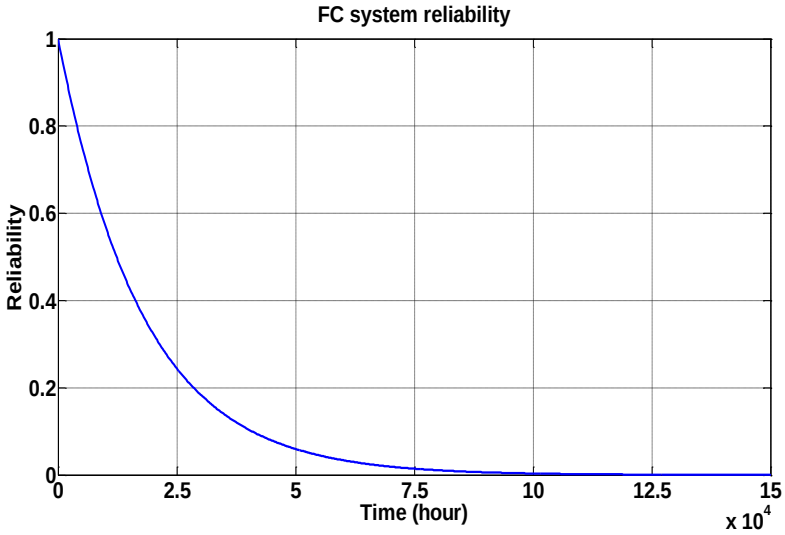

Fig.13 (b). FC subsystem reliability function using a combined FC failure rate of λ_{fc}=46.798x10^{-6} failures/hour

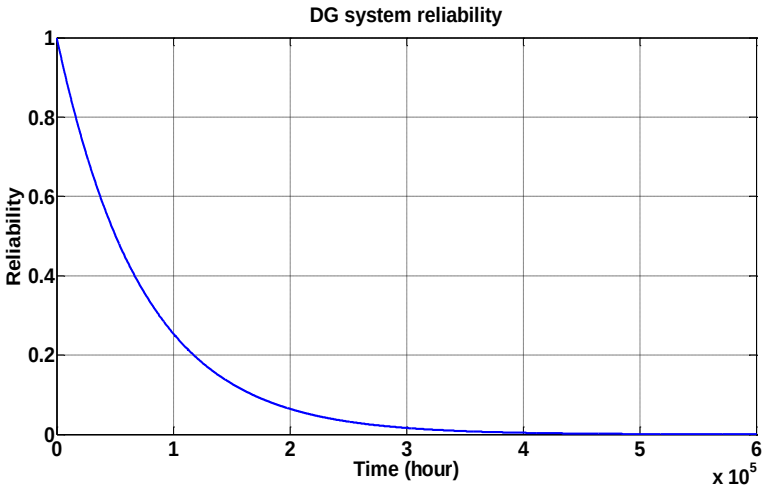

Fig.13 (c). DG subsystem reliability function using a combined DG failure rate of λ_{dg}=13.699x10^{-6} failures/hour

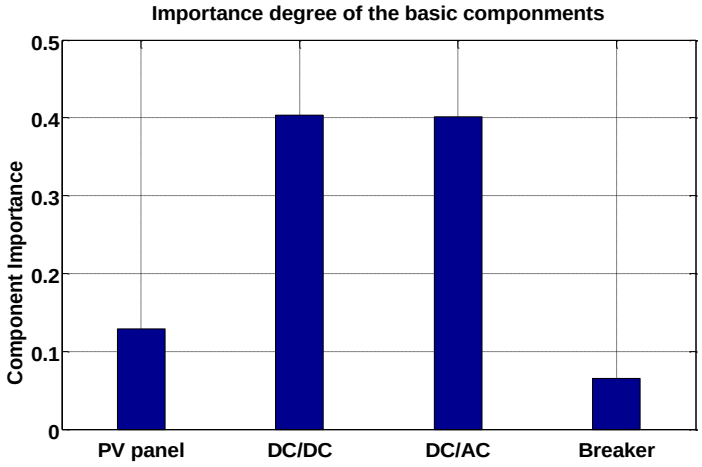

Fig.14 (a). Component importance of PV subsystem

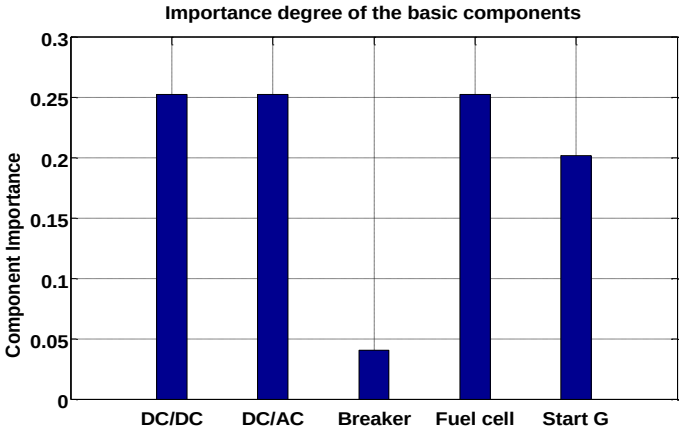

Fig.14 (b). Component importance of FC subsystem

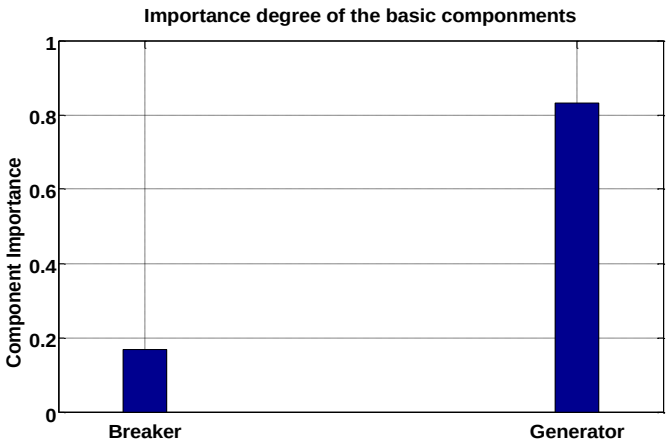

Fig.14 (c). Component importance of DG subsystem

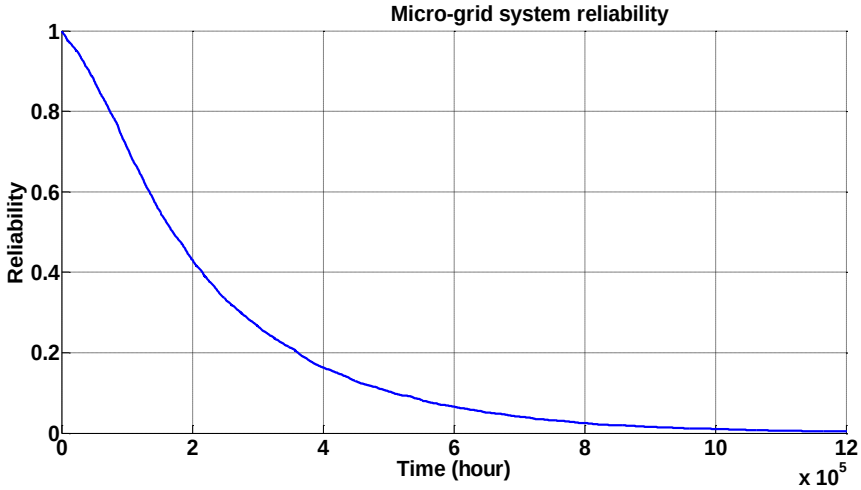

Fig.15 (a). Microgrid system reliability of the first objective to support a 3.3kW critical load

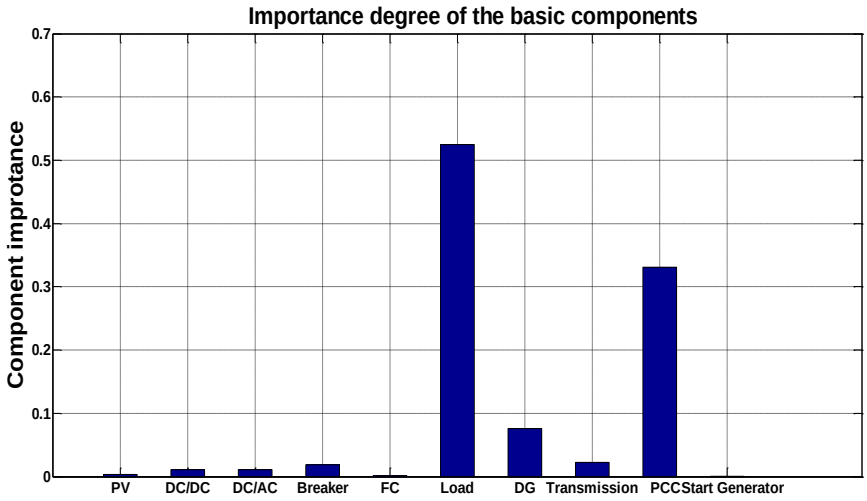

Fig.15 (b). Microgrid system impotance degree of components of the first objective to support a 3.3 kWcricical load

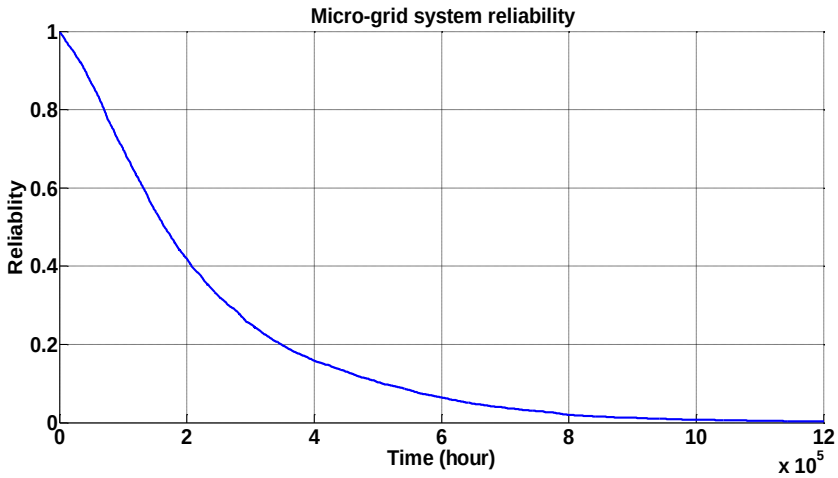

Fig.16 (a). Microgrid system reliability of the second objective to support a 150kW critical load

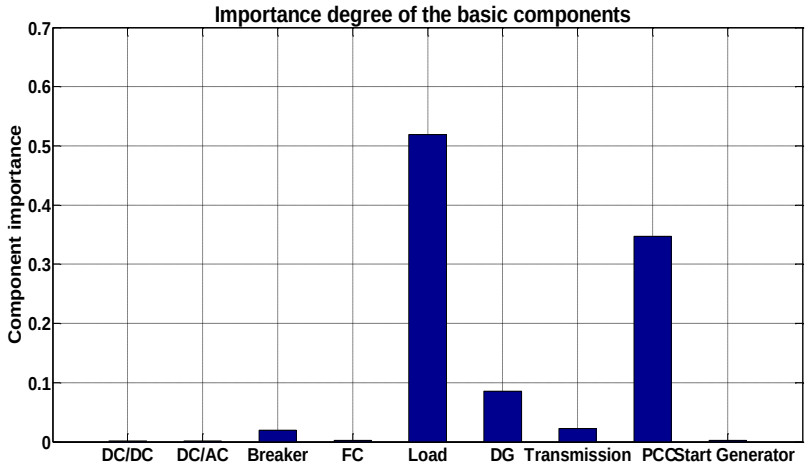

Fig.16 (b). Microgrid system impotance degree of components of the second objective to support a 150kW critical load

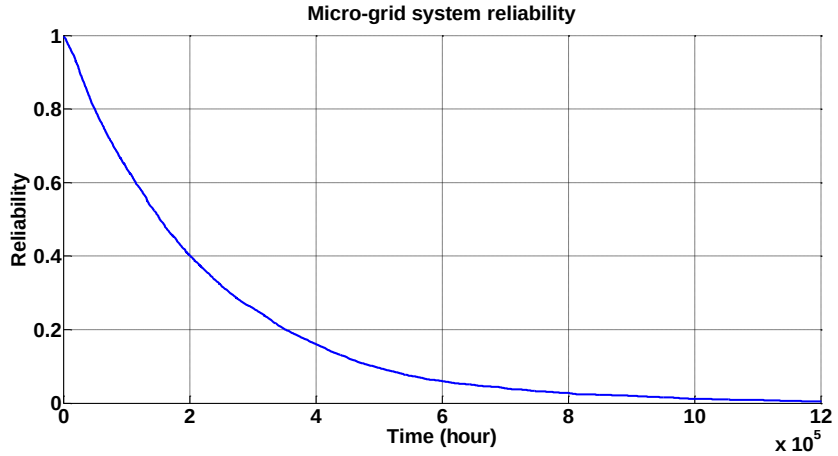

Fig.17 (a). Microgrid system reliability of the third objective to support a 400kW critical load

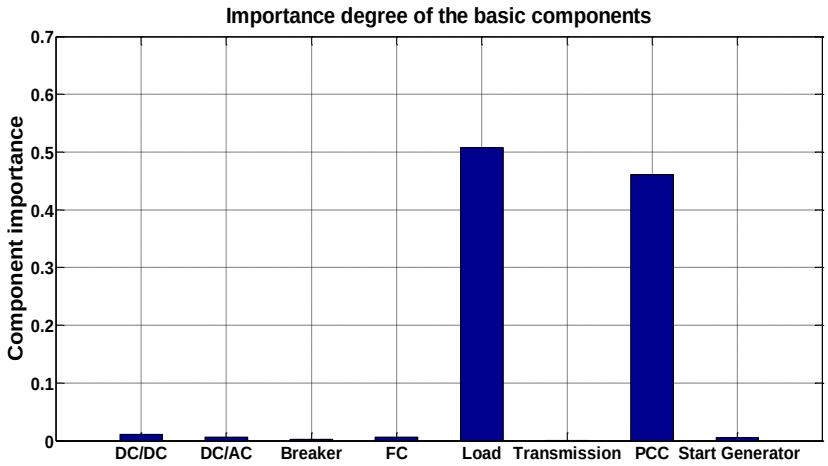

Fig. 17 (b). Microgrid system impotance degree of components of the third objective to support a 400 kW critical load

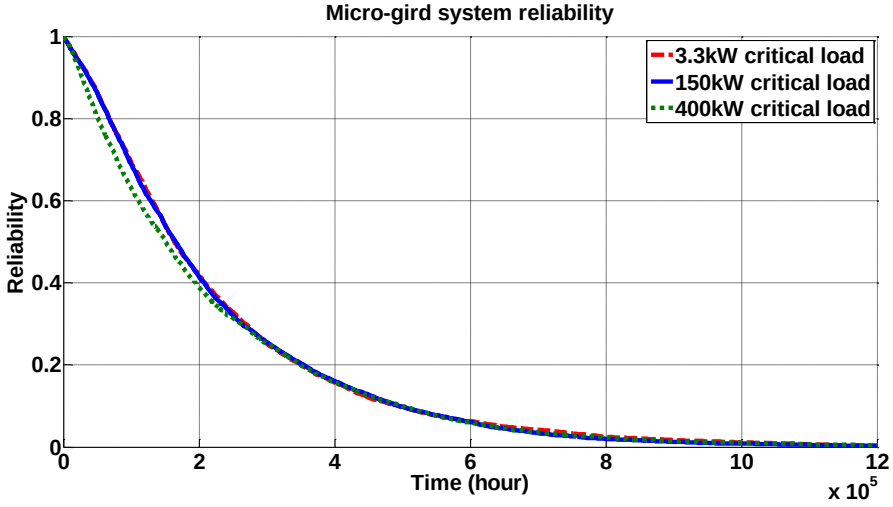

Fig. 18 (a) Micro-grid system reliability of the three objectives

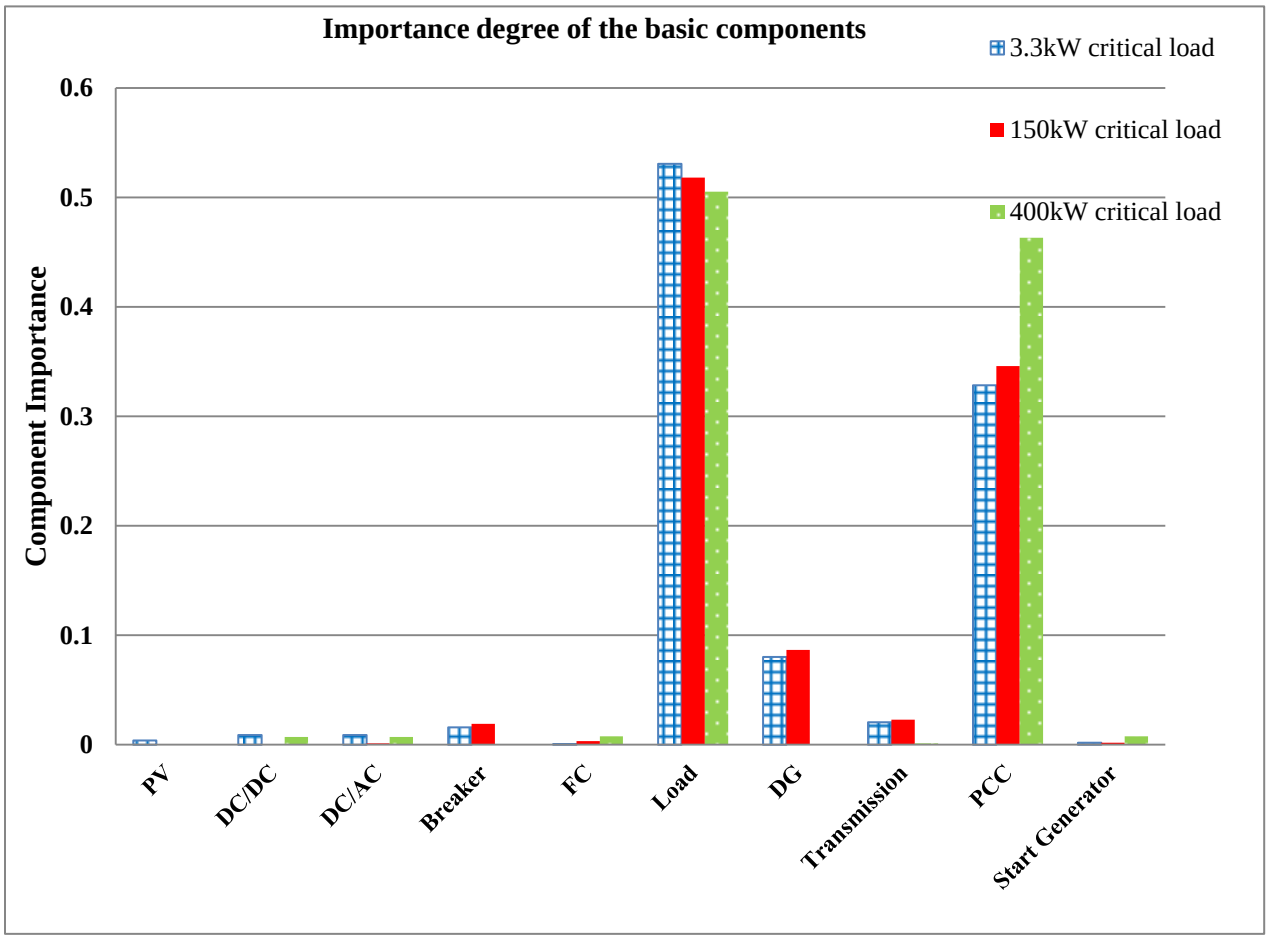

Fig. 18 (b) Micro-grid system importance degree of components of the three objectives

It is clear from the component importance result that higher critical load has lower component importance in the micro-grid system. With the lower critical load, micro-grid has more distributed generators, so the micro-grid overall system has higher reliability.

4.2.3 Fuzzy Fault Tree Analysis (FFTA) Method

As in the theoretical analysis of conventional fault tree method, people treat the event occurrence probability or system failure rate as an exact value. However, inaccuracy of the data will have effect on the determination of the top event occurrence probability, thus fuzzy numbers are also used to describe the probability of events. They do not only overcome the limitation of

the failure probability or relationship between events, but also can combine with the engineering and technical personnel of practical experience to construct fuzzy membership function [53-55]. Fig.19 represents a triangular fuzzy number of event *i* as an example, and it is defined by a triplet. In Fig.19, a_1 to a_3 is the failure probability range of an event and that has its membership function as shown in (4.7). $\mu_A(x)$ is the membership function associated with the fuzzy set.

$$\mu_A(x) = \begin{cases} 0 & x \le a_1 \\ \dfrac{x-a_1}{a_2-a_1} & a_1 \le x \le a_2 \\ \dfrac{a_3-x}{a_3-a_2} & a_2 \le x \le a_3 \\ 0 & x \ge a_3 \end{cases} \tag{4.7}$$

If P_1', P_2',…, Pn' are the possibility functions of *n* basic events, and $P_{T'}$ is for the top event, then the fuzzy "AND" and "OR" gates are defined in (4.8).

$$P_T' = ANDFUZZY(P_1', P_2', \ldots Pn') = (\prod_{i=1}^{n} a_{i1,} \prod_{i=1}^{n} a_{i2,} \prod_{i=1}^{n} a_{i3})$$
$$P_T' = ORFUZZY(P_1', P_2', \ldots Pn') = 1 - \prod_{i=1}^{n} (1 - (a_{i1,} a_{i2,} a_{i3})) \tag{4.8}$$

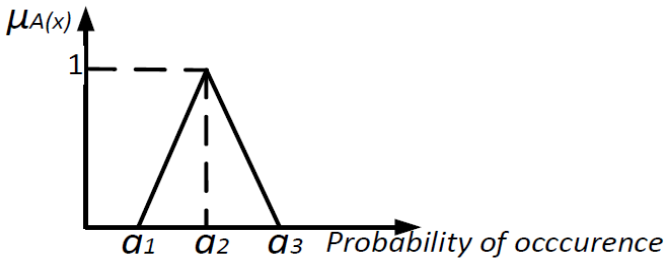

Fig.19. Membership function of fuzzy number

Fuzzy number FTA needs to get the practical experience data of the probability. As an example of using the fuzzy method, here the approximate fuzzy failure probability values are obtained by ranging the failure rates in Table 3 by ±20%, which are shown by three fuzzy

numbers of each component in Table 5. For example, the MTTF of PV is 25 years (0.04 times per year). a_1 is 0.032 times per year and a_3 is 0.048 times per year by ranging 0.04 by ±20%. Now the failure probability is a range from 0.032 times per year to 0.048 times per year rather than a constant 0.04 times per year.

The possibility of the occurrence of the top event is calculated by using equation (4.8) based on the values in Table 5, which comes out to be (0.016, 0.02, 0.024), shown in Fig.20. This means that the maximum possibility of micro-grid failure of objective one in the first case in Fig.8 (a) is 2% per year and the failure possibility will lie between 1.6% and 2.4%. Other membership functions of fuzzy number may have different results.

TABLE 5. FUZZY NUMBER FOR FAILURE POSSIBILITY OF BASIC EVENTS

Component	a_1 (per year)	a_2 (per year)	a_3 (per year)
PV panel	0.032	0.04	0.048
DC/DC	0.1	0.125	0.15
DC/AC	0.1	0.125	0.15
Breaker	0.016	0.02	0.024
Fuel cell	0.1	0.125	0.15
Diesel generator	0.08	0.1	0.12
Start generator	0.08	0.1	0.12
Transmission system	0.016	0.02	0.024
PCC	0.016	0.02	0.024
Load	0.016	0.02	0.024

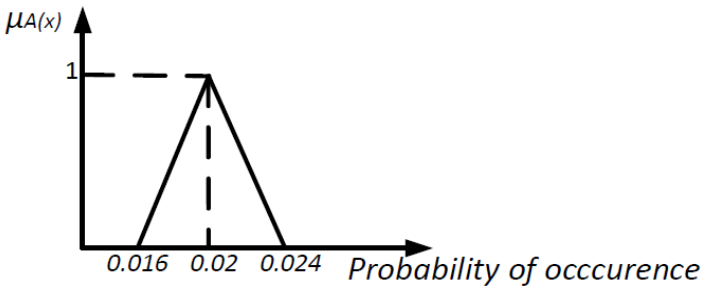

Fig.20. Micro-grid top event failure possibility of occurrence with the first objective of supporting a 3.3kW critical load

4.3 MRM Method for Case #1 UConn Micro-grid System Reliability

The models in Sections 4.1 and 4.2 are both based on the assumption that the components or the systems can be only in two states: a success state or a failed state. In this section, stochastic Markov chains are introduced. Markov reliability modeling is also a useful and powerful modeling and analysis technique with applications in reliability analysis. The reliability characteristics or behavior of a system are represented using a state transition diagram. Using the PV subsystem in Fig.21 as an example, and to simplify the example, assume that only one component can fail, since the components in a PV branch are in series and failure of one can lead to a PV subsystem failure. The Markov model of the PV subsystem is in Fig.22, and the probability distribution vector and transition matrix can be obtained as shown in (4.9) and (4.10) based on section 2.2.4.

Table 6 shows all the states and probabilities of the PV subsystem used in the MRM without considering recovery. A Markov simulation in MATLAB is used to approximate the predicted reliability of the PV system. The MATLB code can be found in Appendix B. The flow chart is shown in Fig.23 and $\dot{P}(t)$ in it can be calculated by the Chapman-Kolmogorov equation in (4.11). In this example, X=[1,0,0,0,0] at the starting time, C=[1,0,0,0,0] since the system is healthy only at state 0. The results of FT-MCS (blue solid curve) and MRM (red dashed curve) are given in Fig.24 (a). Figs.24 (b) and (c) are the FC and DG subsystems reliability functions, respectively, using the failure rates in Table 3. This similarity is expected as MCS covers most

possible fault occurrences at different random times. Both simulation methods can be easily implemented in small size systems with simple logic gate relationships.

Fig.21 PV subsystem example

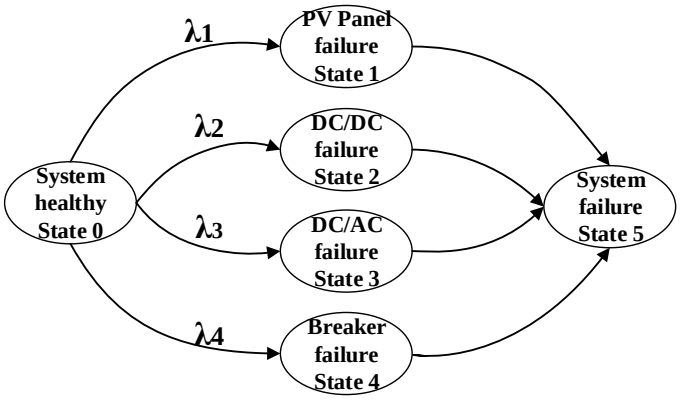

Fig.22 Markov model of PV system

$$P(t) = \begin{bmatrix} P_{00}(t) & P_{01}(t) & P_{02}(t) & P_{03}(t) & P_{04}(t) \end{bmatrix} \tag{4.9}$$

$$A = \begin{bmatrix} -\lambda_1 - \lambda_2 - \lambda_3 - \lambda_4 & \lambda_1 & \lambda_2 & \lambda_3 & \lambda_4 \\ 0 & 0 & 0 & 0 & 0 \\ 0 & 0 & 0 & 0 & 0 \\ 0 & 0 & 0 & 0 & 0 \\ 0 & 0 & 0 & 0 & 0 \end{bmatrix} \tag{4.10}$$

$$\dot{P}(t) = P(t) \bullet A \tag{4.11}$$

TABLE 6. PV SERIES SYSTEM STATES AND PROBABILITY OF EACH STATE

State X	PV panel $R(1)$	DC/DC $R(2)$	DC/AC $R(3)$	Breaker $R(4)$	System state C	Probability of the state P
0	Success	Success	Success	Success	Success	$R(1)*R(2)*R(3)*R(4)$
1	Failure	Success	Success	Success	Failure	$(1-R(1))*R(2)*R(3)*R(4)$
2	Success	Failure	Success	Success	Failure	$R(1)*(1-R(2))*R(3)*R(4)$
3	Success	Success	Failure	Success	Failure	$R(1)*R(2)*(1-R(3))*R(4)$
4	Success	Success	Success	Failure	Failure	$R(1)*R(2)*R(3)*(1-R(4))$

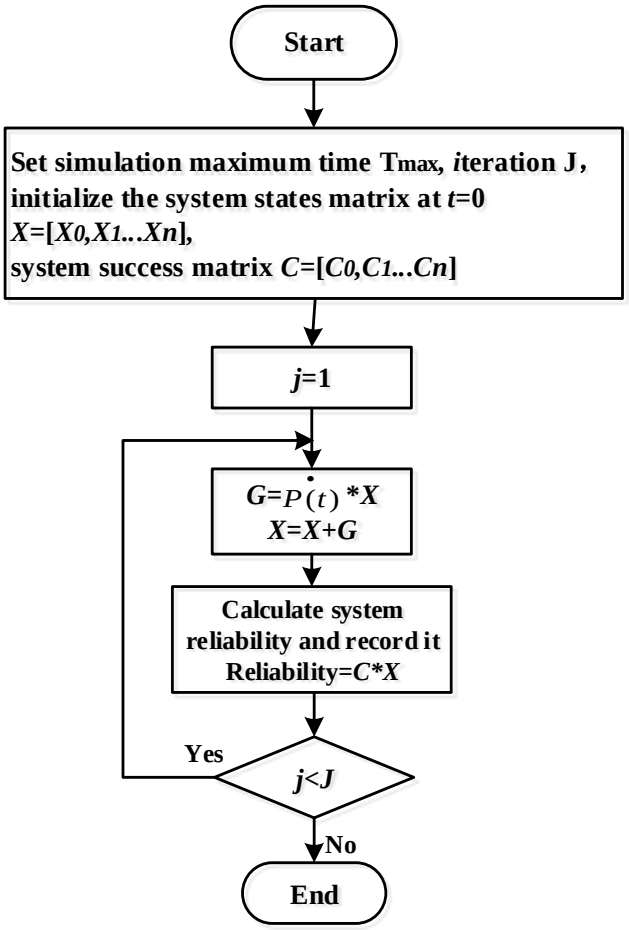

Fig.23 Markov reliability modeling flow chart

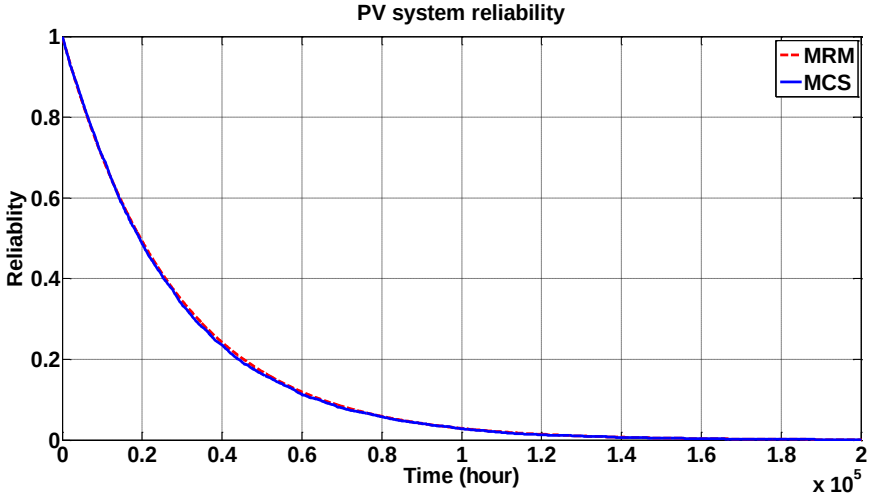

Fig.24 (a).MRM VS MCS result of PV system

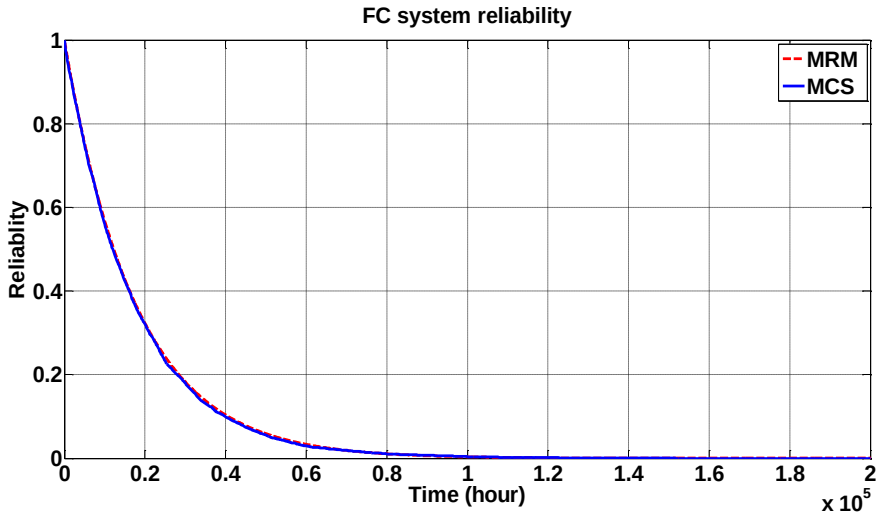

Fig.24 (b). MRM VS MCS result of FC system

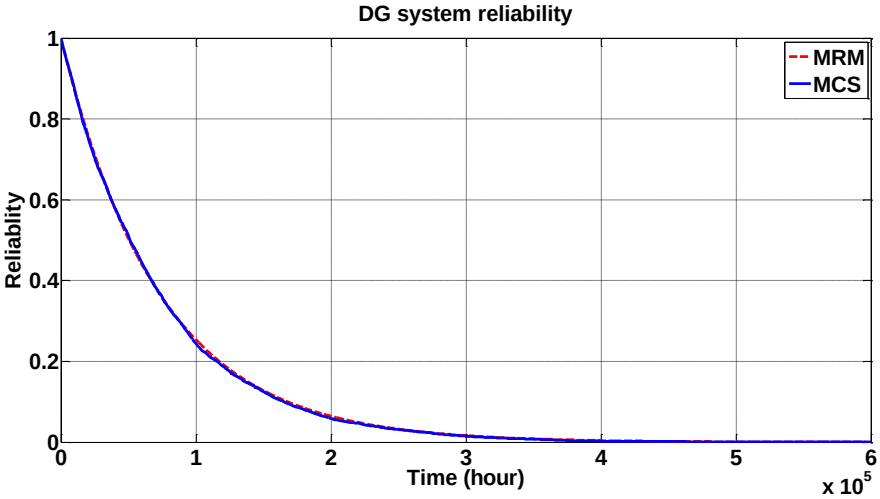

Fig.24 (c). MRM VS MCS result of DG system

For the overall micro-grid system, considering the large number of components in Fig.12 (c), take the micro-grid system in Fig.25 as an example here, four components with (2^4) 16 states in total are shown in Table 7. The fuel cell system is lumped as a whole component m_{fc} and it is the main component in the micro-grid to support a 400kW critical load. When reading the states in Table 7, state X_0(t) is the initial state where components are operating properly, state X_1(t) is when m_{fc} fails but the system survives, state X_2(t) is when component m_{18} fails but the system survives, state X_3(t) is when component m_{20} fails but the system survives, State X_5(t) is when

components m_{18} and m_{fc} fail but the system survives. The final state X_{15}(t) is reached when all four components have failed. Based on the last column of Table 7, the reliability of the micro-grid system is calculated as shown in (4.12) which reflects the total probability of system survival.

$$R(t) = P_0(t) + P_1(t) + P_2(t) + P_3(t) \quad (4.12)$$

TABLE 7. COMPONENTS AND SYSTEM STATES OF FIG.24

State Number	m_{fc} state	m_{18} state	m_{20} state	m_{21} state	System state
0	Success	Success	Success	Success	Success
1	Failure	Success	Success	Success	Success
2	Success	Failure	Success	Success	Success
3	Success	Success	Failure	Success	Success
4	Success	Success	Success	Failure	Failure
5	Failure	Failure	Success	Success	Success
6	Failure	Success	Failure	Success	Failure
7	Failure	Success	Success	Failure	Failure
8	Success	Failure	Failure	Success	Failure
9	Success	Failure	Success	Failure	Failure
10	Success	Success	Failure	Failure	Failure
11	Failure	Failure	Failure	Success	Failure
12	Failure	Failure	Success	Failure	Failure
13	Failure	Success	Failure	Failure	Failure
14	Success	Failure	Failure	Failure	Failure
15	Failure	Failure	Failure	Failure	Failure

TABLE 8. STATE PROBABILITY VECTORS AND DIFFERENTIALS OF ALL THE VECTORS

State NO	State probability vector $P(t)$	Differential equation $\dot{P(t)}$
0	$P_0(t) = R_1(t) \times R_2(t) \times R_3(t) \times R_4(t)$	$P_0^{'}(t) = -(\lambda_1 + \lambda_2 + \lambda_3 + \lambda_4) P_0(t)$
1	$P_1(t) = (1 - R_1(t)) \times R_2(t) \times R_3(t) \times R_4(t)$	$P_1^{'}(t) = -(\lambda_2 + \lambda_3 + \lambda_4) P_2(t) + \lambda_1 P_1(t)$
2	$P_2(t) = R_1(t) \times (1 - R_2(t)) \times R_3(t) \times R_4(t)$	$P_2^{'}(t) = -(\lambda_1 + \lambda_3 + \lambda_4) P_3(t) + \lambda_2 P_1(t)$
3	$P_3(t) = R_1(t) \times R_2(t) \times (1 - R_3(t)) \times R_4(t)$	$P_3^{'}(t) = -(\lambda_1 + \lambda_2 + \lambda_4) P_4(t) + \lambda_3 P_1(t)$
4	$P_4(t) = R_1(t) \times R_2(t) \times R_3(t) \times (1 - R_4(t))$	$P_4^{'}(t) = -(\lambda_1 + \lambda_2 + \lambda_3) P_5(t) + \lambda_4 P_1(t)$
5	$P_5(t) = (1 - R_1(t)) \times (1 - R_2(t)) \times R_3(t) \times R_4(t)$	$P_5^{'}(t) = -(\lambda_3 + \lambda_4) P_6(t) + \lambda_2 P_2(t) + \lambda_1 P_3(t)$
6	$P_6(t) = (1 - R_1(t)) \times R_2(t) \times (1 - R_3(t)) \times R_4(t)$	$P_6^{'}(t) = -(\lambda_2 + \lambda_4) P_7(t) + \lambda_3 P_2(t) + \lambda_1 P_4(t)$
7	$P_7(t) = (1 - R_1(t)) \times R_2(t) \times R_3(t) \times (1 - R_4(t))$	$P_7^{'}(t) = -(\lambda_2 + \lambda_3) P_8(t) + \lambda_4 P_2(t) + \lambda_1 P_5(t)$
8	$P_8(t) = R_1(t) \times (1 - R_2(t)) \times (1 - R_3(t)) \times R_4(t)$	$P_8^{'}(t) = -(\lambda_1 + \lambda_4) P_9(t) + \lambda_3 P_3(t) + \lambda_2 P_4(t)$
9	$P_9(t) = R_1(t) \times (1 - R_2(t)) \times R_3(t) \times (1 - R_4(t))$	$P_9^{'}(t) = -(\lambda_1 + \lambda_3) P_{10}(t) + \lambda_4 P_3(t) + \lambda_2 P_5(t)$
10	$P_{10}(t) = R_1(t) \times R_2(t) \times (1 - R_3(t)) \times (1 - R_4(t))$	$P_{10}^{'}(t) = -(\lambda_1 + \lambda_2) P_{11}(t) + \lambda_4 P_4(t) + \lambda_3 P_5(t)$
11	$P_{11}(t) = (1 - R_1(t)) \times R_2(t) \times (1 - R_3(t)) \times R_4(t)$	$P_{11}^{'}(t) = -\lambda_4 P_{12}(t) + \lambda_3 P_6(t) + \lambda_2 P_7(t) + \lambda_1 P_9(t)$
12	$P_{12}(t) = (1 - R_1(t)) \times (1 - R_2(t)) \times R_3(t) \times (1 - R_4(t))$	$P_{12}^{'}(t) = -\lambda_3 P_{13}(t) + \lambda_4 P_6(t) + \lambda_2 P_8(t) + \lambda_1 P_{10}(t)$
13	$P_{13}(t) = (1 - R_1(t)) \times R_2(t) \times (1 - R_3(t)) \times (1 - R_4(t))$	$P_{13}^{'}(t) = -\lambda_2 P_{14}(t) + \lambda_4 P_7(t) + \lambda_3 P_8(t) + \lambda_1 P_{11}(t)$
14	$P_{14}(t) = R_1(t) \times (1 - R_2(t)) \times (1 - R_3(t)) \times (1 - R_4(t))$	$P_{14}^{'}(t) = -\lambda_1 P_{15}(t) + \lambda_4 P_9(t) + \lambda_3 P_{10}(t) + \lambda_2 P_{11}(t)$
15	$P_{15}(t) = (1 - R_1(t)) \times (1 - R_2(t)) \times (1 - R_3(t)) \times (1 - R_4(t))$	$X_{15}^{'}(t) = \lambda_1 P_{15}(t) + \lambda_2 P_{14}(t) + \lambda_3 P_{13}(t) + \lambda_4 P_{12}(t)$

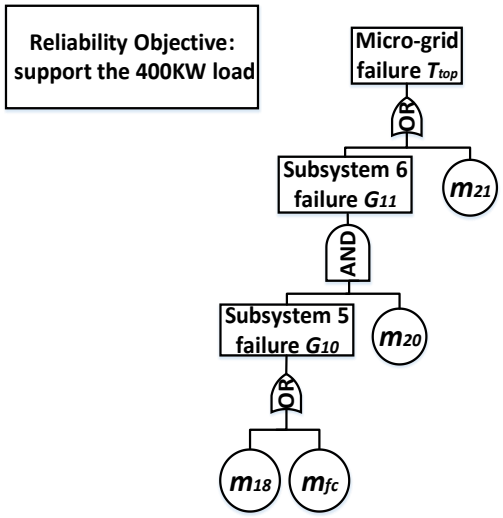

Fig.25. Equivalent fault tree of Fig.12 (c) for MRM example where the objective is to support a 400kW critical load

The state probability vectors and a set of differential equations associated with the state vectors are given by equations in Table 8. Take State 5 as an example,

$$\begin{aligned} P_5(t) &= (1-R_1(t))\times(1-R_2(t))\times R_3(t)\times R_4(t) \\ &= (1-e^{-\lambda_1 t})\times(1-e^{-\lambda_2 t})\times e^{-\lambda_3 t}\times e^{-\lambda_4 t} \\ &= e^{-(\lambda_3+\lambda_4)t} - e^{-(\lambda_1+\lambda_3+\lambda_4)t} - e^{-(\lambda_2+\lambda_3+\lambda_4)t} + e^{-(\lambda_1+\lambda_2+\lambda_3+\lambda_4)t} \\ P_5'(t) &= -(\lambda_3+\lambda_4)\times e^{-(\lambda_3+\lambda_4)t} + (\lambda_1+\lambda_3+\lambda_4)\times e^{-(\lambda_1+\lambda_3+\lambda_4)t} \\ &\quad + (\lambda_2+\lambda_3+\lambda_4)\times e^{-(\lambda_2+\lambda_3+\lambda_4)t} - (\lambda_1+\lambda_2+\lambda_3+\lambda_4)\times e^{-(\lambda_1+\lambda_2+\lambda_3+\lambda_4)t} \\ &= -(\lambda_3+\lambda_4)P_6(t) + \lambda_2 P_2(t) + \lambda_1 P_3(t) \end{aligned} \tag{4.13}$$

Based on the flow chart in Fig. 23, the reliability of the overall micro-grid system can be obtained by integrating the differential equations.

Since there are 21 components in Fig. 12 (a), the total states of the system will be 2^21, considering the large number of components in Fig.12 (a), the subsystems G_6, and G_7 are set as two new components in the overall system MRM simulation in the dashed block in Fig.26 (a).

The equivalent failure rates of all components are shown in Table 9. The curves in Fig.27 (a) give the reliability functions of the overall micro-grid system for the first objective of supporting a 3.3kW critical load (FT-MCS (blue curve), MRM (red curve), and RBD (green curve)).

To simplify the calculation, Fig.26 (b) is the equivalent FT of Fig.12 (b) with the equivalent failure rates shown in Table 10. Fig. 27 (b) is the FT-MCS (blue curve), MRM (red curve) and RBD (green curve) comparison results for the second reliability objective of supporting a 150kW critical load. Fig 25 is the equivalent FT of Fig.12 (c) and Fig. 27 (c) is the FT-MCS (blue curve), MRM (red curve) and RBD (green curve) comparison results.

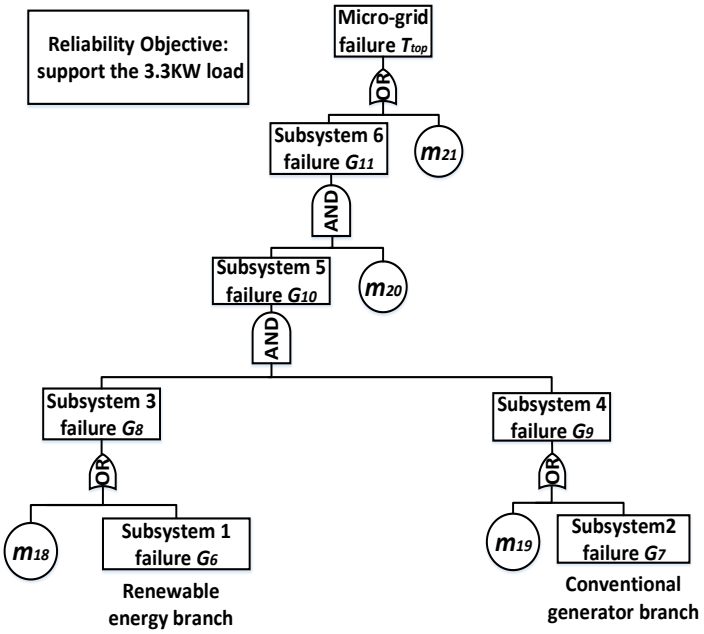

Fig. 26 (a). Equivalent fault tree of Fig.12 (a)

TABLE 9. EQUIVALENT FAILURE RATES USED IN MRM OF FIG.12 (A)

Component	Failure rate (failures/hour)	Component	Failure rate (failures/hour)
m_{18}	2.2831×10^{-6}	m_{20}	2.2831×10^{-6}
G_6 (renewable energy branch combined)	21.0114×10^{-6}	G_7 (DG systems combined)	9.0800×10^{-6}
m_{19}	2.2831×10^{-6}	m_{21}	2.2831×10^{-6}

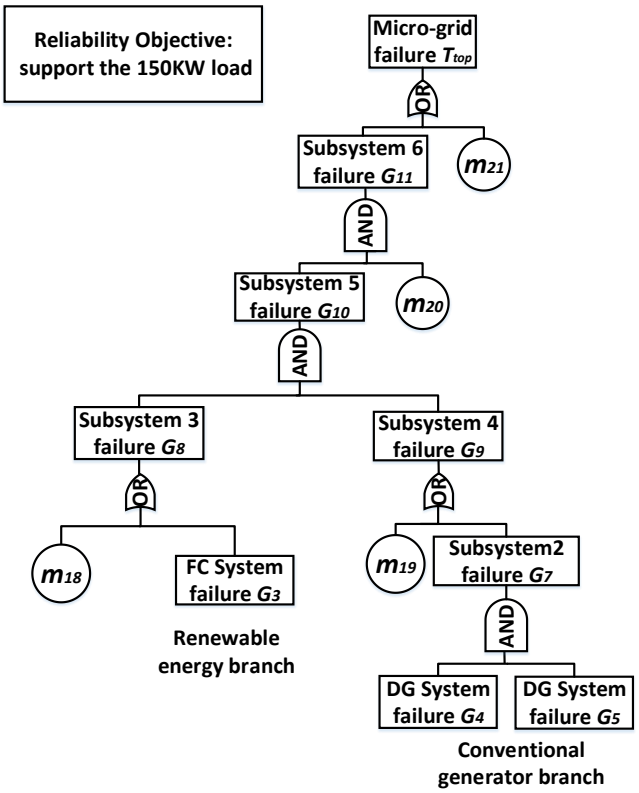

Fig. 26 (b). Equivalent fault tree of Fig.12 (b)

TABLE 10. EQUIVALENT FAILURE RATES USED IN MRM OF FIG.12 (B)

Component	Failure rate (failures/hour)	Component	Failure rate (failures/hour)
G_3 (renewable energy branch combined)	56.512 x10^{-6}	G_5 (one DG system combined)	13.6992 x10^{-6}
m_{18}	2.2831 x10^{-6}	m_{20}	2.2831 x10^{-6}
m_{19}	2.2831 x10^{-6}	m_{21}	2.2831 x10^{-6}
G_4 (one DG system combined)	13.6992 x10^{-6}		

TABLE 11. EQUIVALENT FAILURE RATES USED IN MRM OF FIG.12 (C)

Component	Failure rate (failures/hour)	Component	Failure rate (failures/hour)
m_{18}	2.2831 x10^{-6}	m_{20}	2.2831 x10^{-6}
m_{fc}	56.512 x10^{-6}	m_{21}	2.2831 x10^{-6}

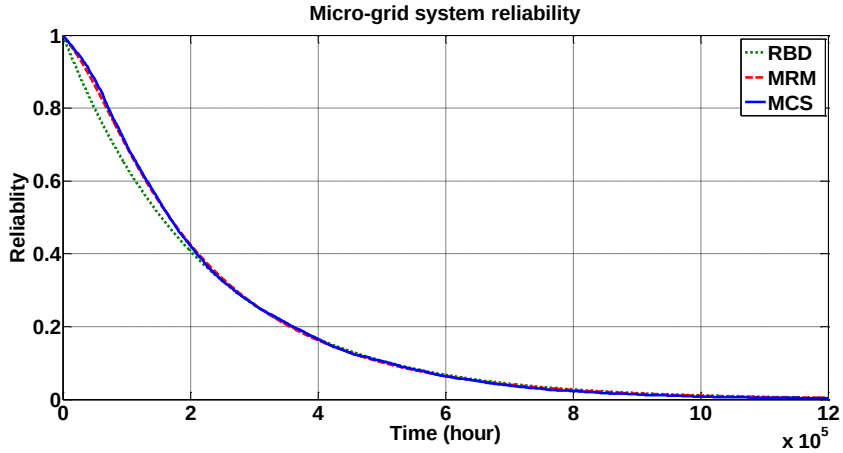

Fig.27 (a). RBD,MRM, and MCS result of overall micro-grid system with the first objective of supporting a 3.3kWcritical load

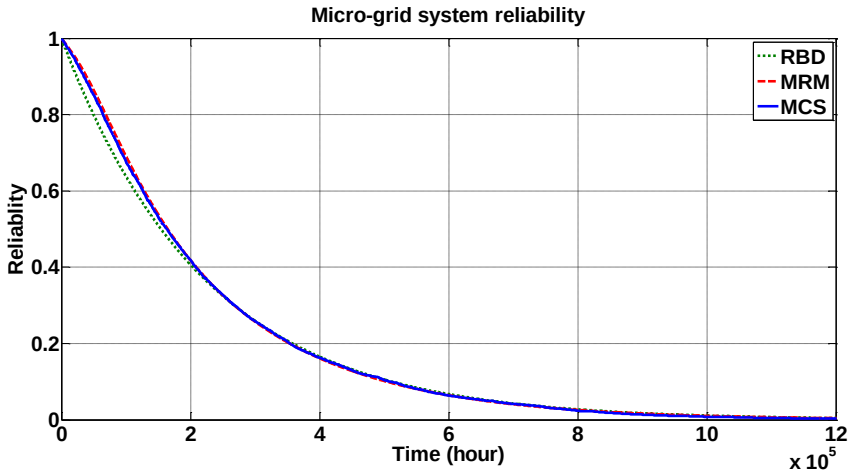

Fig.27 (b). RBD, MRM, and MCS result of overall micro-grid system with the second objective of supporting a 150kW critical load

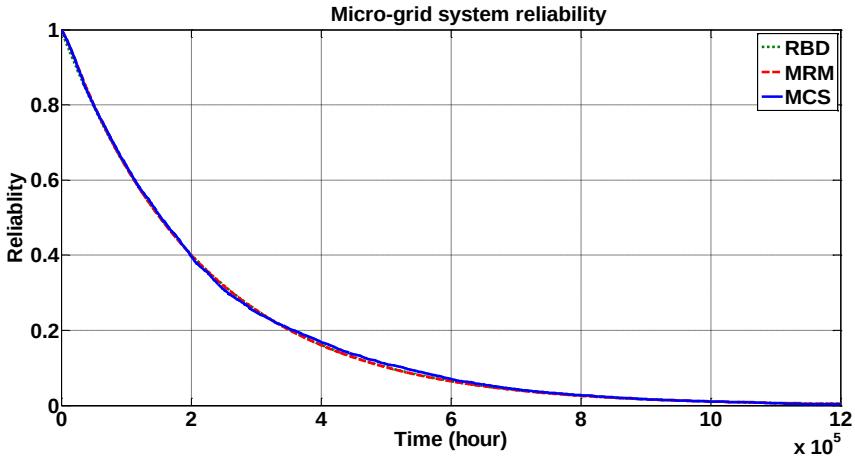

Fig.27 (c). RBD, MRM, and MCS result of overall micro-grid system with the third objective of supporting a 150kW critical

In this Chapter, micro-grid at UConn with three reliability objectives is studied. The MTTFs of three objectives are similar since the critical load, the transmission system and the PCC have small failure rates compared to the other components. But the slight difference between MTTFs also can illustrate the system reliability characteristic, micro-grid of the first objective of supporting a 3.3kW critical load has larger MTTF since it has more parallel distributed generation resources. When doing the reliability analysis and modeling, the objective changes, the result will be changed. Changing the failure rate of the components in a real system will give a huge different result, especially the failure rate of the component with large importance. The detail comparison of the MTTFs can be found in Chapter VII.

V. RELIABILITY ANALYSIS METHODS APPLICATION ON THE SECOND AND THIRD CASE STUDIES: KING'S PLAZA AND NEW YORK UNIVERSITY

5.1 Reliability Analysis of Case Study #2 King's Plaza Micro-grid System

The one-line diagram of Fig.9 was transformed into an RBD as shown in Fig. 28. Two feeders coming from Con-Edison with Gridlink converters, and gas engines are in parallel supporting the King's Plaza Mall. In each feeder, all the devices are in series. If Con-Edison fails, the generators can support the King's Plaza Mall. In RBD analysis, it is assumed that Con-Edison fails twice per year, and all the other failure rates are found using average lifetime information found in the literature. The failure rates shown in Table 12 are estimated from the literature [56-69] for this case. Another assumption is that all switchgear have the same failure rate λ_{sg} and all transformers have the same failure rate $\lambda_{tr,}$ λ_{lo} is the failure rate of the load itself irrespective of the rest of the rest of the micro-grid system, i.e. the inability of a load to receive power due to an internal load fault even though power is available from the micro-grid.

TABLE 12. FAILURE RATES OF COMPONENTS AS APPROXIMATED FROM THE LITERATURE IN CASE TWO AND THREE [56-69]

Device	Failure rate (failures/hour)	Device	Failure rate (failures/hour)
Switchgear (SG unit)	λ_{sg} =4.5662 x10^{-6}	Converter	$\lambda_{dc/ac}$ =$\lambda_{ac/dc}$ =14.2692 x10^{-6}
Transformer	λ_{tr} =4.5662 x10^{-6}	Gas Turbine	λ_{gt} =11.4155 x10^{-6}
Fuse	λ_{fu} =2.5368 x10^{-6}	Con-Edison	λ_{co} =228.32 x10^{-6}
Diesel generator	λ_{dg}=11.4155 x10^{-6}	Loads (Mall)	λ_{lo} =456.64 x10^{-6}
Filter	λ_{fi}=14.2692 x10^{-6}	Bus/bus	λ_{bus} =2.8539 x10^{-6}
Gridlink	λ_{gl}=14.2692 x10^{-6}		

Kings Plaza fails a few times per year, now due to the engines not being able to follow load changes, or a trip of a generator, which similarly causes large load swings. It is envisioned that the Gridlink system will eliminate this by using power from Con-Edison for very short load balancing requirements. So here we have following four detail case for Kings' Plaza system reliability study.

A. King's Plaza system with the critical load (λ_{lo} =4/8760 failures/hour)

As shown below, $\lambda_{1,KP,}$ $\lambda_{2,KP,}$ $\lambda_{3,KP}$ are the failure rates of the three top and parallel block groups in dashed lines yielding $MTTF_{1,KP}$, $MTTF_{2,KP}$, $MTTF_{3,KP}$, respectively and $MTTF_{all,KP}$ for the whole system.

Since the King's Plaza Mall itself is assumed to fail four times per year in this case, the total system MTTF is quite small since the Mall itself has the largest importance in all the components. Note that these MTTF values are approximated using the RBD shown in Fig.28 and may not reflect actual values, mainly due to the approximate failure rate values used.

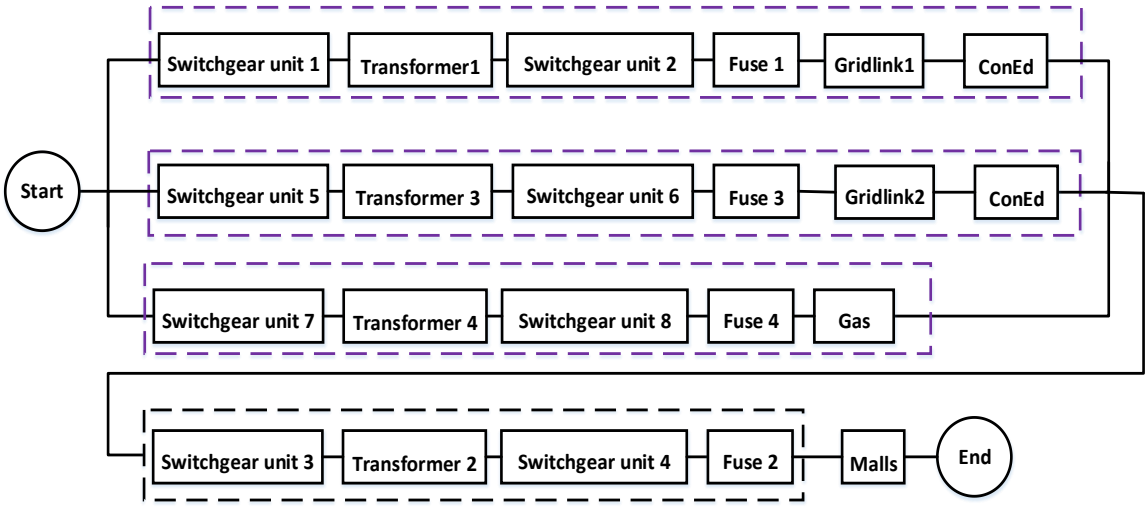

Fig.28 RBD of KP micro-grid system with the critical load and Gridlink

$$MTTF_{1,KP} = \frac{1}{2\lambda_{sg} + \lambda_{tr} + \lambda_{fu} + \lambda_{gl} + \lambda_{co}} = 0.4411 years$$

$$MTTF_{2,KP} = \frac{1}{2\lambda_{sg} + \lambda_{tr} + \lambda_{fu} + \lambda_{gl} + \lambda_{co}} = 0.4411 years$$

$$MTTF_{3,KP} = \frac{1}{2\lambda_{sg} + \lambda_{tr} + \lambda_{fu} + \lambda_{gas}} = 5.2570 years$$

$$MTTF_{all,KP} = \frac{1}{\lambda_{paraller,KP} + 2\lambda_{sg} + \lambda_{tr} + \lambda_{fu} + \lambda_{mall}} = 0.2312 years$$

Fig.29 is the fault tree of the KP system with the objective of supporting the King's Plaza mall at 2MW and λ_{lo} =4/8760 failures/hour. The component importance and system reliability function can be found in Fig.38 using FT-MCS method. In the FT-MCS, simulation iteration equals to 5000, the MTTF is found to be 0.2456 years. The MRM result is shown in Fig.30 in red curve compared with the FT-MCS result in blue curve and RBD result in green curve. In the MRM, simulation iteration also equals to 5000, the MTTF is found to be 0.2389 years.

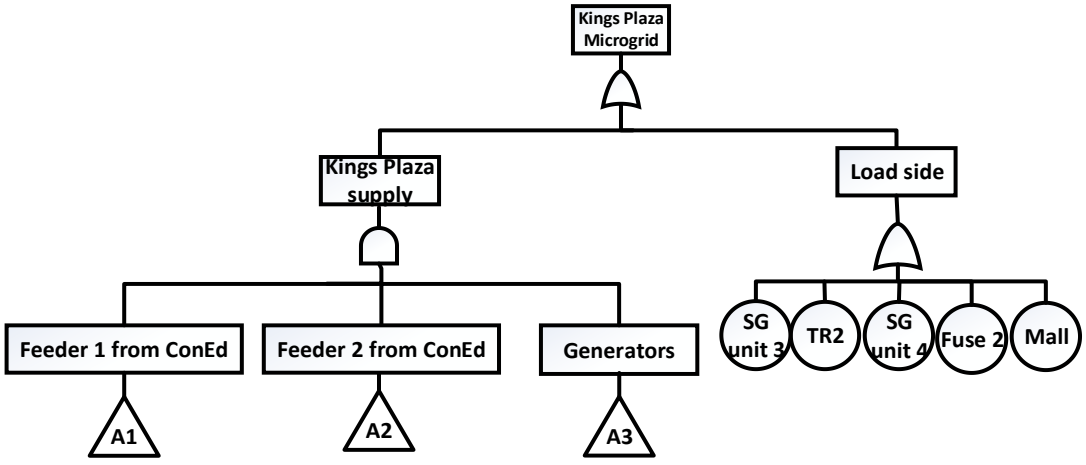

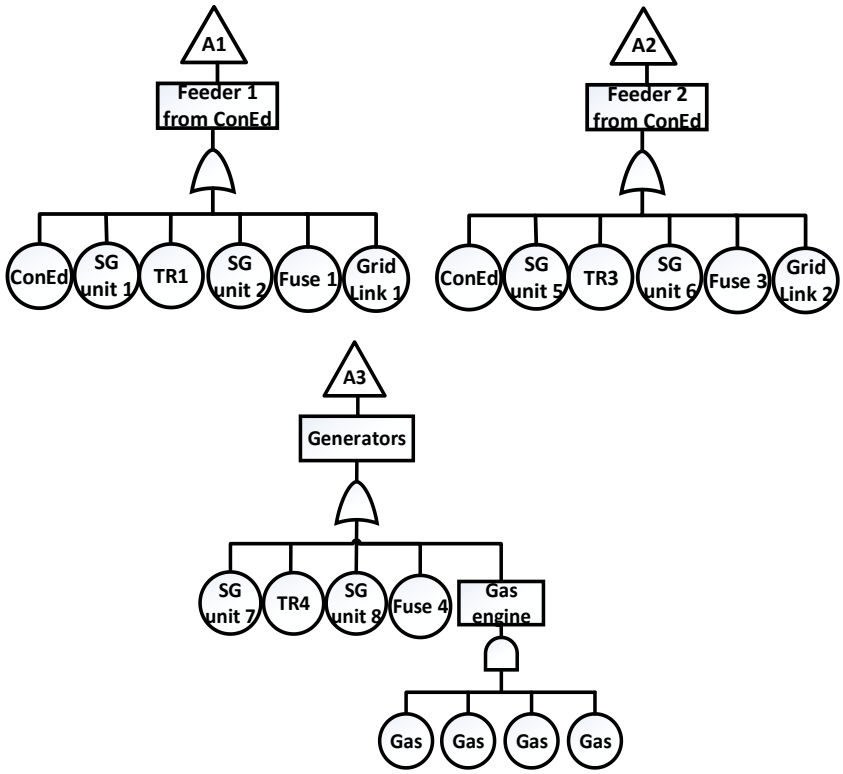

Fig. 29 Fault tree of KP micro-grid system with an objective to support the 2MW load

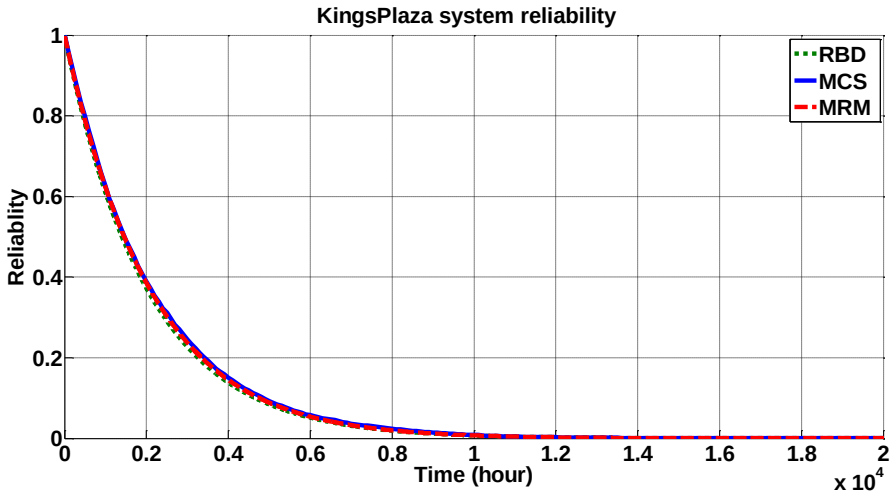

Fig.30 RBD, MRM, and MCS results of the King's Plaza system reliability with critical load (λ_{lo} =4/8760 failures/hour)

B. King's Plaza system with the critical load (λ_{lo} =0.2/8760 failures/hour)

When the failure rate of the mall is once per five years (λ_{lo} =0.2/8760 failures/hour), RBD and fault tree of the system are not changed. The MTTF of the overall King's Plaza system is

calculated as

$$MTTF_{all,KP} = \frac{1}{\lambda_{paraller,KP} + 2\lambda_{sg} + \lambda_{tr} + \lambda_{fu} + \lambda_{mall}} = 1.9947\,years$$

The MRM result is shown in Fig.31 in red curve compared with the FT-MCS result in blue curve, and RBD result in green curve and FT-MCS results can be found in Fig.38. In the FT-MCS, simulation iteration equals to 5000, the MTTF is found to be 2.0865 years. In the MRM, simulation iteration also equals to 5000, the MTTF is found to be 2.0779 years.

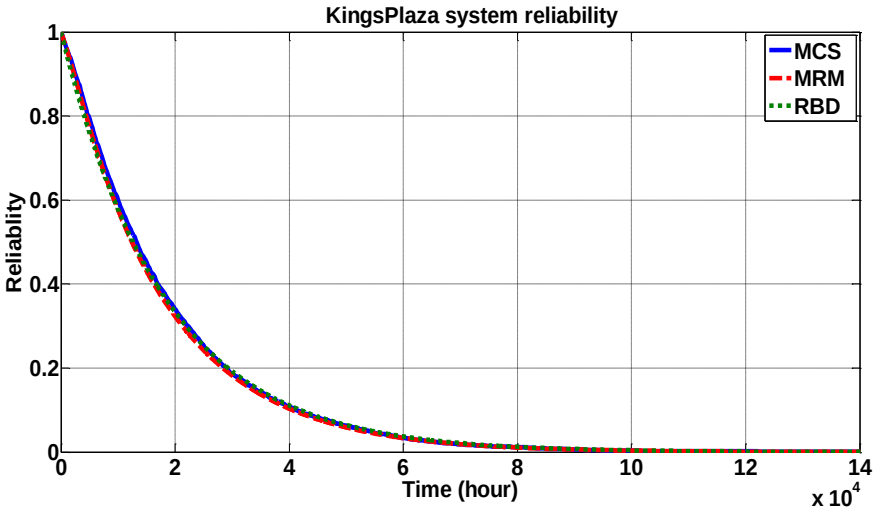

Fig.31 RBD, MRM, and MCS result of the King's Plaza system reliability with critical load (λ_{lo} =0.2/8760)

C. King's Plaza system with ideal critical load (load never fails)

When there is an ideal load (Mall) in the King's Plaza system, RBD and fault tree of the system are shown in Fig. 32 and Fig. 33. The MTTF of the overall system is calculated as

$$MTTF_{all,KP} = \frac{1}{\lambda_{1,KP}} + \frac{1}{\lambda_{2,KP}} + \frac{1}{\lambda_{3,KP}} - \frac{1}{\lambda_{1,KP} + \lambda_{2,KP}} - \frac{1}{\lambda_{1,KP} + \lambda_{3,KP}} - \frac{1}{\lambda_{2,KP} + \lambda_{3,KP}} + \frac{1}{\lambda_{1,KP} + \lambda_{2,KP} + \lambda_{3,KP}}$$
$$= 5.3134\,years$$

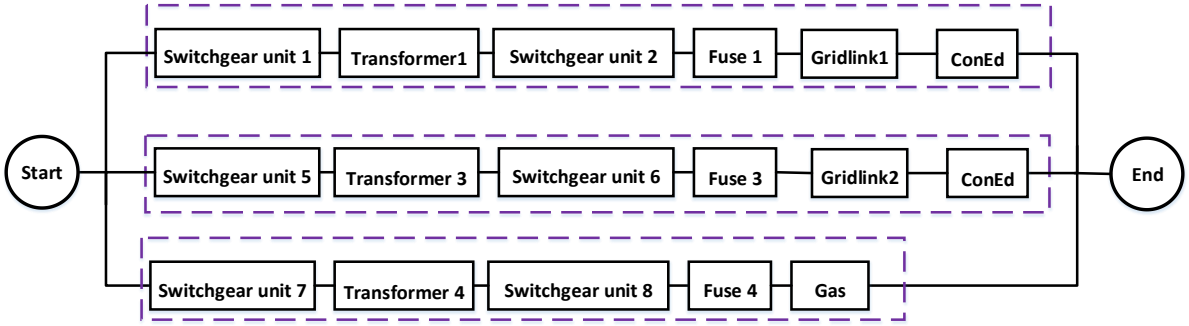

Fig.32. RBD of the King's Plaza system with ideal critical load

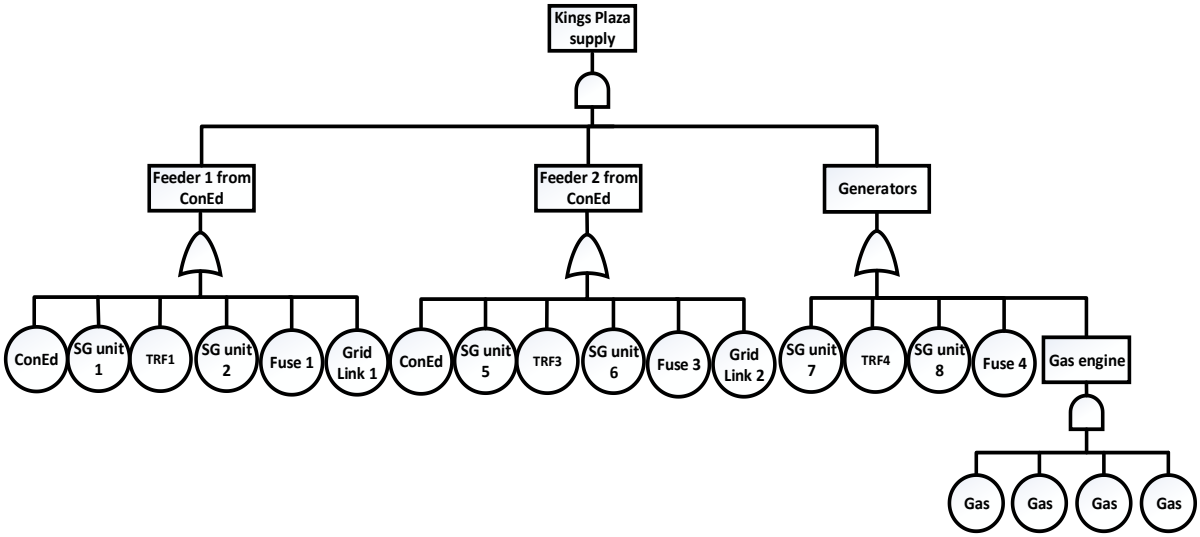

Fig.33 Fault tree of the King's Plaza system with ideal critical load

The component importance and system reliability function are shown in Fig.38 using FT-MCS method. In the FT-MCS, simulation iteration equals to 5000, the MTTF is found to be 5.4688 years. The MRM result is shown in Fig.34 in red curve compared with the FT-MCS result in blue curve and RBD result in green curve. In the MRM, simulation iteration also equals to 5000, the MTTF is found to be 5.3276 years.

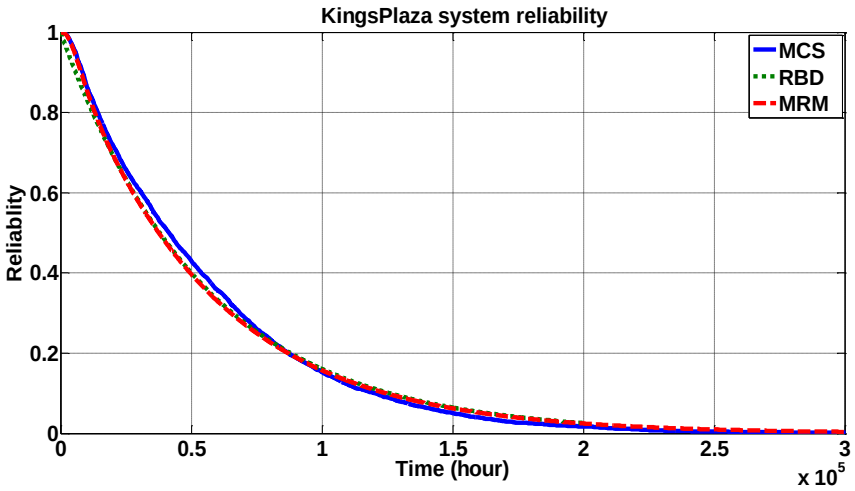

Fig.34 RBD, MRM, and MCS result of the King's Plaza system reliability with ideal critical load

D. King's Plaza system without Gridlink converters but with the critical load (λ_{lo}=4/8760 failures/hour)

When this is no Gridlink in the system, the micro-grid is synchronous connection, RBD and fault tree of the system are shown in Fig.35 and Fig. 36. $\lambda_{1,KP,}$ $\lambda_{2,KP,}$ $\lambda_{3,KP}$ are the failure rates of the three top and parallel block groups in dashed lines yielding $MTTF_{1,KP}$, $MTTF_{2,KP}$, $MTTF_{3,KP}$, respectively and $MTTF_{all,KP}$ for the whole system are calculated below.

$$MTTF_{1,KP} = \frac{1}{2\lambda_{sg} + \lambda_{tr} + \lambda_{fu} + \lambda_{gl} + \lambda_{co}} = 0.4668 years$$

$$MTTF_{2,KP} = \frac{1}{2\lambda_{sg} + \lambda_{tr} + \lambda_{fu} + \lambda_{gl} + \lambda_{co}} = 0.4668 years$$

$$MTTF_{3,KP} = \frac{1}{2\lambda_{sg} + \lambda_{tr} + \lambda_{fu} + \lambda_{gas}} = 5.2570 years$$

$$MTTF_{all,KP} = \frac{1}{\lambda_{paraller,KP} + 2\lambda_{sg} + \lambda_{tr} + \lambda_{fu} + \lambda_{mall}} = 0.2364 years$$

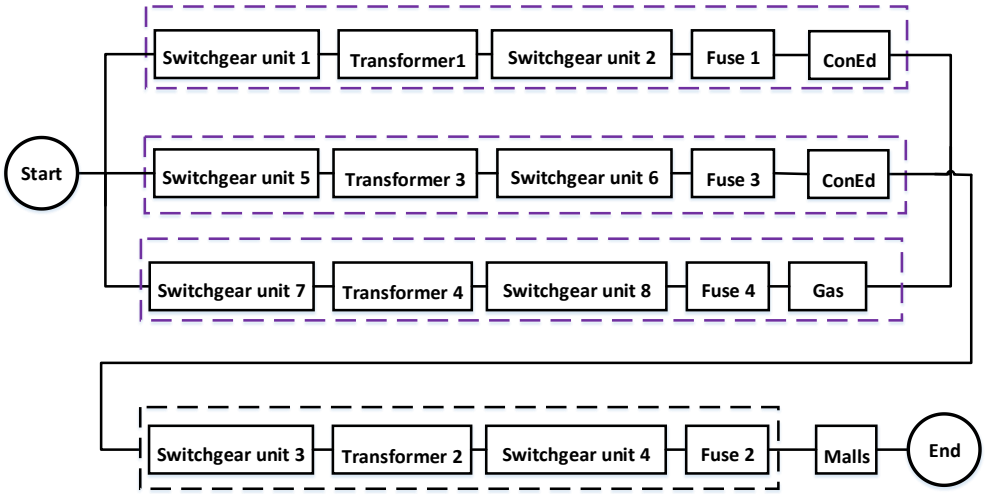

Fig.35 RBD of the King's Plaza system without Gridlink

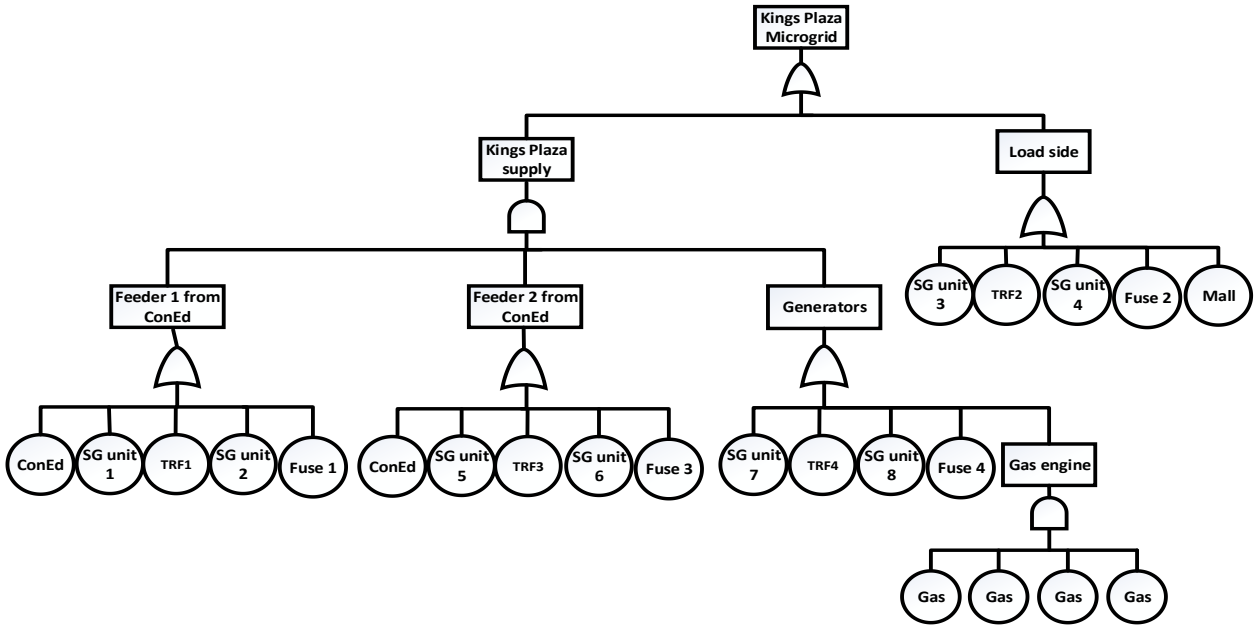

Fig.36 Fault tree of the King's Plaza system without Gridlink

The comparison of the component importance and system reliability function of four situations are shown in Fig.38 using FT-MCS method. In the FT-MCS, simulation iteration equals to 5000, the MTTF is found to be 0.2488 years. The MRM result is shown in Fig.37 in red curve compared with the FT-MCS result in blue curve and RBD result in green curve. In the MRM, simulation iteration also equals to 5000, the MTTF is found to be 0.2393 years.

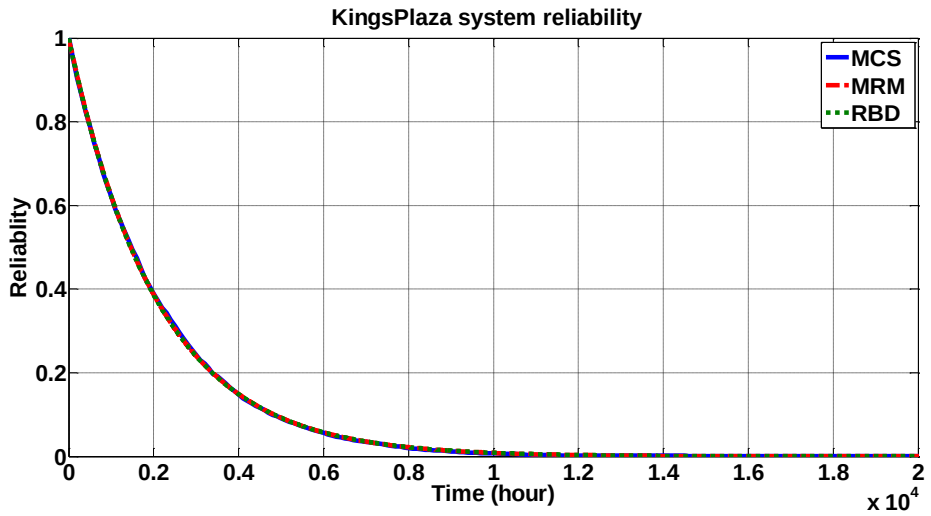

Fig.37 RBD, MRM, and MCS result of the King's Plaza system reliability without Gridlink

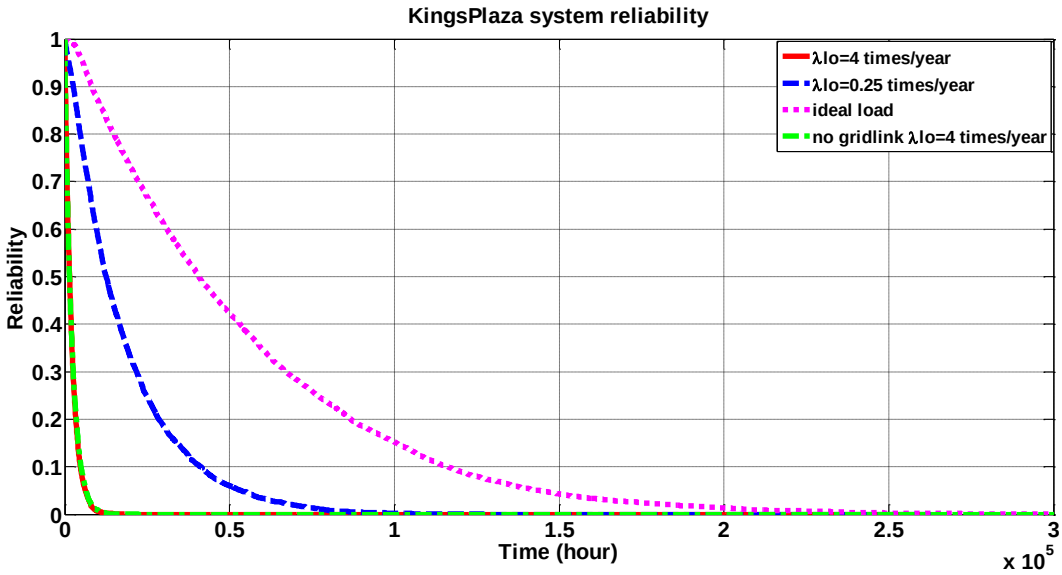

Fig.38 (a) King's Plaza micro-grid reliability comparison (λ_{lo} =4/8760 failures/hour, λ_{lo} =0.2/8760 failures/hour, ideal load, and no gridlink)

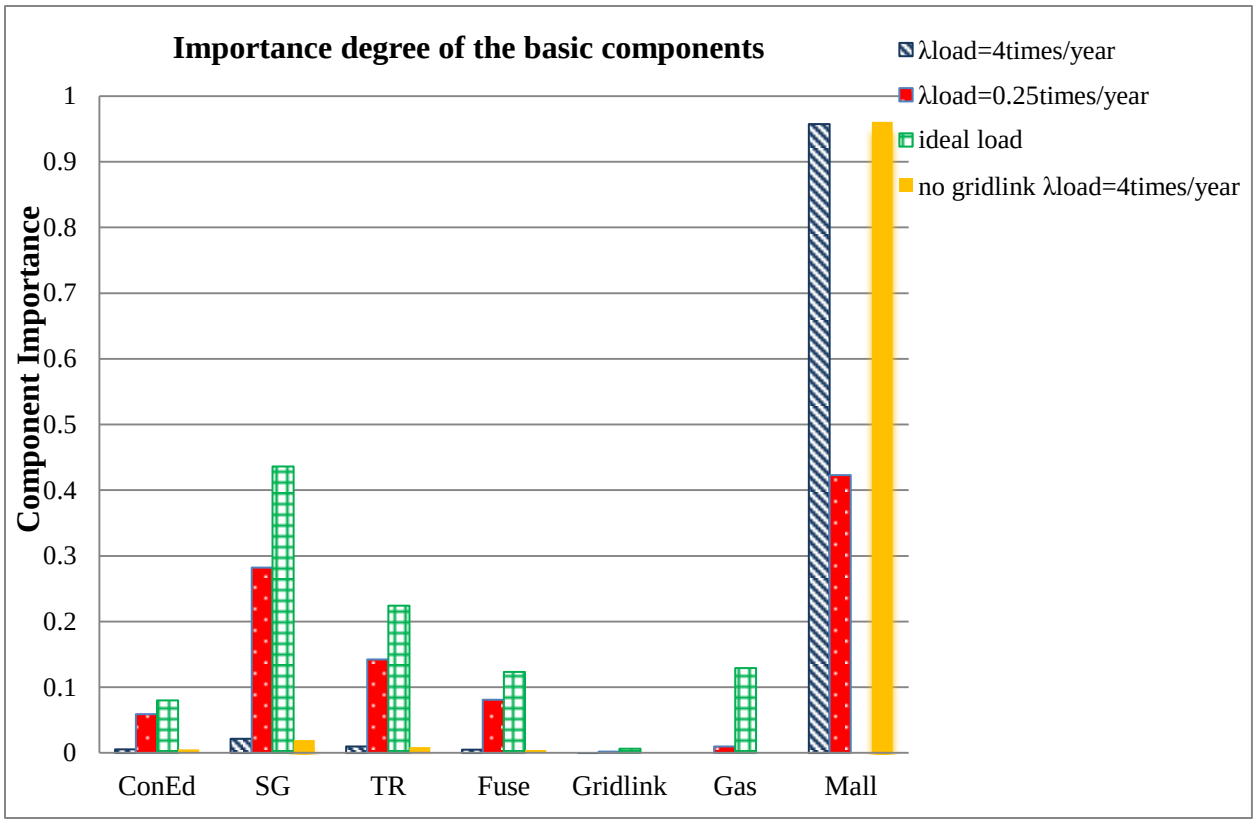

Fig.38 (b) Importance degree of the basic components in King's Plaza system (λ_{lo} =4/8760 failures/hour, λ_{lo} =0.2/8760 failures/hour, ideal load and no gridlink)

5.2 Reliability Analysis of Case Study #3 New York University Micro-grid System

The simplified RBDs of the critical loads in the NYU micro-grid, which mainly considers supporting the critical loads, are shown in Fig. 39. It's learned from the one line diagram in Fig.10 (a) that transformers 1 and 2 support Bus C, so if one of the transformers fails, it will not affect the Bus C sub-system. Silver Tower Garage, Broadway Block Substation NO.3 and Central Heating Plant have their own bus sub-systems as shown in Fig. 39. Substation NO.3 and Silver Tower Garage have the same RBD. The MTTFs in Fig.39 are calculated below, $MTTF_1$ $MTTF_{2,}$ and $MTTF_{3,}$ are the results with the failure rates of the critical loads equal to 4/8760, 1/8760, or 0.1/8760 failures/hour to study the impact of load failure rate on the system reliability. Assuming

all the transformers have the same failure rate λ_{tr}, buses have failure rate λ_{bus}, and the failure rate of the critical loads λ_{lo} in all RBDs. λ_1 is the failure rate of the dotted block in Fig.39 (c). The other components' failure rates are estimated from the literature and some industry norms as shown in Table 12.

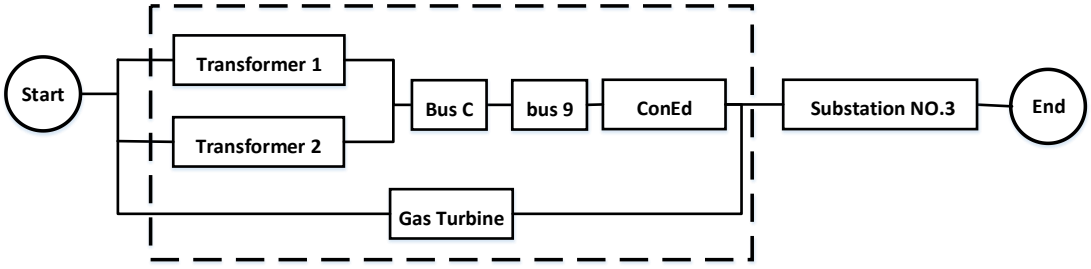

Fig.39 (a).Substation NO.3 RBD

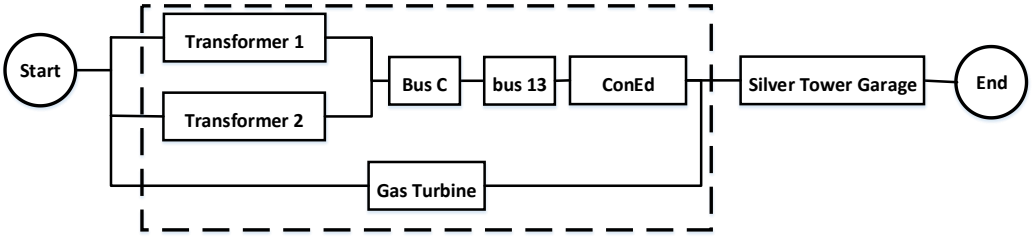

Fig.39 (b). Silver Tower Garage RBD

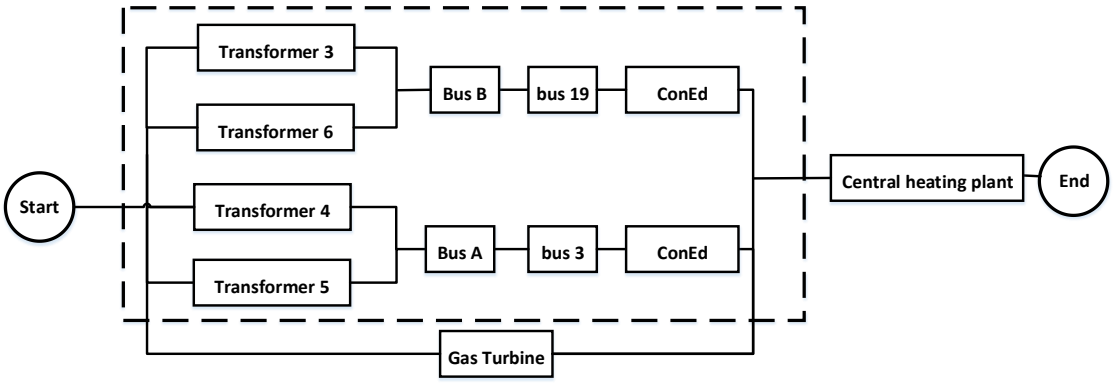

Fig.39 (c). Central heating plant RBD

$$MTTF_{substation,NYU} = \frac{1}{\lambda_{gas}+\lambda_{lo}} - \frac{2}{\lambda_{tr}+\lambda_{gas}+2\lambda_{bus}+\lambda_{lo}+\lambda_{coned}} + \frac{2}{\lambda_{tr}+2\lambda_{bus}+\lambda_{lo}+\lambda_{coned}}$$
$$- \frac{1}{2\lambda_{tr}+2\lambda_{bus}+\lambda_{lo}+\lambda_{coned}} + \frac{1}{2\lambda_{tr}+2\lambda_{bus}+\lambda_{lo}+\lambda_{gas}+\lambda_{coned}}$$

$MTTF_{substation,NYU1} = 0.2466 \ years \ (\lambda_{lo} = 4/8760 \ failures/hour)$

$MTTF_{substation,NYU2} = 0.9195 \ years \ (\lambda_{lo} = 1/8760 \ failures/hour)$

$MTTF_{substation,NYU3} = 5.0208 \ years \ (\lambda_{lo} = 0.1/8760 \ failures/hour)$

$$MTTF_{garage,NYU} = \frac{1}{\lambda_{gas}+\lambda_{lo}} - \frac{2}{\lambda_{tr}+\lambda_{gas}+2\lambda_{bus}+\lambda_{lo}+\lambda_{coned}} + \frac{2}{\lambda_{tr}+2\lambda_{bus}+\lambda_{lo}+\lambda_{coned}}$$
$$- \frac{1}{2\lambda_{tr}+2\lambda_{bus}+\lambda_{lo}+\lambda_{coned}} + \frac{1}{2\lambda_{tr}+2\lambda_{bus}+\lambda_{lo}+\lambda_{gas}+\lambda_{coned}}$$

$MTTF_{garage,NYU1} = 0.2466 \ years \ (\lambda_{lo} = 4/8760 \ failures/hour)$

$MTTF_{garage,NYU2} = 0.9195 \ years \ (\lambda_{lo} = 1/8760 \ failures/hour)$

$MTTF_{garage,NYU3} = 5.0208 \ years \ (\lambda_{lo} = 0.1/8760 \ failures/hour)$

$$MTTF_{heatingplant,NYU} = \frac{1}{2\lambda_1+\lambda_{gas}+\lambda_{load}} - \frac{2}{\lambda_{gas}+\lambda_{lo}+\lambda_1} + \frac{2}{\lambda_{lo}+\lambda_1} + \frac{1}{\lambda_{gas}+\lambda_{lo}} - \frac{1}{2\lambda_1+\lambda_{lo}}$$

$MTTF_{heatingplant,NYU1} = 0.2570 \ years \ (\lambda_{lo} = 4/8760 \ failures/hour)$

$MTTF_{heatingplant,NYU2} = 0.9400 \ years \ (\lambda_{lo} = 1/8760 \ failures/hour)$

$MTTF_{heatingplant,NYU3} = 5.0610 \ years \ (\lambda_{lo} = 0.1/8760 \ failures/hour)$

The fault trees in Fig.40 have the same objectives to supporting three critical loads silver tower garage, substation NO.3 and central heating plant in Fig.39. Since the Silver Tower Garage and Substation NO.3 have the same one-line diagram, their fault trees are the same and the reliability modeling analysis result has no differences. Here only the result of the Silver Tower Garage is shown.

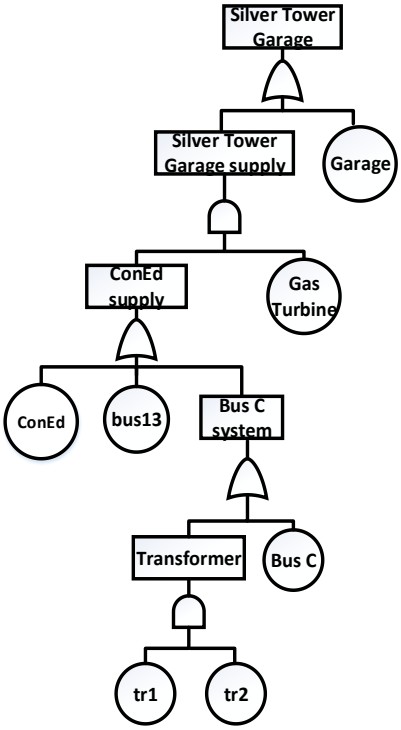

Fig. 40 (a). Silver tower garage fault tree

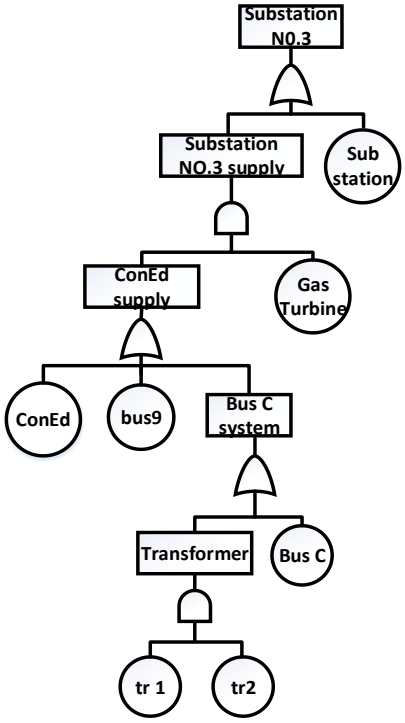

Fig. 40 (b). Substation NO.3 fault tree

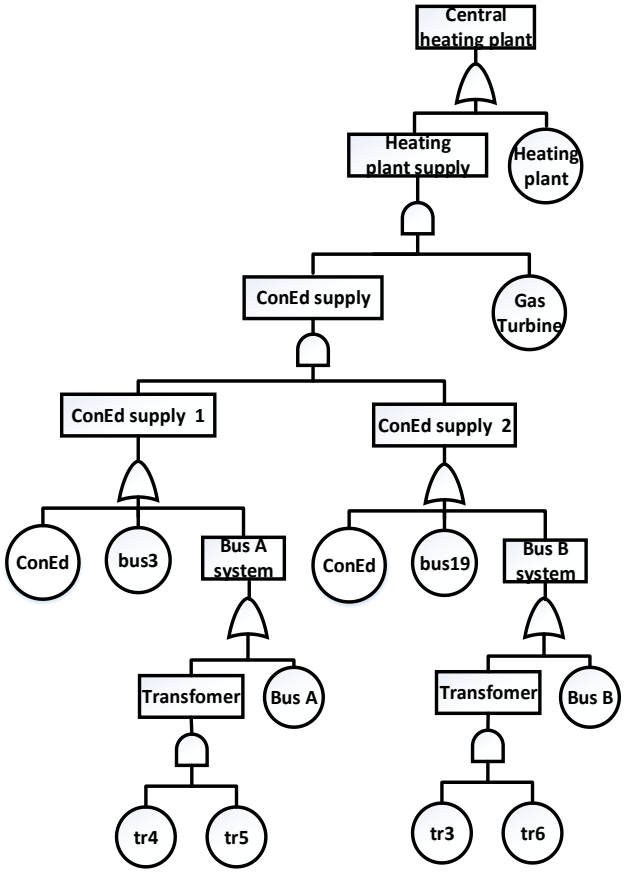

Fig. 40 (c). Central heating plant fault tree

The FT-MCS results of the silver tower garage (critical load) system reliability with the failure rate of the critical load at 4/8760, 1/8760, and 0.1/8760 failures/hour are shown in Fig.41 and the importance of the components are shown in Fig.42. We can see that the garage is the most important component under all these three situations since it is in series with all the other devices. This implies that the garage load should be very reliable itself. With the increase of the reliability of the load, its importance decreases, as shown in Fig.42. The different failure rates of the same component will result in a different component importance of all the components. The MTTFs of the systems in Fig.41 are 0.2496 years, 0.9171 years, and 5.0028 years in the MCS simulation. The MRM simulation results can be found in Fig.43 in red curves compared with the RBD results in green curve and MCS results in blue curves. The MTTFs in MRM are 0.2459 years, 0.9110 years, and 4.9810 years.

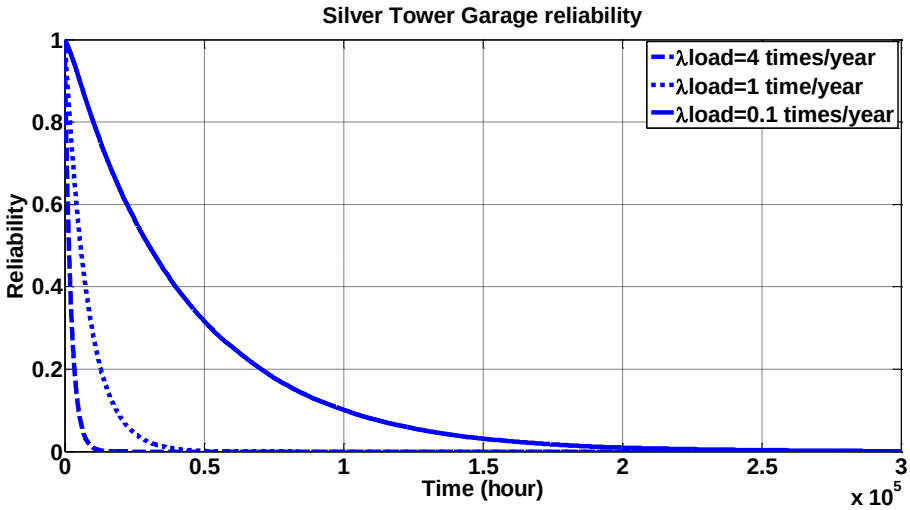

Fig. 41. Silver Tower Garage reliability (λ_{lo}=4/8760 failures/hour, λ_{lo}=1/8760 failures/hour, and λ_{lo}=0.1/8760 failures/hour)

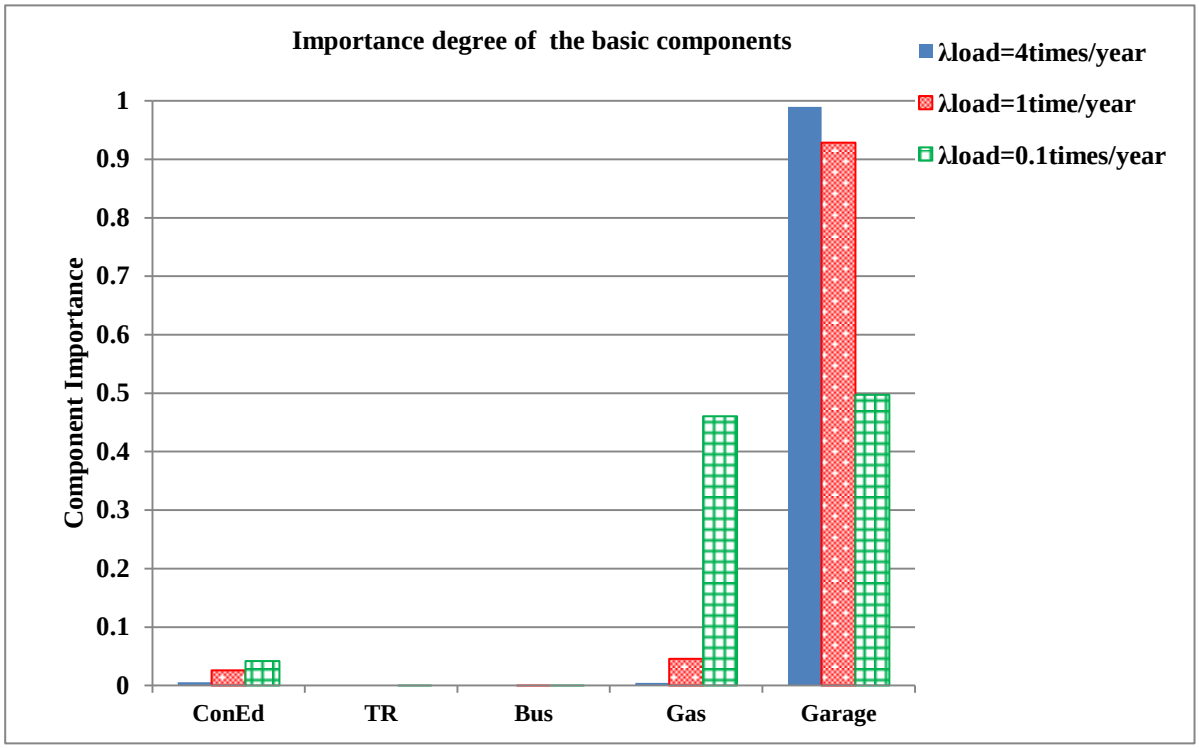

Fig. 42. Silver Tower Garage system component importance (λ_{lo}=4/8760 failures/hour, λ_{lo}=1/8760 failures/hour, and λ_{lo}=0.1/8760 failures/hour)

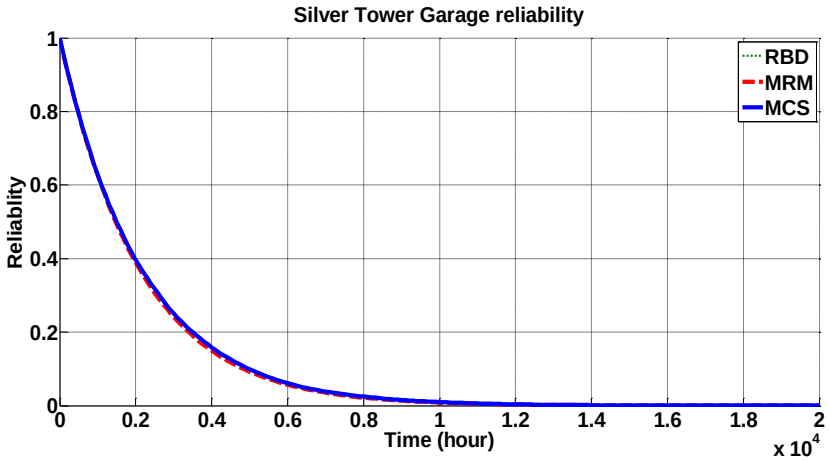

Fig. 43 (a). RBD, MCS, and MRM result comparison of Silver Tower Garage reliability (λ_{lo}=4/8760 failures/hour)

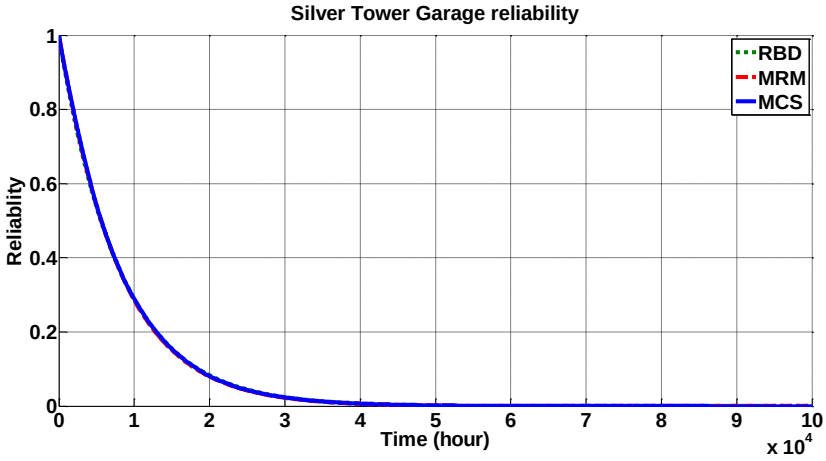

Fig. 43 (b). RBD, MCS, and MRM result comparison of Silver Tower Garage reliability (λ_{lo}=1/8760 failures/hour)

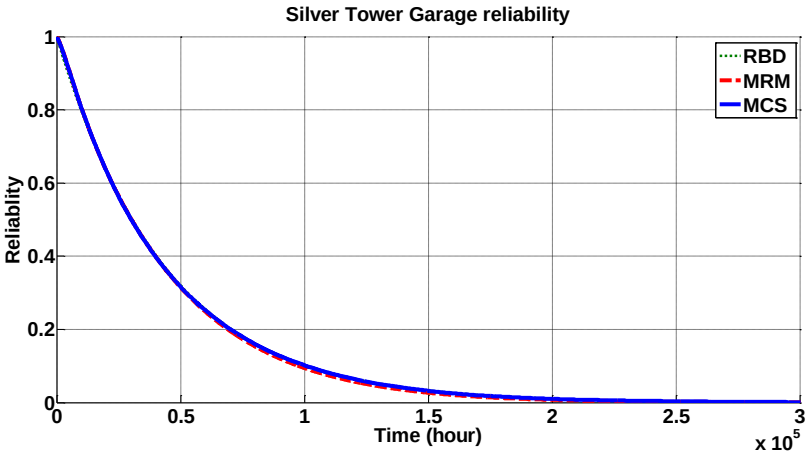

Fig. 43 (c). RBD, MCS, and MRM result comparison of Silver Tower Garage reliability (λ_{lo}=0.1/8760 failures/hour)

Since the failure rate of the central heating plant is also difficult to obtain, here in the simulation, three failure rates (4/8760, 1/8760, and 0.1/8760 failures/hour) are assumed. The simulation results of the central heating plant system are shown below. Fig.44 and Fig.45 are the results of the FT-MCS and the comparisons between RBD (green curve), MCS (blue curves) and MRM (red curves) are shown in Fig.46. MTTFs of the systems in Fig.44 are 0.2610 years, 0.9600 years, and 5.1000 years in the FT-MCS simulation. The MTTFs in MRM are 0.2500 years, 0.9243 years, and 5.0290 years.

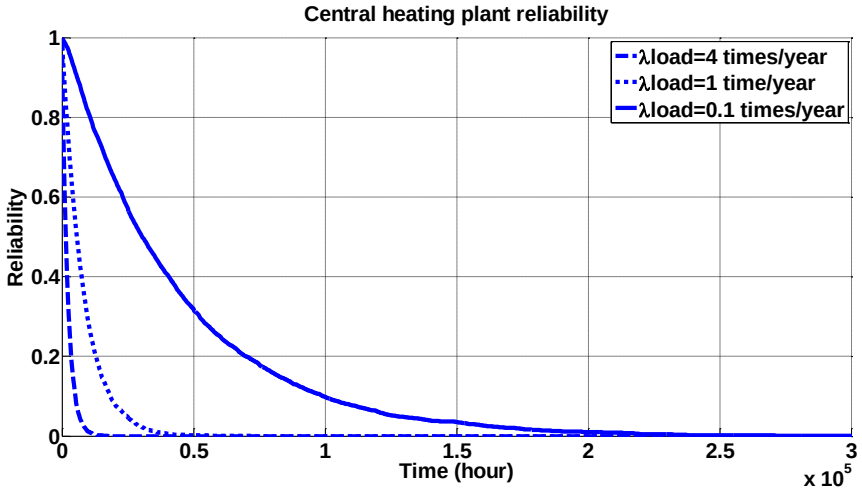

Fig. 44. Central heating plant reliability (λ_{lo}=4/8760 failures/hour, λ_{lo}=1/8760 failures/hour, λ_{lo}=0.1/8760 failures/hour)

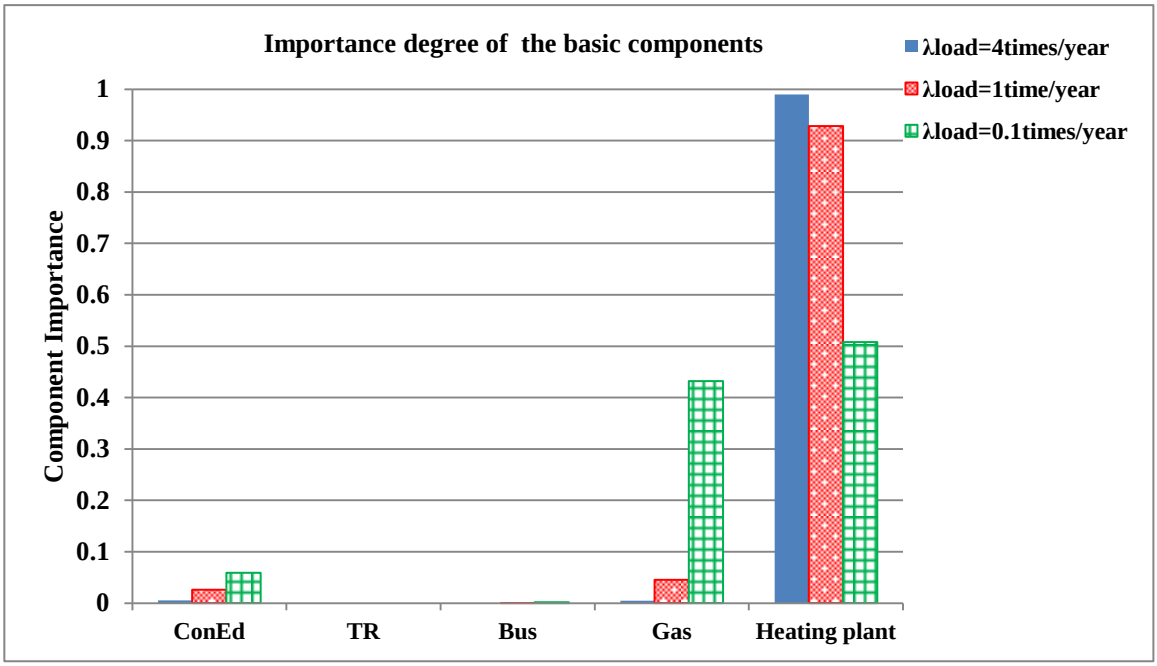

Fig. 45 . Central heating plant system component importance (λ_{lo}=4/8760 failures/hour, λ_{lo}=1/8760 failures/hour, λ_{lo}=0.1/8760 failures/hour)

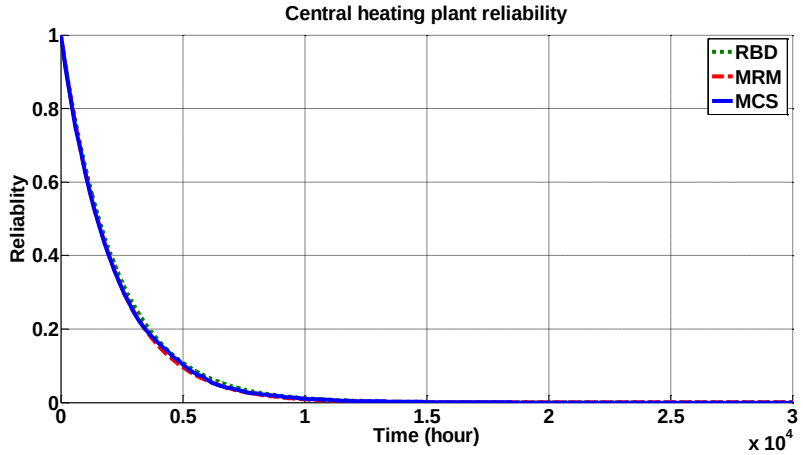

Fig. 46 (a). RBD, MCS, and MRM result comparison of Central Heating Plant reliability (λ_{lo}=4/8760 failures/hour)

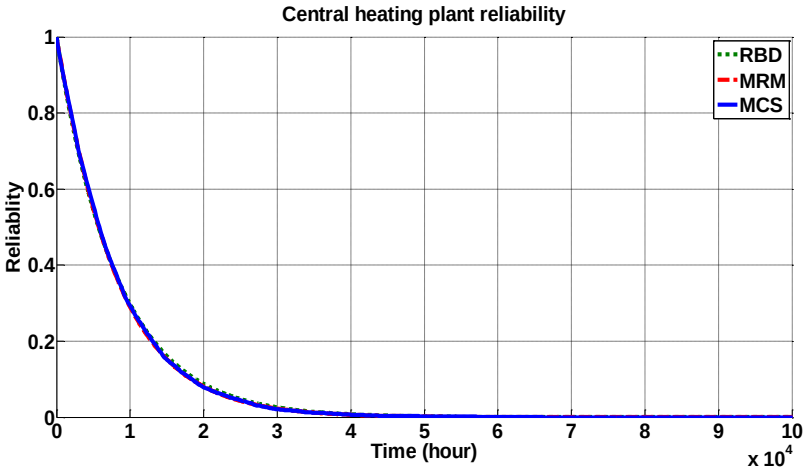

Fig. 46 (b). RBD, MCS, and MRM result comparison of Central Heating Plant reliability (λ_{lo}=1/8760 failures/hour)

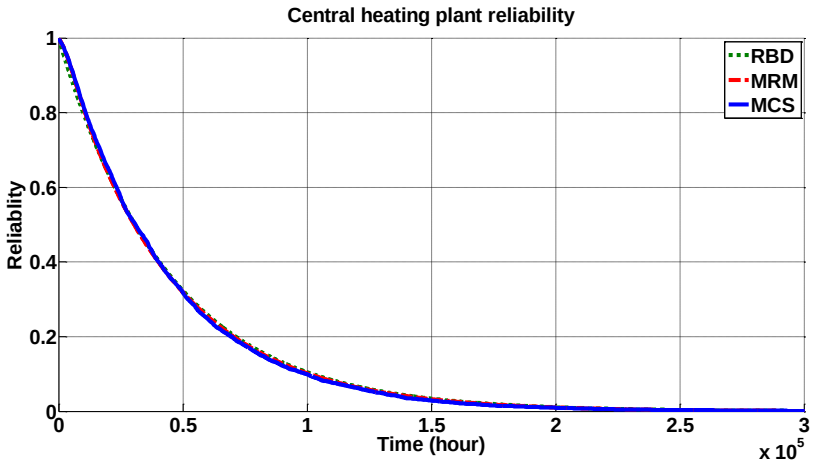

Fig. 46 (c). RBD, MCS, and MRM result comparison of Central Heating Plant reliability (λ_{lo}=0.1/8760 failures/hour)

In this chapter, two micro-grid systems are studied. King's Plaza micro-grid with four cases and NYU micro-grid with variable loads are discussed. In both micro-grid systems, the critical loads under study play a very important role in the overall systems. Figs. 38 (a), 41, and 44 clearly show the different system reliabilities with different failure rates of the loads. Comparing the first case to the forth case in King's Plaza system study, the MTTFs with and without Gridlink are similar after calculation and simulation using three methods. Therefore, if there is a series of Gridlink inverters added into system and other performance of the overall King's Plaza system can be improved in terms of fault ride through and non-synchronous interconnection, then the little decrease of the MTTF is not a significant issue. Detailed comparison of the MTTFs can be found in Chapter VII.

VI. DESIGN FOR RELIABILITY

6.1 RBD Method for PV Micro-grid System Reliability Design

With several reliability modeling and analysis methods introduced in Chapter III, and applied to micro-grids in Chapters IV and V, it is now possible to utilize such methods to close the micro-grid design loop. This will achieve a design-for-reliability approach. RBD is chosen as the method to be used due to its simplicity, but other methods can follow a similar design-for-reliability approach.

Photovoltaic (PV) panels which are fundamental components in PV systems and micro-grids are reliable and have a long performance period of around 20-25 years. But, power electronic converters are fundamental components in PV energy conversion and have shorter expected lifetimes. Thus, studying the effect of power electronics on solar PV system reliability is of interest.

The proposed PV system design for reliability method is illustrated in Fig. 47. The process starts with multiple electrical system configurations in terms of DC/DC and DC/AC conversion stages distributed across the system. Then, an RBD is established for each configuration. An arbitrary failure rate is assigned to each converter in the configuration where the failure rate is of an unknown value, then a reliability function is symbolically derived. However, failure rates used are not completely arbitrary as a meaningful range of each failure rate is determined from literature search. Sensitivity analysis of the reliability function's MTTF is performed by sweeping over this range for each arbitrary failure rate. The MTTF of each configuration is thus plotted against converters' failure rate variations to extract desired converters' failure rates that yield a target system-level MTTF. Thus, if the desired system MTTF is known, converters and their components can be selected to meet this MTTF.

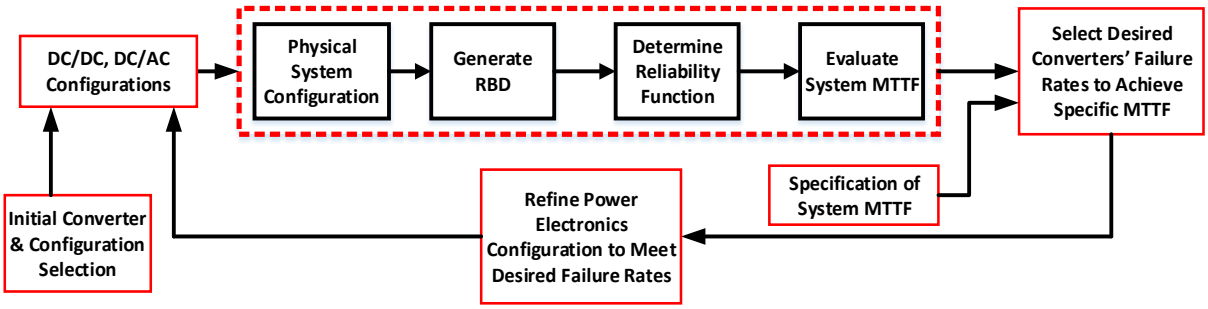

Fig.47. Description of the steps taken to evaluate the reliability of various system configurations

Several PV system configurations are shown in Fig.48. All the modules with a centralized converter or inverter are connected in both series Fig.48 (a,1) and parallel Fig.48 (a,2) configurations. The series configuration is widely used because of its low cost and ability to produce a higher DC bus voltage.

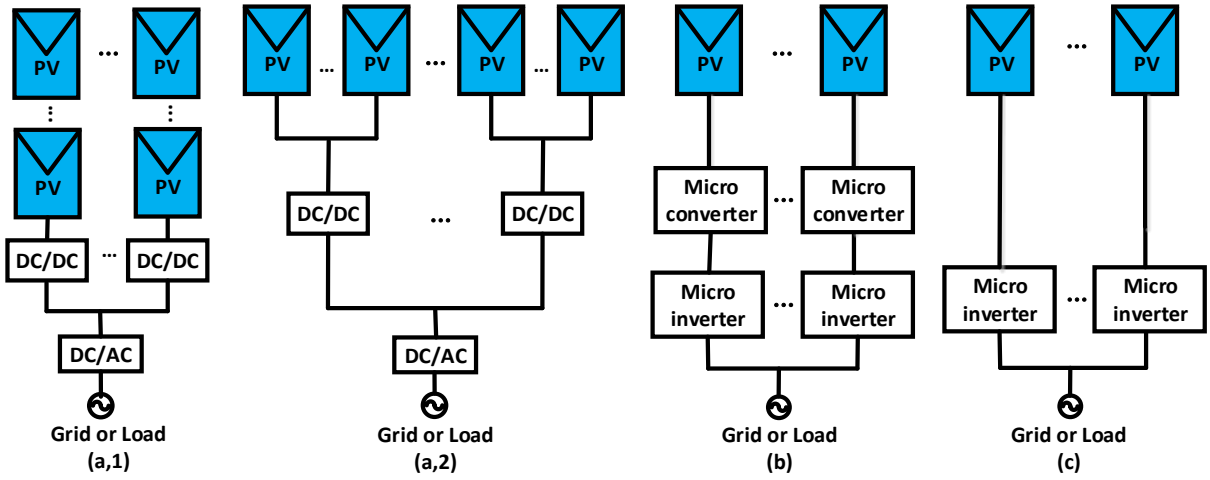

Fig. 48 Different electrical configurations of PV panel: (a,1) Series connection with central inverter, (a,2) Parallel connection with central inverter, (b).Panel with micro-converter and micro-inverter, (c) Panel with single-stage micro- inverter, e.g. boost inverter

However, micro-converter [70] (Fig. 48(b)) and micro-inverter [71] (Fig. 48 (c)) topologies have been proposed as alternatives due to their ability to extract more PV energy. The converters are usually similar in (a) and (b) except for the different power levels and thus failure rates.

For the PV panels in series and parallel configurations shown in Figs. 48(a,1) and (a,2) with

a central inverter, the RBD should be the same even though their electrical systems are different. Fig. 49 (a) shows the RBD of Figs. 48 (a,1) and (a,2). With appropriate protection systems, these configurations maintain operation even if one DC/DC stage fails. The RBD of the systems with two-stage micro-inverters shown in Fig. 48 (b) and single-stage micro-inverters shown in Fig. 48 (c) are shown in Figs. 49 (b) and (c), respectively. Assuming that the components are non-repairable, DC/DC and micro-converter failure rates are assumed to be λ_2, the centralized inverter failure rate as λ_1, the micro-inverter failure rate in Fig.49 (b) as λ_3, and the micro-inverter failure rate in Fig. 49(c) as λ_4. Micro-inverter2 is more complex than micro-inverter1 since the former includes a single-stage, e.g. boost inverter [72], and therefore they have different failure rates.

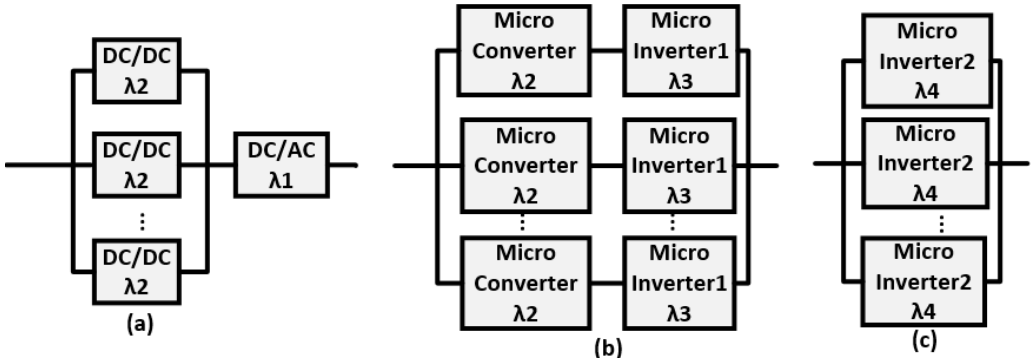

Fig.49 (a) RBD with centralized inverter

(b) RBD with two-stage micro-inverter (micro-converter and micro-inverter)

(c) RBD with single-stage micro-inverter

By implementing equations (2.8)-(2.11) to the RBDs in Figs. 49 (a)-(c), MTTF estimates for each RBD can be analytically found as shown in equations (6.1)-(6.3). The Gamma function (Γ) is defined as $\Gamma(n)=(n-1)!$. Assuming *n* DC/DC converters, *n* micro-converters, and *n*

micro-inverters are in Fig.48. $MTTF_a$, $MTTF_b$, and $MTTF_c$ are the MTTFs of the systems in Fig.49 (a)-(c), respectively.

$$MTTF_a = \frac{1}{\lambda_1} - \frac{\Gamma(\frac{\lambda_1}{\lambda_2})\Gamma(1+n)}{\lambda_2\Gamma(1+n+\frac{\lambda_1}{\lambda_2})} \tag{6.1}$$

$$MTTF_b = \frac{1}{\lambda_2+\lambda_3}\sum_{x=1}^{n}\binom{n}{x}\frac{(-1)^{x+1}}{x} \tag{6.2}$$

$$MTTF_c = \frac{1}{\lambda_4}\sum_{x=1}^{n}\binom{n}{x}\frac{(-1)^{x+1}}{x} \tag{6.3}$$

Numerical MTTF values can then be determined by implementing equations (6.1)-(6.3) in MATLAB for given values of λ_1, ..., λ_4. Theoretically, if a PV panel has a lifetime of 20-30 years, the converter and the inverter systems should also have a 20-30 year lifetime in order to maintain the system reliability, but this is not the case in real systems. Since values of λ_1, ..., λ_4 are difficult to determine in an accurate manner, ranges for these failure rates are used to evaluate the MTTF of each configuration. Based on the literature review of the failure rates for different converters, a thorough review of MTTFs and failure rates of the converters is presented in Table 13, which can be used as a reference to choose the suitable converters, more details of the converters can be found in [73-83]. Since some of the failure rates in the table are too small to affect the system MTTF, or too large to dominate the system's reliability, failure rates in the range of 2.5-25e^{-6} failures/hour are considered here.

TABLE 13. EXAMPLE CONVERTER TYPES AND MTTFS [73-83]

Type	MTTF (year)	Failure rate (failures/hour 10^{-6})	Type	MTTF (year)	Failure rate (failures/hour 10^{-6})
Rectifier/inverter	3.67-4.3	26.6-31.09	IBH converter	2.03-14.27	8-56.23
Intermediate bus converter	1.16-9.51	12-98	Inverter	9.71	11.75
Boost converter	6.93	16.4718	Boost inverter	4.07-16.3	7-28
DC/DC converter	9.92-17.84 14.38-24.82	6.4-11.5 (MOSFET based) 4.6-7.94 (IGBT based)	DC/AC converter	6.52-11.41 10.99-17.84	10-17.5 (MOSFET based) 6.4-10.38 (IGBT based)
Buck converter	25.41-26.11	4.372-4.494	Fly-back inverter	20.47	5.577
Back-to-back converter	3.68	31	Matrix converter	3.98	28.66
F3E-based PV inverters	11.4155	10			

By sweeping over ranges of λ_1, ..., λ_4, Fig.50 shows plots of $MTTF_a$, $MTTF_b$, and $MTTF_c$. To demonstrate how these MTTFs are used, a system-level MTTF between 20 and 30 years is used as an example with n=10, which leads to specific ranges for λ_1, ..., λ_4 highlighted in yellow in Figs. 50 (d)-(f). For example, Fig. 50 (e) shows that λ_2 and λ_3 should be between 0.9 and 1.5 x 10^{-6} failures per hour to achieve a desired system-level MTTF between 20 and 30 years.

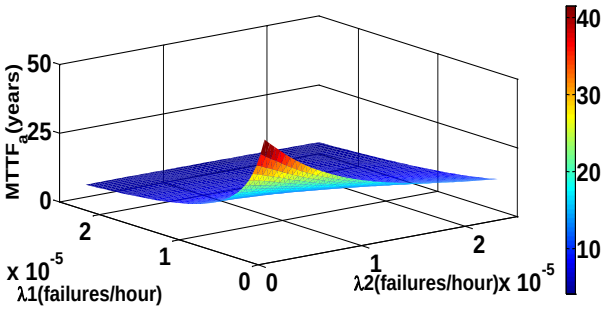

(a)

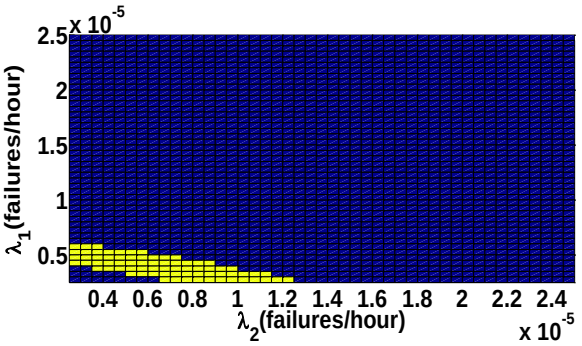

(d)

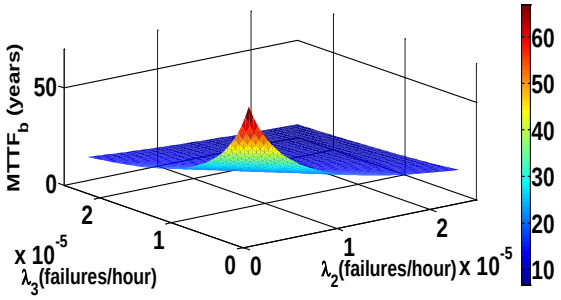

(b)

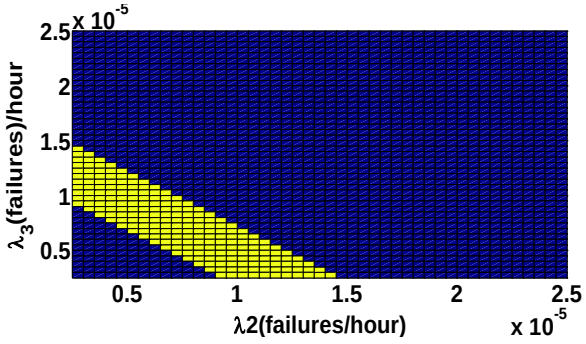

(e)

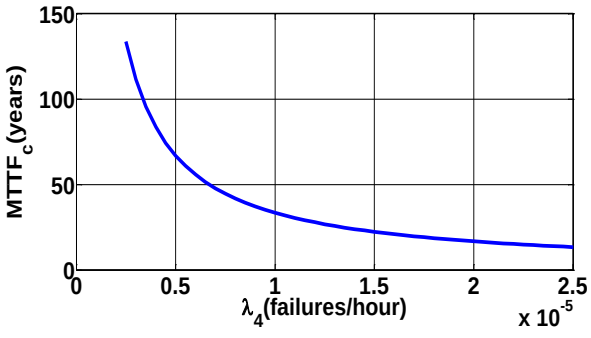

(c)

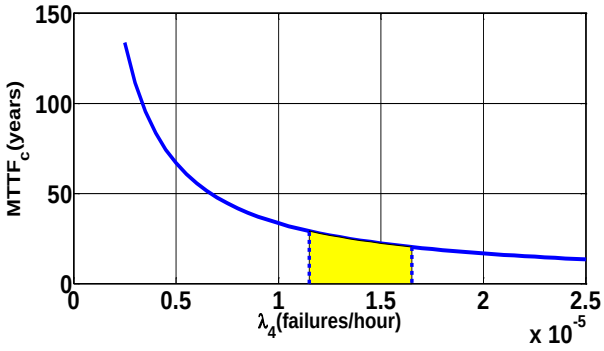

(f)

Fig.50 Variation of (a) $MTTF_a$, (b) $MTTF_b$, and (c) $MTTF_c$ 3D plots, and 2D plots (d), (e), and (f), respectively at n=10

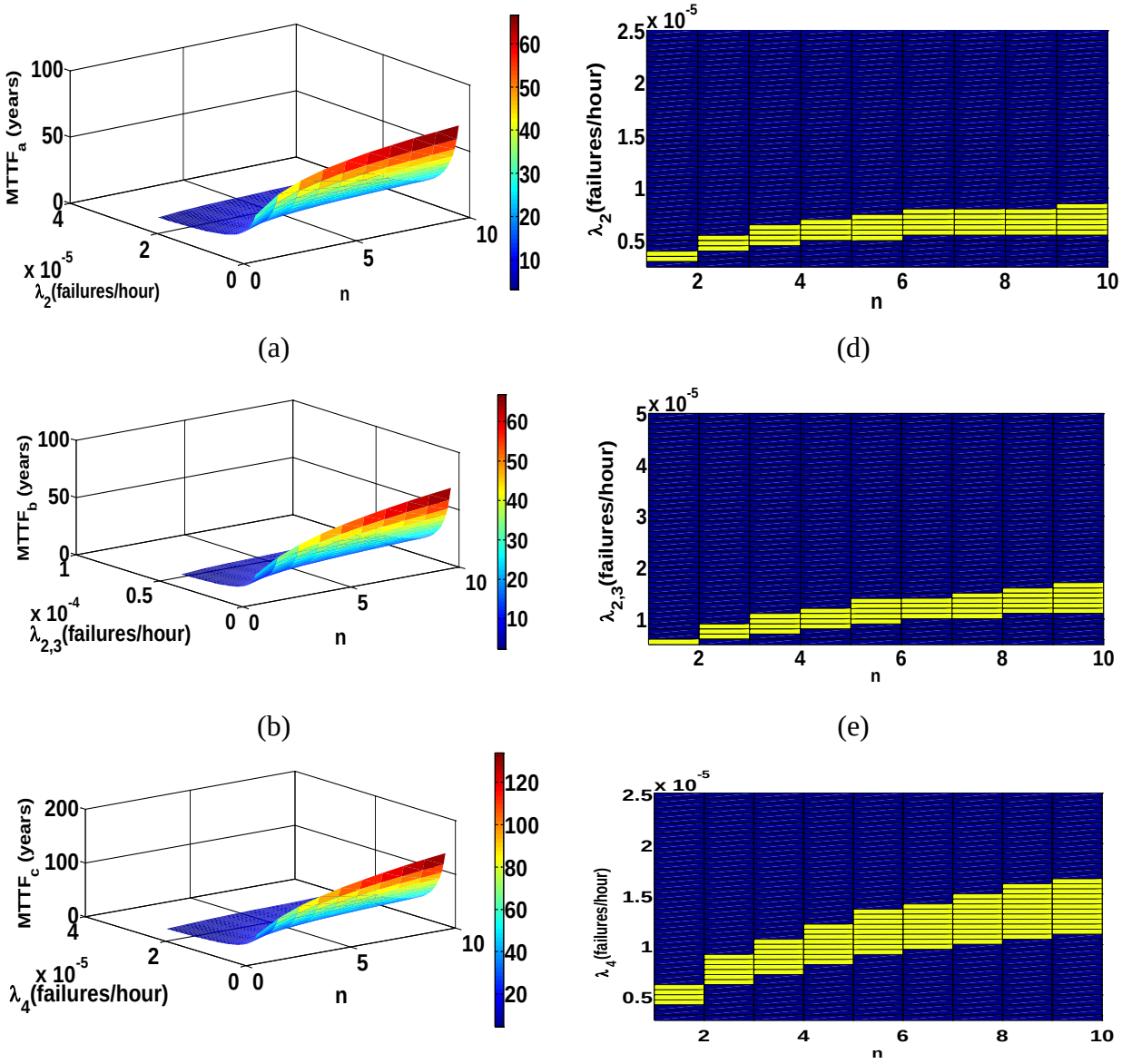

Fig.51 Variation of (a) $MTTF_a$, (b) $MTTF_b$, and (c) $MTTF_c$ 3D plots, and 2D plots (d), (e), and (f), respectively at *various* n with an assumption that $\lambda_1 = \lambda_2 = \lambda_3$.

The effect of different number of panels is studied by varying *n*. For simpler visualization, λ_1, λ_2, and λ_3 are all assumed equal. Results for varying *n* are shown in Fig. 51. Note that as *n* increases, all configurations are shown to tolerate higher failure rates as expected due to redundant PV panels being available in the system. Note that for configurations in Figs. 48 (b)

and (c), the number of converters also increases with the number of panels and thus converters need to be more reliable with small values of *n* to ensure a 20-30 year system MTTF is achieved. Note that the failure rate ranges and choice of specific system MTTF ranges are shown for illustrative purposes to demonstrate the proposed methodology.

The proposed design-for-reliability approach for PV systems based on the results in Figs. 50 and 51 can thus be summarized as shown in the dotted box of Fig.52. Future work can address other portions of this proposed approach

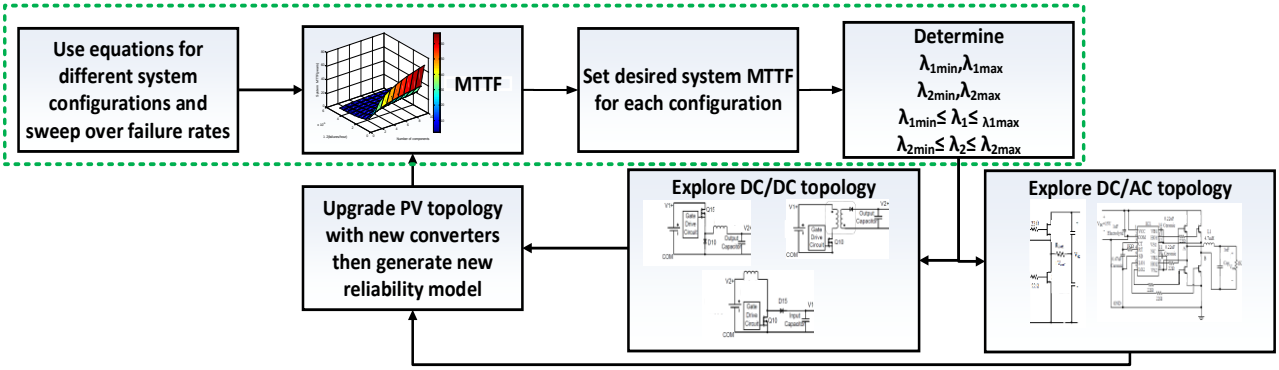

Fig.52. PV system design for reliability approach

This Chapter presents an RBD-based approach to evaluate PV system reliability for various configurations to aid in the design-for-reliability of power electronics. The proper number and type of converters, inverters, and PV panels are determined based on a desired system MTTF, and desired converter failure rates are extracted. The proposed system-level design procedure is explained through three main PV system configurations for which MTTFs are evaluated for a range of converter failure rates. Tighter failure rate ranges are then extracted for desired MTTFs for each system, and are expected to be used with power electronic converter design and selection. The proposed approach is expected to be scalable to larger systems, adjustable to

various PV system configurations, and applicable to other energy systems where the reliability of power electronics is a design criterion.

VII. DISCUSSION AND COMPARISON

The MTTF results from the three reliability modeling and analysis methods for three cases with different reliability objectives show how each method can be applied to micro-grid reliability evaluation. The MTTFs calculated using the RBD method are approximately equal to the results in the MCS and MRM, as shown in Tables 14-17. The MTTFs in Table 14 are similar since the failure rate of the critical load is not changed. The only change is the equivalent failure rates of the distributed generation resources which has small importance compared to the critical load. In Tables 15-17, the MTTFs are different because of the variable failure rates of the loads.

However, FTA on its own does not consider components' failure rates and considers the structure importance rates which differ with the reliability objective defined.

Based on applying these three different methods to example micro-grid case studies, comparisons can be drawn as summarized in Tables 18 and 19.

TABLE 14. THE COMPARISON OF THREE METHODS OF THREE OBJECTIVES FOR CASE STUDY #1 UCONN MICRO-GRID

Methods	MTTF (years)		
	First objective	Second objective	Third objective
RBD	25.466	25.213	25.067
FTA-MCS	25.683	25.415	25.083
MRM	26.236	26.060	25.830

TABLE 15 MTTF COMPARISON OF CASE STUDY #2 KING'S PLAZA MALL

Method	MTTF(year)			
	λ_{load}=1/0.25 year	λ_{load}=1/5 year	Ideal load	No Gridlink
RBD	0.2312	1.9947	5.3134	0.2364
FTA-MC	0.2456	2.0865	5.4688	0.2488
MRM	0.2389	2.0779	5.3676	0.2393

TABLE 16 MTTF COMPARISON OF CASE STUDY #3 NYU (SILVER TOWER GARAGE)

Method	MTTF(year)		
	λ_{load}=0.25 year	λ_{load}=1 year	λ_{load}=10 year
RBD	0.2466	0.9195	5.0208
FTA-MC	0.2496	0.9171	5.0028
MRM	0.2459	0.9110	4.9810

TABLE 17 MTTF COMPARISON OF CASE STUDY #3 NYU (CENTRAL HEATING PLANT)

Method	MTTF(year)		
	λ_{load}=0.25 year	λ_{load}=1 year	λ_{load}=10 year
RBD	0.2570	0.9400	5.0610
FTA-MC	0.2610	0.9600	5.1000
MRM	0.2500	0.9234	5.0290

TABLE 18. THE COMPARISON OF THREE METHODS

Characteristics	RBD	FTA	FTA-MCS	MRM
Static: the diagram changes without time	o	o		
Dynamic: the diagram changes with time			o	o
Logic based: depends on the "AND" and "OR" relationship between the failures	o	o	o	
State based: depends on the system states when the faults happen.				o
Top-down: depends on system hierarchy	o	o	o	

TABLE 19. SUMMARY OF ADVANTAGES (A) AND DISADVANTAGES (D) OF THE THREE METHODS

Method	Advantages	Disadvantages
RBD	A1: Easy to build simple logic diagrams A2: Can evaluate system reliability ($R(t)$, MTTF)	D1: Some complex structures and component sharing cannot be clearly represented. D2: Formulations of MTTF can become very complicated
FTA	A1: Easy to build for simple systems with a small number of failures A2: Can show multiple failures or combinations of failures A3: Quickly exposes critical cut sets that lead to system failure	D1: Time consuming to build for larger systems D2: Requires detailed knowledge of the design, construction and operation of the system D3: Cannot account for failure rates or repair rates are state-dependent
MRM	A1: Sequential system states and fault propagation can be accounted for A2: Captures fault coverage rates and state-dependent failure rates	D1: Incredibly large number of states for complex systems D2:Hard to get accurate failure rates for state transitions

VIII. CONCLUSIONS

This thesis provides an overview of the fault universe of major components in a micro-grid and how these failures can affect the reliability of a micro-grid. In the thesis, three reliability analysis approaches RBD, FTA, and MRM used to evaluate the micro-grid system reliability are analyzed and compared. Focus is given to physical system failure. Reliability analysis of three case studies is shown using the three different methods: RBD, FTA, and MRM. The MTTF of various micro-grids with different reliability objectives and loads are calculated using the estimated failure rates. The FT-MCS and MRM methods are implemented in software such as MTALAB to get the reliability functions of the each micro-grid case. Results show sample reliability models of the micro-grid for a reliability objective being to support a critical load, but other objectives such as full operation in islanding mode can be used to generate different reliability models and other distributions of the component failure function will lead to different result. Results illustrate that all methods provide similar MTTF approximation but will with different approaches. The effect of critical load reliability is also studied. A design-for-reliability approach is proposed to get higher standards for micro-grid power electronics reliability through a close loop iterative design process.

These reliability modeling methods can also be applied to other larger power and energy systems for lifetime estimation and to enhance the system's reliability at the design stage.

References

1. DOE, “Final report on the august 14, 2003 blackout in the united states and canada,” U.S.-Canada Power System Outage Task Force, 2004.
2. Marko Cepin, Assessment of power system reliability methods and applications, 2011
3. [Online] Available: http://www.solarcurator.com/2012/06/13/module-failure-from-an-otherworldly-source/
4. [Online] Available: http://livewireinnovation.com/
5. M. Rausand and A. Høyland, System Reliability Theory: Models, Statistical Methods, and Applications, 2nd ed. Hoboken, NJ: Wiley, 2005.
6. W. Li, et al. "Power system reliability analysis system based on PSASP and fault enumeration method and applications." in IEEE China International Conference on Electricity Distribution (CICED), pp.1323-1326, 2014
7. S. Babu, H. Patrik, and J. H. Jurgensen. "On the status of reliability studies involving primary and secondary equipment applied to power system," in IEEE International Conference on Probabilistic Methods Applied to Power Systems (PMAPS), pp. 1-6, 2014.
8. Y. Xiang, L. Wang, and F. Tian. "A preliminary study of power system reliability considering cloud service reliability," in IEEE International Conference on Power System Technology (POWERCON), pp. 2031-2036, 2014.
9. W. Peng, et al. "A Bayesian approach for system reliability analysis with multilevel pass-fail, lifetime and degradation data sets," IEEE Trans. Reliab., vol.62, no.3, pp 689-699, 2013
10. IEEE Guide for Electric Power Distribution Reliability Indices
11. F. Z. Peng, Y. W. Li and L. M. Tolbert, "Control and protection of power electronics interfaced distributed generation systems in a customer-driven microgrid," in IEEE Power & Energy Society General Meeting, pp.1-8, 2009.
12. J. Hare, X. Shi, S. Gupta and A. Bazzi “A review of faults and fault diagnosis in micro-grids electrical energy infrastructure,” in Energy Conversion Congress and Exposition (ECCE), PP.3325-3332, 2014.
13. W. Herrmann, W. Wiesner and W. Vaassen, "Hot spot investigations on PV modules-new concepts for a test standard and consequences for module design with respect to bypass diodes," in IEEE Photovoltaic Specialists Conference, pp. 1129-1132, 1997.
14. T. Takashima, et al., "Experimental studies of fault location in PV module strings," Solar Energy Materials and Solar Cells, vol. 93, no. 6, pp. 1079-1082, 2009.
15. Yu, Yong, et al. "Fault diagnosis and life prediction of dc-link aluminum electrolytic capacitors used in three-phase ac/dc/ac converters," in IEEE Instrumentation, Measurement, Computer, Communication and Control (IMCCC), pp.825-830, 2012.
16. F. J. Espadafor, J. B. Villanueva and M. T. García, "Analysis of a diesel generator crankshaft failure," Engineering Failure Analysis, vol. 16, no. 7, pp. 2333-2341, 2009.
17. J. Yang, L. Pu, Z. Wang, Y. Zhou and X. Yan, "Fault detection in a diesel engine by analysing the instantaneous angular speed," Mechanical Systems and Signal Processing, vol. 15, no. 3, pp. 549-564, 2001.

18. M. A. S. K. Khan, T. S. Radwan and M. A. Rahman, "Real-time implementation of wavelet packet transform-based diagnosis and protection of three-phase induction motors," IEEE Transactions on Energy Conversion, vol. 22, no. 3, pp. 647-655, 2007.
19. J. A. Haylock, et. al. , "Operation of fault tolerant machines with winding failures," IEEE Transactions on Energy Conversion, vol. 14, no. 4, pp. 1490-1495, 1999.
20. M. Biet and A. Bijeire, "Rotor faults diagnosis in synchronous generators using feature selection and nearest neighbors rule," in IEEE International Symposium on Diagnostics for Electric Machines, Power Electronics & Drives, pp.300-306, 2011.
21. J. Wu, et al., "A review of PEM fuel cell durability: degradation mechanisms and mitigation strategies," Journal of Power Sources, vol. 184, no. 1, pp. 104-119, 2008.
22. H. Li, Y. Tang, Z. Wang, Z. Shi, S. Wu, D. Song, J. Zhang, et al., "A review of water flooding issues in the proton exchange membrane fuel cell," Journal of Power Sources, vol. 178, no. 1, pp. 103-117, 2008.
23. T. Escobet, D. Feroldi, S. De Lira, V. Puig, J. Quevedo, J. Riera and M. Serra, "Model-based fault diagnosis in PEM fuel cell systems," Journal of Power Sources, vol. 192, no. 1, pp. 216-223, 2009.
24. Z. Hameed, Y. S. Hong, Y. M. Cho, S. H. Ahn and C. K. Song, "Condition monitoring and fault detection of wind turbines and related algorithms: A review," Renewable and Sustainable energy reviews, vol. 13, no. 1, pp. 1-39, 2009.
25. M. Nie and L. Wang, "Review of condition monitoring and fault diagnosis technologies for wind turbine gearbox," Procedia CIRP, vol. 11, pp. 287-290, 2013.
26. “Timken bearing damage analysis with lubrication reference guide,” The Timken Company, 2011
27. A. Yazidi, H. Henao, G. A. Capolino, D. Casadei, F. Filippetti and C. Fossi, "Simulation of a doubly-fed induction machine for wind turbine generator fault analysis," in IEEE International Symposium on Diagnostics for Electric Machines, Power Electronics and Drives, pp.1-6, 2005.
28. H. Arabian-Hoseynabadi, H. Oraee and P. J. Tavner, "Failure modes and effects analysis (FMEA) for wind turbines," International Journal of Electrical Power & Energy Systems, vol. 32, no. 7, pp. 817-824, 2010.
29. D. Shah, S. Nandi and P. Neti, "Stator-interturn-fault detection of doubly fed induction generators using rotor-current and search-coil-voltage signature analysis," IEEE Transactions on Industry Applications, vol. 45, no. 5, pp. 1831-1842, 2009.
30. N. A. Al-Nuaim and H. A. Toliyat, "A novel method for modeling dynamic air-gap eccentricity in synchronous machines based on modified winding function theory," IEEE Transactions on Energy Conversion, vol. 13, no. 2, pp. 156-162, 1998.
31. S. Jan, R. Afzal, and A. Khan, "Transformer Failures, Causes & Impact," in International Conference Data Mining, Civil and Mechanical Engineering, pp. 49-52, 2015
32. A. Franzén and S. Karlsson. "Failure modes and effects analysis of transformers," Electrical Engineering, Royal Institute of Technology KTH: Stokholm Sweden, 2007

33. Top Five Switchgear Failure Causes [On line] Available: www. Netaworld.org/sites/default/files/public/neta-jounals/NWsu10-NoOutage-Genutis.pdf
34. B. Yao et al. "Reliability and failure analysis of DC/DC converter and case studies," in IEEE Quality, Reliability, Risk, Maintenance, and Safety Engineering International Conference, pp.1133-1135, 2013.
35. M. Paolone, et al., "Lightning induced disturbances in buried cables-part II: experiment and model validation," IEEE Transactions on Electromagnetic Compatibility, vol. 47, no. 3, pp. 509-520, 2005.
36. H. Gargama and S. K. Chaturvedi, "Criticality Assessment Models for Failure Mode Effects and Criticality," vol. 60, no. 1, pp. 102–110, 2011.
37. H. S. Son, R. Y. C. Kim, and Y. B. Park, "Test Case Generation from Cause-Effect Graph Based on Model Transformation," in Information Science and Applications (ICISA), pp. 1–4, 2014.
38. J. T. Olson, J. W. Rozenblit, C. Talarico, and W. Jacak, "Hardware/Software Partitioning Using Bayesian Belief Networks," IEEE Trans. Syst. Man, Cybern. - Part A Syst. Humans, vol. 37, no. 5, pp. 655–668, Sep. 2007.
39. J. D. Andrews and S. J. Dunnett, "Event-tree analysis using binary decision diagrams," IEEE Trans. Reliab., vol. 49, no. 2, pp. 230–238, Jun. 2000.
40. H. Aliee and H. Zarandi, "A fast and accurate fault tree analysis based on stochastic logic implemented on field-programmable gate arrays," IEEE Trans. Reliab., vol. 62, no. 1, pp. 13–22, 2013.
41. P. Henneaux, S. Member, P. Labeau, and J. Maun, "Blackout Probabilistic Risk Assessment and Thermal Effects : Impacts of Changes in Generation," IEEE Trans. Power syst., vol. 28, no. 4, pp. 4722–4731, 2013.
42. Y. Li, E. Zio, S. Member, Y. Lin, and M. Carlo, "A Multistate Physics Model of Component Degradation Based on Stochastic Petri Nets and Simulation," IEEE Trans. Reliab., vol. 61, no. 4, pp. 921–931, 2012.
43. W. Wang, J. M. Loman, R. G. Arno, P. Vassiliou, E. R. Furlong, and D. Ogden, "Reliability Block Diagram Simulation Techniques Applied to the IEEE Std. 493 Standard Network," IEEE Trans. Ind. Appl., vol. 40, no. 3, pp. 887–895, May 2004.
44. M. Vázquez and I. ReyIStolle, "Photovoltaic module reliability model based on field degradation studies," Prog. Photovoltaics Research and Applications, no. March, pp. 419–433, 2008.
45. "Military Handbook Reliability Prediction of Electronics Equipment," MIL-HDBK-217F, Department of Defense, 1995.
46. M. Vázquez and I. ReyIStolle, "Photovoltaic module reliability model based on field degradation studies," in Progress in Photovoltaics: Research and Applications,pp.419-433,2008.
47. T. Khatib, a. Mohamed, K. Sopian, and M. Mahmoud, "Optimal sizing of building integrated hybrid PV/diesel generator system for zero load rejection for Malaysia," Energy Build., vol. 43, no. 12, pp. 3430–3435, 2011.

48. 2011 Alkaline Membrane Fuel Cell Workshop Final Report [Online] Available at: http://www.nrel.gov/docs/fy12osti/54297.pdf
49. Purecell system model 400 [Online] Available at: http:// sites.ieee.org /isgt/ files/2013/03/ Hayes6B.pdf
50. Powered With Preventive Maintenance: Longer Standby Generator Life [Online]Available at: http:// www. maintenancetechnology.com /2012 / 03/powered - with - preventive-maintenance- longer- standby- generator- life/
51. [Online] Available at: http://freeenergygenerator.us/
52. How to predict life span of the switchgear? [Online] Available at: http://electrical-engineering-portal.com/how-to-predict-life-span-of-the-switchgear
53. V. Renjith, G. Madhu, V. Nayagam, and B. Bhasi, "Two-dimensional fuzzy fault tree analysis for chlorine release from a chlor-alkali industry using expert elicitation," Journal of hazardous materials, vol. 183, no. 1–3, pp. 103–10, 2010.
54. S. Agarwal and M. Kansal, "Fuzzy fault tree analysis of a power transformer," in IEEE Int. Conf. Qual. Reliab. Risk, Maintenance, Saf. Eng., pp. 1000–1004, 2012.
55. D. Singer, "A fuzzy set approach to fault tree and reliability analysis," Fuzzy sets and systems vol.34, no.2, pp.145-155, 1990
56. Z. Dan, C. Li, and Z. Wang. "Power transformer lifetime modeling," in IEEE Conference on Prognostics and System Health Management (PHM), pp.1-7, 2012.
57. P. Gill, "Electrical power equipment maintenance and testing," CRC press, 2008.
58. H. Picard et al. "Decision model for End of Life management of switchgears," in IEEE Electrical and Instrumentation Applications in the Petroleum & Chemical Industry, pp.1-10, 2007.
59. J.Shi. "Multi-factors ageing condition inspection and lifetime prediction for low voltage fuse," in IEEE Computer Science and Information Processing (CSIP), pp.1227-1231, 2012.
60. J. Shi, et al. "Ageing assessment, condition inspection and lifetime evaluation for safety related fuse in nuclear power plant," in 18th International Conference on Nuclear Engineering. American Society of Mechanical Engineers, pp.1-5, 2010.
61. [Online]Available:http://www.cooperindustries.com/content/dam/public/bussmann/Electrical/Resources/solution-center/frequently_asked_questions/BUS_Ele_FAQ_Fuse_Element_Fatigue.pdf
62. [Online]Available:http://www.electricaltechnology.org/2013/01/what-is-normal-or-average-life.html
63. [Online] Available: https://stevenengineering.com/tech_support/PDFs/45TMEDVOLT.pdf
64. [Online]Available:https://blog.summit.com/wp-content/uploads/2010/06/GE-DEA491A-QL-Ultra- Transformers- Flyer-4 -28.pdf
65. [Online]Available:http://www.dynamicelec.com/zlargefilespdf/Transformer%20Life%20Expectancy.pdf
66. [Online]Available:http://renewablesgrid.eu/uploads/media/Electricity_Transmission_Costing_Study_Parsons_Brinckerhoff.pdf

67. [Online]Available:http://www.energy.siemens.com/us/pool/hq/energy-topics/pdfs/en/gas-turbines-power-plants/5_Lifetime_Extension_for_Siemens.pdf
68. [Online] Available: http://www.ct.gov/csc/lib/csc/lifecycle-1996.pdf
69. [Online] Available: http://www.jcmiras.net/surge/p151.htm
70. S. Harb, H. Hu, N. Kutkut, I. Batarseh, and Z. Shen, "A three-port Photovoltaic (PV) micro-inverter with power decoupling capability," in IEEE Twenty-Sixth Annu. IEEE Appl. Power Electron. Conf. Expo.,pp. 203–208, 2011.
71. H. Gui, Z. Zhang, X. He, and Y. Liu, "A high voltage-gain LLC micro-converter with high efficiency in wide input range for PV applications," in IEEE Appl. Power Electron. Conf. Expo.(APEC), pp. 637–642, 2014.
72. P. G. Barbosa, H. Antonio, C. Braga, and S. Member, "Boost Current Multilevel Inverter and Its Application Photovoltaic Systems," IEEE Trans. Power Electron. vol. 21, no. 4, pp. 1116–1124, 2006.
73. Aten, M., et al. "Reliability comparison of matrix and other converter topologies," IEEE Trans. Aerosp. Electron. Syst., vol.42, no.3, pp.867-875,2006.
74. A. Mehdipour and S. Farhangi, "Comparison of three isolated bi-directional DC/DC converter topologies for a backup photovoltaic application," in IEEE Int. Conf. Electr. Power Energy Convers. Syst., pp. 1–5, 2011.
75. C. Rodriguez and G. a. J. Amaratunga, "Long-Lifetime Power Inverter for Photovoltaic AC Modules," IEEE Trans. Ind. Electron., vol. 55, no. 7, pp. 2593–2601, 2008.
76. M. K. Alam and F. H. Khan, "Reliability analysis and performance degradation of a Boost converter," in IEEE Energy Convers. Congr. Expo., pp. 5592–5597, 2013.
77. F. Chan, H. Calleja, and S. Member, "Reliability Estimation of Three Single-Phase Topologies in Grid-Connected PV Systems," IEEE Trans. Ind. Electron., vol. 58, no. 7, pp. 2683–2689, 2011.
78. D. Strickland and N. Mukherjee, "Second Life Battery Energy Storage Systems: Converter Topology and Redundancy Selection," in IEEE IET Int. Conf. Power Electron. Mach. Drives, pp. 1-6, 2014.
79. V. Javadian and S. Kaboli, "Reliability assessment of some high side MOSFET drivers for buck converter," in IEEE Int. Conf. Electr. Power Energy Convers. Syst., pp. 1–6, 2013.
80. S. Harb, S. Member, R. S. Balog, and S. Member, "Reliability of Candidate Photovoltaic Topologies — A Usage Model Approach," IEEE Trans. Power Electron., vol. 28, no. 6, pp. 3019–3027, 2013.
81. M. Arifujjaman, "Reliability comparison of power electronic converters for grid-connected 1.5kW wind energy conversion system," Renew. Energy, vol. 57, pp. 348–357, 2013.
82. P. W. Wheeler, J. C. Clare, L. De Lillo, and K. J. Bradley, "A Comparison of the Reliability of a Matrix Converter and a Controlled Rectifier-Inverter," in IEEE Power Electronics and Applications, pp.1-7,2005.
83. K. Gopfrich, "PV-inverter with improved efficiency and lifetime." in IEEE Power Electronics and Applications, pp.1-6, 2009.

Appendix A: Publications

[1]. X. Shi and A. Bazzi, "Fault tree reliability analysis of a micro-grid using Monte Carlo simulations," in Proc. IEEE Power and Energy Conference at Illinois (PECI), pp. 1-5, 2015.
[2]. X. Shi and A. Bazzi, “Reliability Modeling and Analysis of a Micro-grid with Significant Clean Energy Penetration,” in ICPE, ECCE Asia, pp. 202-207, 2015.
[3]. X. Shi and A. Bazzi, “Solar Photovoltaic Power Electronic Systems: Design for Reliability Approach” in EPE, ECCE Europe 2015, Accepted.
[4]. J. Hare, X. Shi, S. Gupta and A. Bazzi “A review of faults and fault diagnosis in micro-grids electrical energy infrastructure” in Proc. IEEE Energy Conversion Congress and Exposition (ECCE), pp. 3325-3332, 2014.

Appendix B: Matlab Code

1. MCS for the first objective of supporting a 3.3kW critical load of UConn micro-grid:

```
function MonteCarlo3p3KW()
clc;
lambda=[4.5662,14.269,14.269,2.2831,  4.5662,14.269,14.269,2.2831,
14.269,14.269,14.269,11.416, 2.2831,   11.416,2.2831,11.416,2.2831,  2.2831,
2.2831,2.2831,2.2831].*0.000001;
name={'PV','DC/DC','DC/AC','Breaker', 'PV','DC/DC','DC/AC','Breaker',
'FC','DC/DC','DC/AC','Start Generator','Breaker', 'DG','Breaker','DG','Breaker',
'Transmission','Transmission','PCC','Load'};
[m,n]=size(lambda);
T_max=150*8760;
inter_t=200;
t=zeros(1,n);
N=5000;
mm=T_max/inter_t;
fs=zeros(1,mm);
Rs=zeros(1,mm);
Ps=zeros(1,mm);
delta_m=zeros(1,mm);
component_m=zeros(1,n);
component_w=zeros(1,n);

for j=1:N
    component=zeros(1,n);
    t=time(lambda,n);
    [t_f,index]=sort(t);
    for k=1:n
        if(t_f(k))>=T_max
         delta_m(end)=delta_m(end)+1;
         break;
        end
        component(index(k))=1;
        top_event=top_function(component);
        if top_event ~= 0
           if mod(t_f(k),inter_t)==0
              delta_m(fix(t_f(k)/inter_t))=delta_m(fix(t_f(k)/inter_t))+1;
           else delta_m(fix(t_f(k)/inter_t)+1)=delta_m(fix(t_f(k)/inter_t)+1)+1;
           end
```

```
            component_m(index(k))=component_m(index(k))+1;
            break;
        end
    end

end
fs=cumulativefailure(delta_m,mm);
fs_m=zeros(1,mm+1);
fs_m(2:end)=fs;
Rs=1.-fs;
Rs_m=ones(1,mm+1);
Rs_m(2:end)=Rs;
Ps=failureprobability(delta_m,mm);
component_w=componentweight(component_m,n);
name_s={'PV','DC/DC','DC/AC','Breaker','FC','Load','DG','Transmission','
PCC','   Start Generator'};
component_s=zeros(1,10);
component_s(1)=component_w(1)+component_w(5);
component_s(2)=component_w(2)+component_w(6)+component_w(10);
component_s(3)=component_w(3)+component_w(7)+component_w(11);
component_s(4)=component_w(4)+component_w(8)+component_w(13)+component_w(15)+
component_w(17);
component_s(5)=component_w(9);
component_s(6)=component_w(21);
component_s(7)=component_w(14)+component_w(16);
component_s(8)=component_w(18)+component_w(19);
component_s(9)=component_w(20);
component_s(10)=component_w(12);

figure(2);
hold on;
plot(0:inter_t:T_max,Rs_m);
title('System reliability');
hold off;
figure;
bar(component_s,0.5);
set(gca, 'XTickLabel', name_s);
title('Importance degree of the basic components');%display(component_w);
MTTF=mean_life(Ps,inter_t,T_max);
display(MTTF);
end
```

```
 function t=time(lambda,n)
monte_random=rand(1,n);
t=-log(monte_random)./lambda;
end

 function fs=cumulativefailure(delta_m,mm)
fs=zeros(1,mm);
mr=0;
total=sum(delta_m);
for w=1:mm
    mr=mr+delta_m(w);
    fs(w)=mr/total;
end
end

 function Ps=failureprobability(delta_m,mm)
Ps=zeros(1,mm);
total=sum(delta_m);
for w=1:mm
    Ps(w)=delta_m(w)/total;
end
end

 function component_w=componentweight(component_m,n)
component_w=zeros(1,n);
total=sum(component_m);
component_w=component_m./total;
end

 function MTTF=mean_life(Ps,inter_t,T_max)
t=inter_t:inter_t:T_max;
MTTF=sum(Ps.*t);
end

function top_system=top_function(component)
PV_system_1=sum(component(1,1:4));
PV_system_2=sum(component(1,5:8));
FC_system=sum(component(1,9:13));
DG_system_1=component(14)+component(15);
DG_system_2=component(16)+component(17);
```

```
sub_1=PV_system_1*PV_system_2*FC_system;
sub_2=DG_system_1*DG_system_2;
sub_3=component(18)+sub_1;
sub_4=component(19)+sub_2;
sub_5=sub_3*sub_4;
sub_6=sub_5*component(20);
top_system=component(21)+sub_6;
end
```

2. MRM for the first objective of supporting a 3.3kW critical load of UConn micro-grid:

```
%=================================================================
% BY: xiaofang shi
% mircogrid overall system markov 150KW 6states
%=================================================================
clear;
time = 150; % TIME (Years)
lambda_all=[0.02,1/5.2,0.02,1/12.50,0.02,0.02];
%R_trans=0.02;
%R_load=0.02;
%R_pcc=0.02;
%_____________________________________
format long
%=================================================================
%  Initialized Variable
%=================================================================
lambda_all1=lambda_all(1); % Scale
lambda_all2=lambda_all(2); % Scale
lambda_all3=lambda_all(3); % Scale
lambda_all4=lambda_all(4); % Scale
lambda_all5=lambda_all(5); % Scale
lambda_all6=lambda_all(6); % Scale

Divisions = 5000; % Simulation Iterations
dt = time/Divisions % Delta Time Per Iteration
%Rel_PV=zeros(1,Divisions);
%=================================================================
% USING MARKOV_____________
%=================================================================
```

```
X=[1;0;0;0;0;0;0;0;0;0;0;0;0;0;0;0;0;0;0;0;0;0;0;0;0;0;0;0;0;0;0;0;0;0;0;0;0;
0;0;0;0;0;0;0;0;0;0;0;0;0;0;0;0;0;0;0;0;0;0;0;0;0;0;0];%Initial values of the
states
C =
[1,0,1,1,1,1,1,0,0,0,0,0,1,1,1,1,1,1,1,1,1,1,0,0,0,0,0,0,0,0,0,0,1,0,0,0,0,1,
1,1,1,1,1,0,0,0,0,0,0,0,0,0,0,0,0,0,0,0,0,0,0,0,0,0];
%_________________________________________
t = dt;
%______________ Markov Process_________
% X = Summation of (A*X(i))
% ; where i = 0,1,2,...Time
for i = 1:1:Divisions
B=zeros(64);
B(1,1)=-1*(lambda_all1+lambda_all2+lambda_all3+lambda_all4+lambda_all5+lambda
_all6);
B(2,1)=lambda_all6;
B(2,2)=-1*(lambda_all1+lambda_all2+lambda_all3+lambda_all4+lambda_all5);
B(3,1)=lambda_all5;
B(3,3)=-1*(lambda_all1+lambda_all2+lambda_all3+lambda_all4+lambda_all6);
B(4,1)=lambda_all4;
B(4,4)=-1*(lambda_all1+lambda_all2+lambda_all3+lambda_all5+lambda_all6);
B(5,1)=lambda_all3;
B(5,5)=-1*(lambda_all1+lambda_all2+lambda_all4+lambda_all5+lambda_all6);
B(6,1)=lambda_all2;
B(6,6)=-1*(lambda_all1+lambda_all3+lambda_all4+lambda_all5+lambda_all6);
B(7,1)=lambda_all1;
B(7,7)=-1*(lambda_all2+lambda_all3+lambda_all4+lambda_all5+lambda_all6);
B(8,2)=lambda_all5;
B(8,3)=lambda_all6;
B(8,8)=-1*(lambda_all1+lambda_all2+lambda_all3+lambda_all4);
B(9,2)=lambda_all4;
B(9,4)=lambda_all6;
B(9,9)=-1*(lambda_all1+lambda_all2+lambda_all3+lambda_all5);
B(10,2)=lambda_all3;
B(10,5)=lambda_all6;
B(10,10)=-1*(lambda_all1+lambda_all2+lambda_all4+lambda_all5);
B(11,2)=lambda_all2;
B(11,6)=lambda_all6;
B(11,11)=-1*(lambda_all1+lambda_all3+lambda_all4+lambda_all5);
B(12,2)=lambda_all1;
B(12,7)=lambda_all6;
```

```
B(12,12)=-1*(lambda_all2+lambda_all3+lambda_all4+lambda_all5);
B(13,3)=lambda_all4;
B(13,4)=lambda_all5;
B(13,13)=-1*(lambda_all1+lambda_all2+lambda_all3+lambda_all6);
B(14,3)=lambda_all3;
B(14,5)=lambda_all5;
B(14,14)=-1*(lambda_all1+lambda_all2+lambda_all6+lambda_all4);
B(15,3)=lambda_all2;
B(15,6)=lambda_all5;
B(15,15)=-1*(lambda_all1+lambda_all3+lambda_all6+lambda_all4);
B(16,3)=lambda_all1;
B(16,7)=lambda_all5;
B(16,16)=-1*(lambda_all2+lambda_all3+lambda_all4+lambda_all6);
B(17,4)=lambda_all3;
B(17,5)=lambda_all4;
B(17,17)=-1*(lambda_all1+lambda_all2+lambda_all6+lambda_all5);
B(18,4)=lambda_all2;
B(18,6)=lambda_all4;
B(18,18)=-1*(lambda_all1+lambda_all3+lambda_all6+lambda_all5);
B(19,4)=lambda_all1;
B(19,7)=lambda_all4;
B(19,19)=-1*(lambda_all2+lambda_all3+lambda_all6+lambda_all5);
B(20,5)=lambda_all2;
B(20,6)=lambda_all3;
B(20,20)=-1*(lambda_all1+lambda_all4+lambda_all5+lambda_all6);
B(21,5)=lambda_all1;
B(21,7)=lambda_all3;
B(21,21)=-1*(lambda_all5+lambda_all2+lambda_all6+lambda_all4);
B(22,6)=lambda_all1;
B(22,7)=lambda_all2;
B(22,22)=-1*(lambda_all5+lambda_all6+lambda_all3+lambda_all4);
B(23,8)=lambda_all4;
B(23,9)=lambda_all5;
B(23,13)=lambda_all6;
B(23,23)=-1*(lambda_all1+lambda_all2+lambda_all3);
B(24,8)=lambda_all3;
B(24,10)=lambda_all5;
B(24,14)=lambda_all6;
B(24,24)=-1*(lambda_all1+lambda_all2+lambda_all4);
B(25,8)=lambda_all2;
B(25,11)=lambda_all5;
```

```
B(25,15)=lambda_all6;
B(25,25)=-1*(lambda_all1+lambda_all4+lambda_all3);
B(26,8)=lambda_all1;
B(26,12)=lambda_all5;
B(26,16)=lambda_all6;
B(26,26)=-1*(lambda_all4+lambda_all2+lambda_all3);
B(27,9)=lambda_all3;
B(27,10)=lambda_all4;
B(27,17)=lambda_all6;
B(27,27)=-1*(lambda_all1+lambda_all2+lambda_all5);
B(28,9)=lambda_all2;
B(28,11)=lambda_all4;
B(28,18)=lambda_all6;
B(28,28)=-1*(lambda_all1+lambda_all3+lambda_all5);
B(29,9)=lambda_all1;
B(29,12)=lambda_all4;
B(29,19)=lambda_all6;
B(29,29)=-1*(lambda_all2+lambda_all5+lambda_all3);
B(30,10)=lambda_all2;
B(30,11)=lambda_all3;
B(30,20)=lambda_all6;
B(30,30)=-1*(lambda_all1+lambda_all5+lambda_all4);
B(31,10)=lambda_all1;
B(31,12)=lambda_all3;
B(31,21)=lambda_all6;
B(31,31)=-1*(lambda_all2+lambda_all4+lambda_all5);
B(32,11)=lambda_all1;
B(32,12)=lambda_all2;
B(32,22)=lambda_all6;
B(32,32)=-1*(lambda_all3+lambda_all5+lambda_all4);
B(33,13)=lambda_all3;
B(33,14)=lambda_all4;
B(33,17)=lambda_all5;
B(33,33)=-1*(lambda_all1+lambda_all2+lambda_all6);
B(34,13)=lambda_all2;
B(34,15)=lambda_all4;
B(34,18)=lambda_all5;
B(34,34)=-1*(lambda_all1+lambda_all3+lambda_all6);

B(35,13)=lambda_all1;
B(35,16)=lambda_all4;
```

```
B(35,19)=lambda_all5;
B(35,35)=-1*(lambda_all2+lambda_all3+lambda_all6);
B(36,14)=lambda_all2;
B(36,15)=lambda_all3;
B(36,20)=lambda_all5;
B(36,36)=-1*(lambda_all1+lambda_all6+lambda_all4);
B(37,14)=lambda_all1;
B(37,16)=lambda_all3;
B(37,21)=lambda_all5;
B(37,37)=-1*(lambda_all6+lambda_all2+lambda_all4);
B(38,15)=lambda_all1;
B(38,16)=lambda_all2;
B(38,22)=lambda_all5;
B(38,38)=-1*(lambda_all6+lambda_all3+lambda_all4);
B(39,17)=lambda_all2;
B(39,18)=lambda_all3;
B(39,20)=lambda_all4;
B(39,39)=-1*(lambda_all1+lambda_all5+lambda_all6);
B(40,17)=lambda_all1;
B(40,19)=lambda_all3;
B(40,21)=lambda_all5;
B(40,40)=-1*(lambda_all2+lambda_all5+lambda_all6);
B(41,18)=lambda_all1;
B(41,19)=lambda_all2;
B(41,22)=lambda_all4;
B(41,41)=-1*(lambda_all3+lambda_all5+lambda_all6);
B(42,20)=lambda_all1;
B(42,21)=lambda_all2;
B(42,22)=lambda_all3;
B(42,42)=-1*(lambda_all4+lambda_all5+lambda_all6);
B(43,39)=lambda_all1;
B(43,40)=lambda_all2;
B(43,41)=lambda_all3;
B(43,42)=lambda_all4;
B(43,43)=-1*(lambda_all5+lambda_all6);
B(44,36)=lambda_all1;
B(44,37)=lambda_all2;
B(44,38)=lambda_all3;
B(44,42)=lambda_all5;
B(44,44)=-1*(lambda_all4+lambda_all6);
B(45,34)=lambda_all1;
```

```
B(45,35)=lambda_all2;
B(45,38)=lambda_all4;
B(45,41)=lambda_all5;
B(45,45)=-1*(lambda_all6+lambda_all3);
B(46,33)=lambda_all1;
B(46,35)=lambda_all3;
B(46,37)=lambda_all4;
B(46,40)=lambda_all5;
B(46,46)=-1*(lambda_all2+lambda_all6);
B(47,33)=lambda_all2;
B(47,34)=lambda_all3;
B(47,36)=lambda_all4;
B(47,39)=lambda_all5;
B(47,47)=-1*(lambda_all1+lambda_all6);
B(48,30)=lambda_all1;
B(48,31)=lambda_all2;
B(48,32)=lambda_all3;
B(48,42)=lambda_all6;
B(48,48)=-1*(lambda_all4+lambda_all5);
B(49,28)=lambda_all1;
B(49,29)=lambda_all2;
B(49,32)=lambda_all4;
B(49,41)=lambda_all6;
B(49,49)=-1*(lambda_all3+lambda_all5);
B(50,27)=lambda_all1;
B(50,29)=lambda_all3;
B(50,31)=lambda_all4;
B(50,40)=lambda_all6;
B(50,50)=-1*(lambda_all2+lambda_all5);
B(51,27)=lambda_all2;
B(51,28)=lambda_all3;
B(51,30)=lambda_all4;
B(51,39)=lambda_all6;
B(51,51)=-1*(lambda_all1+lambda_all5);
B(52,25)=lambda_all1;
B(52,26)=lambda_all2;
B(52,32)=lambda_all5;
B(52,38)=lambda_all6;
B(52,52)=-1*(lambda_all3+lambda_all4);
B(53,24)=lambda_all1;
B(53,26)=lambda_all3;
```

```
B(53,31)=lambda_all5;
B(53,37)=lambda_all6;
B(53,53)=-1*(lambda_all2+lambda_all4);
B(54,24)=lambda_all2;
B(54,25)=lambda_all3;
B(54,30)=lambda_all5;
B(54,36)=lambda_all6;
B(54,54)=-1*(lambda_all1+lambda_all4);
B(55,23)=lambda_all1;
B(55,26)=lambda_all4;
B(55,29)=lambda_all5;
B(55,35)=lambda_all6;
B(55,55)=-1*(lambda_all3+lambda_all2);
B(56,23)=lambda_all2;
B(56,25)=lambda_all4;
B(56,28)=lambda_all5;
B(56,34)=lambda_all6;
B(56,56)=-1*(lambda_all1+lambda_all3);
B(27,23)=lambda_all3;
B(57,24)=lambda_all4;
B(57,27)=lambda_all5;
B(57,33)=lambda_all6;
B(57,57)=-1*(lambda_all2+lambda_all1);
B(58,47)=lambda_all1;
B(58,46)=lambda_all2;
B(58,45)=lambda_all3;
B(58,44)=lambda_all4;
B(58,43)=lambda_all5;
B(58,58)=-1*(lambda_all6);
B(59,51)=lambda_all1;
B(59,50)=lambda_all2;
B(59,49)=lambda_all3;
B(59,48)=lambda_all4;
B(59,43)=lambda_all6;
B(59,59)=-1*(lambda_all5);
B(60,54)=lambda_all1;
B(60,53)=lambda_all2;
B(60,52)=lambda_all3;
B(60,48)=lambda_all5;
B(60,44)=lambda_all6;
B(60,60)=-1*(lambda_all4);
```

```
B(61,56)=lambda_all1;
B(61,55)=lambda_all2;
B(61,52)=lambda_all4;
B(61,49)=lambda_all5;
B(61,45)=lambda_all6;
B(61,61)=-1*(lambda_all3);
B(62,57)=lambda_all1;
B(62,55)=lambda_all3;
B(62,53)=lambda_all4;
B(62,50)=lambda_all5;
B(62,46)=lambda_all6;
B(62,62)=-1*(lambda_all2);
B(63,57)=lambda_all2;
B(63,56)=lambda_all3;
B(63,54)=lambda_all4;
B(63,51)=lambda_all5;
B(63,47)=lambda_all6;
B(63,63)=-1*(lambda_all1);
B(64,63)=lambda_all1;
B(64,62)=lambda_all2;
B(64,61)=lambda_all3;
B(64,60)=lambda_all4;
B(64,59)=lambda_all5;
B(64,58)=lambda_all6;

G=B*X;
X = X + G*dt;
Rel(i)=C*X;
Reliability = C*X;
end
xx=dt:dt:time;
xx=xx.*8760;
figure(2);
hold on;
plot(xx,Rel,'r');
hold off;
xlabel('Time(Hours)');
ylabel('Reliablity');

T=sum(dt.*Rel);
display(T)
```